Full-Duplex Device-to-Device Communication for 5G Network

Hussein Chour

THESE DE DOCTORAT DE

CENTRALESUPELEC

COMUE UNIVERSITE BRETAGNE LOIRE

ECOLE DOCTORALE N° 601
Mathématiques et Sciences et Technologies de l'Information et de la Communication
Spécialité : *Télécommunications*

UNIVERSITE LIBANAISE

École Doctorale des Sciences et de Technologie (EDST)

Par

« Hussein Chour »

« Full-Duplex Device-to-Device Communication for 5G Network »

Thèse présentée et soutenue à Rennes, le 28 octobre 2019
Unité de recherche : UMR 6164 – IETR (Équipe SCEE)
Thèse N° : 2019CSUP0002

Rapporteurs avant soutenance :

Eduard JORSWIECK Professeur des universités au Technische Universität Braunschweig, Allemagne
E. Veronica BELMEGA Professeur associé à l'université de Cergy-Pontoise, France

Composition du Jury :

Président :	Didier Le RUYET	Professeur des universités, au CNAM Paris-France
Examinateurs :	Fabrice VALOIS	Professeur des universités à l'INSA de Lyon-France
	Joumana FARAH	Professeur des universités à l'université Libanaise, Beyrouth-Liban
Encadrant :	Youssef Nasser	Professeur associé à American University of Beirut, Liban
Dir. de thèse :	C. Faouzi BADER	Professeur associé à CentraleSupélec-France
	Oussama BAZZI	Professeur des universités à l'université Libanaise, Beyrouth-Liban

Remerciements

First and foremost, I must acknowledge and thank The Almighty Allah for blessing, protecting and guiding me throughout this period.

I would like to express my gratitude to my supervisors Prof. Faouzi Bader, Prof. Oussamma Bazzi, and Dr. Youssef Nasser for their useful comments, remarks and engagement through the learning process of this PhD thesis. Prof. Bader, Prof. Bazzi, and Dr. Nasser encouraged and guided me from the initial to the final level in developing a deep under-standing of the subject. His instructive comments and evaluation guided and challenged my thinking, substantially improving the thesis outcome.

I am also grateful for the valuable advices and constructive criticisms were given by Prof. Edward Jorswieck and for his hosting me in the Information Theory Lab of the Technical University of Dresden. And I would like to thank Prof. E. Veronica Belmega for her valuable comments and advices.

I would like to extend my gratitude to my parents who provided me with moral support and bared my stress during the whole period, and to my friends who always stand by my side. I really cannot thank them enough and I pray God to preserve them for me.

Abstract

With the rapidly growing of the customers' data traffic demand, improving the system capacity and increasing the user throughput have become essential concerns for the future fifth-generation (5G) wireless communication network. In this context, device-to-device (*D2D*) communication and in-band full-duplex (FD) are proposed as potential solutions to increase the spatial spectrum utilization and the user rate in a cellular network. *D2D* allows two nearby devices to communicate without base station (*BS*) participation or with limited participation. On the other hand, FD communication enables simultaneous transmission and reception in the same frequency band. Due to the short distance property of *D2D* links, exploiting the FD technology in D2D communication is an excellent choice to further improve the cellular spectrum efficiency and the users' throughput. However, practical FD transceivers add new challenges for D2D communication. For instance, the existing FD devices cannot perfectly eliminate the self-interference (SI) imposed on the receiver by the node's own transmitter. Thus, the residual self-interference (RSI) which is tightly related to the transmitter power value highly affects the performance of FD transmission. Moreover, the FD technique creates additional interference in the network which may degrade its performance when compared with the half-duplex transmission. Thus, proper radio resource management is needed to exploit the benefits of FD and guarantee the quality of service (QoS) of the users. The works in this dissertation focus on the power allocation (PA) and channel assignment (CA) of a full-duplex device-to-device (FD-D2D) network. In particular, this thesis first addresses the PA problem and proposes a simple yet efficient centralized optimal PA framework, and next, it derives the optimal joint PA and CA scheme for an FD-D2D network. A simple sub-optimal algorithm for resource allocation named CATPA, based on CA followed by PA, is also derived and proposed. This dissertation also develops, in the end, an efficient decentralized PA using game theory tools that will be an essential part of future works in the context of distributed radio resource management.

Résumé

Avec la croissance rapide de la demande de trafic de données des clients, l'amélioration de la capacité du système et l'augmentation du débit des utilisateurs sont devenues des préoccupations essentielles pour le futur réseau de communication sans fil de cinquième génération. Dans ce contexte, la communication terminal-à-terminal (Device-to-Device D2D) et le Full Duplex (FD) sont proposés comme solutions potentielles pour augmenter l'efficacité spectrale et le débit des utilisateurs dans un réseau cellulaire. Le D2D permet à deux périphériques proches de communiquer sans participation de la station de base ou avec une participation limitée. D'autre part, la communication en FD permet une transmission et une réception simultanées dans la même bande de fréquence. En raison de la propriété de distance courte des liaisons D2D, exploiter la technologie FD dans la communication D2D est un excellent choix pour améliorer encore plus l'efficacité spectrale cellulaire et le débit des utilisateurs. Cependant, les émetteurs-récepteurs FD constituent de nouveau défis pour la communication D2D. Par exemple, en FD les émetteurs-récepteurs ne peuvent pas supprimer d'une manière parfaite l'auto-interférence (SI) générée au niveaux des récepteurs lors de la transmission des données (par le propre émetteur du dispositif cellulaire). Ainsi, l'auto-interférence résiduelle qui est étroitement liée à la valeur de la puissance de l'émetteur affecte fortement les performances de la transmission FD. De plus, la technique en FD crée des interférences supplémentaires dans le réseau, ce qui peut dégrader ses performances par rapport à la transmission en semi-duplex (Half-duplex HD). Ainsi, une bonne gestion des ressources radio est nécessaire pour exploiter les avantages de la FD et garantir la qualité de service (QoS) des utilisateurs. Les travaux de cette thèse portent sur l'allocation de puissance et l'attribution de canaux d'un réseau FD-D2D. En particulier, cette thèse aborde d'abord le problème de l'allocation de puissance et propose une méthode d'allocation de puissance (PA) optimale centralisée simple mais efficace, puis développe le schéma optimal conjoint d'AP et d'AC pour un réseau FD-D2D. Un algorithme de complexité réduite CATPA, basé sur une allocation CA suivie d'une allocation PA, est aussi développée et proposé. La thèse présente à la fin une stratégie efficace d'AP décentralisée en utilisant les outils de la théorie des jeux.

Résumé Etendu en Français

Contexte et Motivation

En réponse à la croissance rapide de la demande en trafic de données des utilisateurs et à la rareté du spectre radioélectrique [1], les technologies de communication terminal-à-terminal (Device-to-Device D2D) avec un mode d'accès Full Duplex (FD) sont proposées pour améliorer l'utilisation du spectre des communications cellulaires et l'expérience des utilisateurs pour les futurs réseaux cinquième génération (5G) [2,3]. D'une part, le dispositif D2D permet à deux terminaux proches de contourner la station de base et de communiquer directement en tant que paire de communication [4]. D'autre part, le mode FD permet à un appareil d'émettre et de recevoir simultanément dans la même bande de fréquence et dans le même intervalle de temps [3]. Comme le système D2D fonctionne à courte distance, l'intégration de la technologie FD au D2D peut encore plus améliorer l'efficacité spectrale et le débit des utilisateurs 5G [5].

Cependant, l'utilisation pratique du mode d'accès FD ajoute de nouveaux défis à la communication D2D et à la communication cellulaire traditionnelle. Par exemple, en FD les émetteurs-récepteurs ne peuvent pas supprimer d'une manière parfaite l'auto-interférence (SI) générée au niveau des récepteurs lors de la transmission des données (par le propre émetteur du dispositif cellulaire) [3]. Ainsi, l'interférence résiduelle qui est étroitement liée à la valeur de la puissance d'émission affecte fortement les performances de transmission du système de communication en mode FD. En outre, l'utilisation de la technique FD crée des interférences supplémentaires dans le réseau qui risquent de dégrader le lien de communication cellulaire classique. Malgré cet environnement d'interférence complexe, l'intégration FD-D2D peut générer un gain non négligeable si une gestion efficace des interférences et des algorithmes d'allocation de ressources sont appliqués [6]. Cette thèse aborde le problème d'allocation de ressources (RA) d'un réseau FD-D2D et vise à proposer des algorithmes de RA efficaces en termes de complexité, d'efficacité spectrale et énergétique afin d'ouvrir la voie au déploiement des technologies FD-D2D dans les futurs réseaux 5G.

Objectifs et Contributions

Comme il a été décrit précédemment, le principal défi d'un réseau cellulaire FD-D2D de type ''underlaying" est son milieu d'interférence complexe. Cette thèse porte sur la manière d'améliorer les performances d'un réseau cellulaire incluant des dispositifs FD-D2D par le biais d'une conception et d'une coordination appropriées des techniques de gestion des ressources radio. Plus précisément, nous reconnaissons l'importance de l'allocation optimale de puissance et de l'affectation des canaux pour réaliser les promesses en terme de gain et d'efficacité des communications FD-D2D dans les futur réseaux 5G. Les grandes lignes de cette thèse, ainsi que les différentes contributions et publications, sont décrites ci-dessous.

Après une présentation de l'état de l'art sur les réseaux D2D dans le premier chapitre, nous abordons, dans le chapitre 2, l'allocation de puissance d'un réseau FD-D2D qui se compose d'une paire de dispositifs D2D partageant la bande passante d'un système de communication cellulaire (cellular user-CU). Dans la première section de ce chapitre, nous cherchons à dériver la performance ergodique du système pour avoir une vue d'ensemble des différents paramètres qui peuvent affecter le comportement du réseau. Pour ce faire, nous dérivons l'expression analytique de la capacitée ergodique, puis nous formulons le problème de maximisation de la capacitée ergodique. Le problème formulé s'est avéré non convexe, c'est pourquoi nous proposons une solution sous-optimale en supposant un système à interférence limitée et un rapport signal interférence élevé. La solution proposée montre directement l'impact de la localisation des utilisateurs CUs, de la capacité de l'annuleur d'interférence (SIC), et de la distance D2D sur la performance du réseau.

Dans la deuxième section du chapitre 2, nous nous concentrons sur le problème de l'allocation instantanée de la puissance qui est normalement utilisée dans tous les systèmes réels. Nous présentons d'abord la technique d'optimisation convexe séquentielle (sequential convex optimization-SCO) qui est largement utilisée dans la littérature pour résoudre le problème de l'allocation de puissance (PA) non convexe. Ensuite, nous développons une nouvelle méthode d'optimisation géométrique appelée GALEN (Geometrical framework Approach for gLobal optimal powEr allocatioN) qui permet d'obtenir une solution globale optimale au problème PA. En particulier, l'algorithme GALEN profite de la monotonocité inhérente caractéristique de la fonction objectif pour résout le problème d'optimisation seulement sur la frontière de l'ensemble admissible au lieu d'explorer tous les points admissible de l'ensemble. En outre, l'algorithme GALEN montre que la solution du problème sur la frontière des solutions appartient à un ensemble de points dont les coordonnées sont connues et directement liées au gain du canal des utilisateurs, au bruit du récepteur, et à la capacité du SIC à réduire l'auto-interférence. Ce chapitre comprend une partie du contenu des publications à comité de lecture suivantes :

- H. Chour, F. Bader, Y. Nasser, and O. Bazzi, “Galen: A Geometric Framework for Global Optimal Power Allocation in a Full-Duplex D2D Network,” in Proc. IEEE Wireless Communications and Networking Conf (WCNC2019), Apr. 2019.

- H. Chour, O. Bazzi, F. Bader,and Y. Nasser, “Analytical Framework for Joint Mode Selection and Power Allocation for Full-Duplex D2D Network,” in Proc. IEEE Wireless Communications and Networking Conf. (WCNC2019), Apr. 2019.

- H. Chour, Y. Nasser, O. Bazzi,and F. Bader, “Full-duplex or half-duplex D2D Mode Closed Form Expression of the Optimal Power Allocation,” in Proc. 25th Int. Conf. Telecommunications (ICT), Jun.2018.

Le chapitre 3, traite le problème commun d’allocation des canaux (CA) et de PA d’un réseau FD-D2D avec plusieurs paires D2D coexistant avec plusieurs CUs. Ce type de problème est non convexe. Tout au long de cette thèse, nous avons traité le problème conjoint CA et PA comme un problème d’allocation de ressources (RA) que nous utilisons de manière interchangeable. Après avoir formulé le problème du RA, nous montrons que la solution optimale globale peut être obtenue en découplant le problème original du RA en deux sous-problèmes PA-CA. Ensuite, nous résolvons le sous-problème PA en utilisant la théorie de l’optimisation monotone (MO). Précisément, nous proposons un nouvel algorithme de type polybloc nommé, MARIO (polyblock vertices triMming bAsed poweR allocatIOn), qui converge efficacement vers la solution globale du problème PA.

Ensuite, sur la base de la solution optimale pour le PA, le problème du CA se réduit à un problème d’assignation qui peut être résolu par l’algorithme de Khun-Munkers (également connu sous le nom de l’algorithme Hongrois). Le principal inconvénient de la solution basée sur l’optimisation MO est sa grande complexité, c’est pourquoi nous proposons une solution sous-optimale en résolvant le problème original de RA dans l’ordre inverse, c’est-à-dire en assignant d’abord le canal puis la puissance. Les résultats de simulations montrent l’efficacité des algorithmes proposés et fournissent des informations importantes sur les paramètres de conception de la solution, tels que la distance de proximité et la capacité d’annulation de l’auto-interférence. Le contenu de ce chapitre est basé en partie sur les travaux présentés dans la revue à comité de lecture suivante :

- H. Chour, E. Jorswieck, F. Bader, Y. Nasser, and O. Bazzi, “Global Optimal Resource Allocation for Efficient FD-D2D Enabled Cellular Network,” IEEE Access, Vol. 7, pp. 59690-59707, May 2019.

Le chapitre 4 vise à développer un algorithme d’allocation de puissance (PA) distribuée dans un réseau cellulaire FD-D2D en mode ‘’underlaying”. À cette fin, nous formulons d’abord le problème d’allocation de puissance comme un jeu non coopératif dans lequel chaque utilisateur décide de la puissance à transmettre sur le canal qui lui est attribué pour maximiser l’efficacité

énergétique de sa liaison. Ensuite, nous montrons que ce jeu admet un point d'équilibre de Nash unique qui peut être obtenu grâce à un processus itératif. Ensuite, nous comparons l'algorithme distribué que nous proposons avec l'algorithme centralisé du PA développé au chapitre 3. Les résultats de simulation vérifient l'efficacité de l'algorithme distribué proposé. Le contenu de ce chapitre est basé sur les résultats présentés dans la publication à comité de lecture ci-dessous :

- H. Chour, Y. Nasser, F.Bader, and O.Bazzi, "Game-Theoretic Based Power Allocation for a Full-Duplex D2D Network" in Proc. IEEE International Workshop on Computer Aided Modeling and Design of Communication Links and Networks (CAMAD2019), Sept. 2019.

Enfin, le chapitre 5 conclut la thèse et résume les principales contributions. En outre, il souligne les limites de la thèse et fournit une discussion sur les perspectives pour les travaux futurs.

Principaux résultats et conclusion de la thèse

Analyse du comportement du taux ergodique

Dans le but de comprendre les performances générales du réseau FD-D2D et de reconnaître les paramètres susceptibles d'affecter ses gains, nous avons tout d'abord déduit au chapitre 2 l'expression analytique du débit ergodique du D2D. Ensuite, nous avons analysé en détail cette expression et nous avons constaté que la distance entre les utilisateurs de d2d, la capacité SIC du dispositif FD, la distance entre les CUs et la paire D2D jouent un rôle essentiel dans la détermination des performances du réseau. Par conséquent, dans toutes les expériences de simulation, nous validons les algorithmes proposés avec différentes distances de proximité D2D et plusieurs facteurs SIC.

Développer un schéma PA efficace et optimal

En général, le contrôle de la puissance est considéré comme l'un des éléments les plus essentiels pour contrôler les interférences de tout réseau sans fil. En effet, la gestion et le contrôle de la puissance de l'interférence sont directement liées aux opérateurs des réseaux mobiles. Dans cette thèse, nous cherchons également à trouver le meilleur schéma PA du réseau FD-D2D, mais malheureusement, le problème du PA se révèle comme étant un problème non concave. Pour faire face à ce problème, la plupart des travaux connexes ont utilisé l'outil SCO pour fournir une solution PA efficace. Le chapitre 2, se focalise sur ce problème et fournit l'algorithme GALEN qui permet de trouver la stratégie PA optimale en tirant parti de la géométrie de l'ensemble réalisable. En particulier, la solution apportée dans ce chapitre explore la structure de l'ensemble réalisable et restreint le point optimal à l'intérieur d'un ensemble de sommets aux coordonnées connues.

Trouver le gain ultime d'un réseau FD-D2D

Outre le PA, lorsque plusieurs paires D2D coexistent avec des utilisateurs cellulaires, le CA devient un point crucial pour la performance du réseau. Normalement, le problème conjoint CA et PA appartient à la classe de programmation non linéaire à nombres entiers mixtes (Mixed-Integer Non-Linear Programming -MINLP), ce qui en fait un problème très difficile à résoudre. C'est pourquoi la plupart des travaux liés dans le contexte du réseau FD-D2D ont uniquement fourni un schéma d'évaluation de l'état des ressources sous-optimales. Pour combler cette lacune, le chapitre 3 propose une solution RA basée sur la technique OM qui peut permettre d'atteindre une solution optimale. Plus précisément, ce chapitre décompose d'abord le problème RA en sous-problèmes PA et CA. Après cela, il développe un algorithme à base de polybloc appelé MARIO pour résoudre globalement le sous-problème du PA. Ensuite, il utilise l'algorithme Khun-Munkers pour l'attribution CA des utilisateurs. De plus, le chapitre 3 présente une nouvelle solution sous-optimale appelée CATPA (Channel Assignment Then Power Allocation), qui rivalise avec les travaux existants en termes de complexité et de précision.

Proposer un algorithme de PA distribué

Bien que des schémas d'allocations PA et RA optimaux aient été développés aux chapitres 2 et 3 respectivement, les solutions proposées sont du type centralisé, en d'autres termes le CSI de tous les utilisateurs sont supposés connus de l'unité centrale à la station base (BS). Cependant, cette hypothèse n'est pas réaliste et ne peut pas être mise en œuvre dans un scénario de réseau réel. Pour surmonter ce problème, le chapitre 4 exploite la théorie des jeux (GT) pour résoudre le problème des PA de manière distribuée. En particulier, ce chapitre présente le PA comme un jeu non coopératif dans lequel chaque utilisateur décide de la quantité de puissance à transmettre à travers le canal qui lui est attribué afin d'optimiser son propre fonctionnement. L'existence et l'unicité de la solution du jeu sont également abordées dans ce chapitre.

Globalement, les résultats obtenus dans cette thèse montrent que les performances du FD-D2D sont étroitement liées à la technique de réduction des interférences générées dans le réseau. Par conséquent, une étude plus approfondie est nécessaire pour obtenir tous les gains possibles du réseau FD-D2D. La section suivante fournit plusieurs extensions possibles de cette thèse.

Perspectives

Cette thèse a principalement abordé les problèmes PA et RA d'un réseau FD-D2D. Les hypothèses que nous avons formulées et les résultats que nous avons obtenus ouvrent la voie à des perspectives potentielles pour des travaux futurs que nous citons ci-après.

Gestion de l'allocation de ressources avec scénario statistique CSI

Les algorithmes PA et CA proposés aux chapitres 2 et 3 exigent une connaissance parfaite des CSI pour tous les utilisateurs du réseau de communication. En pratique, l'état des canaux entre les utilisateurs de CU / D2D et la station de base peut être obtenu à partir de signaux pilotes. Toutefois, l'état du canal entre deux utilisateurs ne peut être obtenu directement que si l'un de ces utilisateurs, c'est-à-dire les utilisateurs CUs ou D2Ds, le mesure et le rapporte à la station de base. Ce processus augmente et surcharge la signalisation et par conséquent la complexité de calcul; il est donc utile de proposer un schéma RA en considérant un scénario avec une information CSI statistique.

Gestion de l'allocation de ressources avec moins de restrictions sur le partage des canaux

En raison des interférences nuisibles générées dans un réseau FD-D2D, nous supposons dans cette thèse qu'une paire FD-D2D peut réutiliser les ressources du mode ascendant (UL) d'au plus un CU et que ce dernier peut partager ses ressources avec au plus une paire D2D. Bien que cette technique puisse aider à modérer les interférences du réseau, elle peut ne pas améliorer l'efficacité spectrale, en particulier lorsque les CUs expérimentent des canaux de bonne qualité. Ainsi, une extension possible de ce travail consiste à analyser les problèmes du PA et RA en supposant que plusieurs paires FD-D2D puissent partager les mêmes ressources UL, ou qu'une paire FD-D2D puisse réutiliser plusieurs ressources à la fois, ou alors que plusieurs CUs partagent leur bande passante avec plusieurs paires FD-D2D.

Contents

List of Figures

List of Tables

List of Symbols

Acronyms and abbreviations

3GPP	*3^{rd} Generation Partnership Project*
5G	*Fifth-Generation of Wireless Communication Network*
ACCENT5	*Advanced Waveforms, MAC Design and Dynamic Radio Resource Allocation for Device-to-Device in 5G Wireless Networks*
ADC	*Analog-to-Digital Converter*
AWGN	*Additive White Gaussian Noise*
BS	*Base Station*
CA	*Channel Assignment*
CATPA	*Channel Assignment then Power Allocation Algorithm*
CSI	*Channel State Information*
CU	*Cellular User*
CVX	*Matlab Software for Disciplined Convex Programming*
D2D	*Device-to-Device communication*
DAC	*Digital-to-Analog Converter*
DL	*Downlink Channel*
EE	*Energy Efficiency*
FD	*In-Band Full-Duplex*
FD-D2D	*Full-Duplex Device-to-Device communication*
FDD	*Frequency Division Duplex*
GALEN	*Geometric Framework for Global Optimal Power Allocation*
GEE	*Global Energy Efficiency*

GT	*Game Theory*
HD	*Half-Duplex*
HD-D2D	*Half-Duplex Device-to-Device communication*
ISM	*Industrial, Scientific, and Medical Spectrum*
LTE	*Long Term Evolution Network*
MAC	*Medium Access Control*
MAEIO	*Polyblock vertices triMming bAsed poweR allocatIOn Algorithm*
MIMO	*Multiple Input Multiple Output*
MO	*Monotonic Optimization Theory*
NE	*Nash Equilibrium Point*
PA	*Power Allocation*
PDF	*Probability Density Function*
QoS	*Quality of Service*
RA	*Resource allocation*
RF	*Radio Frequency*
RRM	*Radio Resource Management*
RSI	*Residual Self-Interference*
SCO	*Sequential Convex Optimization Theory*
SE	*Spectrum Efficiency*
SI	*Self-Interference*
SIC	*Self-Interference Cancellation*
SINR	*Signal-to-Interference-plus-Noise-Ratio*
SNC	*Social Networking Service*
SNR	*Signal-to-Noise Ratio*
TDD	*Time division duplex*
TTI	*Transmission Time Interval*
UL	*Uplink Channel*
V2V	*Vehicle-to-Vehicle communication*

WSR	*Weighted-Sum Rate*

Mathematical notations

$\mathbb{R}$	*Set of real numbers*
$\mathbf{X}$	*Matrix*
$\mathbf{x}$	*Vector*
x	*Scalar*

Units

dB	*Decibel*
Hz	*Hertz*
J	*Joule*
s	*Second*

Chapter 1

Introduction

Contents

In response to the rapid growth in the users' data traffic demands and the scarcity of the radio spectrum [1], *D2D* communication and FD technologies are proposed to improve the cellular spectrum utilization and the users' experience in the future 5G cellular network [2,3]. *D2D* allows two nearby devices to bypass the base station and communicate directly as a *D2D* communication pair [4]. On the other hand, FD allows a device to simultaneously transmit and receive in the same frequency band at the same time slot [3]. Due to the short distance feature of *D2D* communication, integrating the FD technology with *D2D* communication can further enhance the spectrum efficiency and the users' throughput [5]. However, practical FD devices add new challenges to both *D2D* communication and traditional cellular communication. For instance, the existing FD transceivers cannot perfectly remove the SI imposed on the receiver by the node's own transmitter [3]. Thus, the residual SI, which is tightly related to the transmitter power value, highly affects the performance of FD transmission. Besides, using the FD technique creates additional interference in the network which may overwhelm the conventional cellular link. Despite this complicated interference environment, a non-trivial gain can be earned when integrating FD with *D2D* if efficient interference management and resource allocation algorithms are applied [6].

This dissertation addresses the resource allocation (RA) problem of an FD-D2D network and aims to propose an efficient RA algorithm in terms of complexity and efficiency to pave the way for deploying FD and *D2D* technologies in the emerging 5G network. In this chapter, first, we introduce the concept of *D2D* communication, following by providing a background for the FD transmission. Then, we explore the related state of the arts of FD-D2D communication, and finally, we summarize our contributions and draw the structure of this dissertation.

1.1 D2D background

D2D communication is a new radio technology that authorizes direct communication between nearby devices and bypasses the *BS* as well as the core cellular network. The idea behind *D2D* communication is not novel and several *D2D* based services already exist such as Bluetooth and WiFi-direct. What makes *D2D* communication different is the utilization of the licensed cellular spectrum with QoS guarantees and seamless network detection [4,7]. This new technology provides several benefits to both network operators and cellular users. In the user side, due to the close proximity feature of *D2D* communication, the *D2D* users will experience a high data-rate, low-latency, and energy-efficient communication link comparing to the traditional communication link [4,7]. From the network's perspective, *D2D* communication will help in better utilization of the cellular spectrum and increasing the cell capacity without additional infrastructure cost. Moreover, *D2D* communication will bring new business opportunities to network operators with an estimated revenue of 17 billion dollars as forecasted by the social networking service (SNC) research [8]. Possible *D2D* use cases include, among others, proximity-

based services that are triggered when the communication parties are in proximity of each other such as local information sharing, mobile advertising, vehicle-to-vehicle (V2V) communication, mobile gaming, and social applications [7]. Other applications include emergency services which take advantage of the *D2D* proximity feature to establish an Ad-hoc network even in case of damage to the network infrastructure as happens during the natural disasters, e.g., hurricane, and earthquakes, or during a crowded event like the FIFA world cup games [4,7]. Fig.1.1 shows the possible use-cases of *D2D* communication.

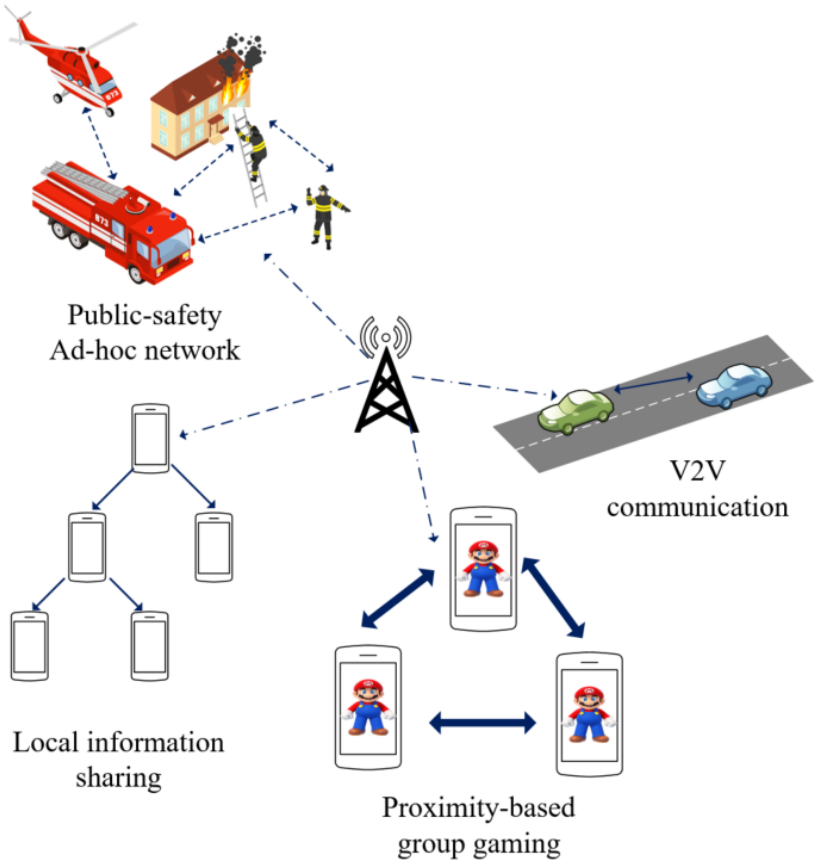

Figure 1.1 – Possible D2D use-cases.

In a *D2D* network, two users can set up a *D2D* link if they are in proximity to each other. Thus, a peer discovery process must be accomplished before initiating a *D2D* link. In general, the *D2D* communication is two-phases-process. The first phase is called as **discovery phase** while the second is named as **communication phase**. The discovery phase allows a user to determine his potential nearby peer before starting a *D2D* link in the communication phase which includes channel estimation, mode selection, resource allocation, power control, and the actual transmission of information.

In general, there are two approaches to *D2D* discovery: direct and network-assisted discovery. Direct discovery uses beaconing signals and scanning, which makes it time- and energy-consuming [4], and it was previously investigated in different license-free wireless technologies like Bluetooth and Wi-Fi direct. However, the unpredictable interference in the unlicensed spectrum prevents these methods to provide a good QoS and also limits its coverage range [4]. Thus, later, the focus has shifted to the licensed band [4, 9]. In this respect, the first step was made by Qualcomm in their "FlashLinQ" communication system, which provided an autonomous peer discovery and *D2D* communication procedure using the Long Term Evolution (LTE) spectrum [10]. Soon after that, this work was integrated into the 3rd Generation Partnership Project (3GPP) standard under the name "LTE-direct" [11]. On the other hand, in network-assisted discovery [12, 13], users rely on the network to detect and identify each other. UE informs the *BS* about its desire to initiate a *D2D* link by sending a request, prompting the BS to order some message exchanges with the devices to acquire identity and information about the link. This approach requires the network to mediate the discovery process to recognize *D2D* candidates, coordinate time and frequency allocations by sending/scanning beacons, and provide identity information [4, 13]. A mix centralized and autonomous *D2D* discovery and communication process can also be assumed to achieve a good trade-off between complexity and signaling overhead and guaranteed QoS, e.g., the work in [14].

The aim of our work is to provide an efficient RA algorithm for an FD-D2D network, and thus, we only focus on the *D2D* communication phase assuming that any two nearby devices have already discovered each other and they are forming a *D2D* pair which looks to assign its communication channel and allocate its transmission power.

1.1.1 D2D classification

Based on the type of spectrum used in *D2D* communication, *D2D* can be categorized into: in-band and out-band *D2D* communication as illustrated in Fig.1.2. The former uses the licensed spectrum while the latter operates in the unlicensed spectrum such as the industrial, scientific, and medical (ISM) band [4]. Due to the stochastic nature of the unlicensed band, in-band has gained much attraction among the research community [4, 15]. Further, the in-band *D2D* communication is grouped into overlay and underlay communication. The *D2D* overlay communication prevents the co-channel interference between the *D2D* and the traditional cellular signals by allocating dedicated cellular resources for the *D2D* links. On the contrary, in the underlaying scenario, the *D2D* devices reuse the spectrum resources of the cellular users (CUs) [15]. Thus, in the underlaying scenario, rigorous interference management is required to improve the network performance. Due to the spectrum scarcity problem, the underlay *D2D* communication has gained much attention [4, 15], and several resource allocation techniques, including channel assignment, mode selection, and power control have

been extensively explored [16–18]. Since spectrum efficiency (SE) is an important criterion in the future 5G network, in this work we consider an underlaying *D2D* scenario.

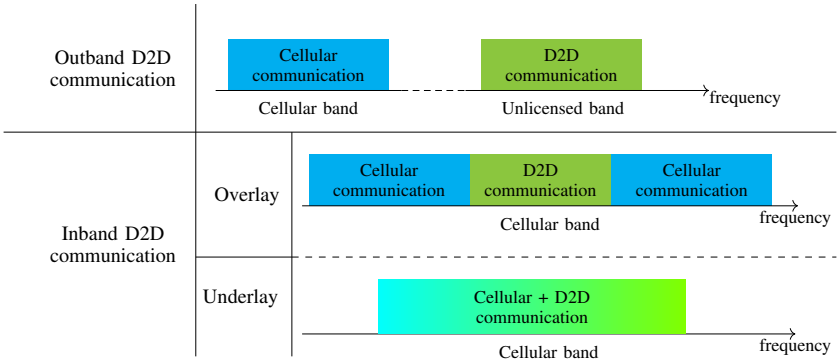

Figure 1.2 – Illustration of in-band overlay, in-band underlay, and out-band D2D communication.

Although *D2D* communication could achieve better performance in terms of SE and user's experience compared to the traditional cellular link, it is insufficient to meet the eager 5G requirements [19]. Accordingly, it is expected to fulfill the 5G targets by combining several new technologies into the state-of-the-art cellular network [19]. The short-range communication feature of the *D2D* network allows the *D2D* users to transmit with relatively lower power compared to the traditional communication links. This, in turn, makes the *D2D* communication an excellent candidate for being integrated with the in-band full-duplex technology for further SE and rate enhancement as we will see in the following section.

1.2 Full-Duplex background

The latest achievements in wireless communication have led to an ever-growth demand on the limited cellular radio spectrum, pushing for innovating new radio technologies that use the spectrum efficiently. Techniques like multiple-input-multiple-output (MIMO) [20, 21], *D2D*, non-orthogonal multiple access (NOMA) [22, 23], cognitive radio [24], and FD radios [3] are among new technologies which aim to enhance the wireless network SE. Due to the potential of doubling SE, as well as the network throughput, without using any additional bandwidth, recently, FD has gained a lot of attraction in academia [25] and industry [26, 27]. The current wireless network uses the conventional half-duplex (HD) as a transmission mode. The latter is a transmission technique that allows a transceiver to avoid the interference between its transmitter and receiver by transmitting and receiving signals over orthogonal frequencies as in the frequency division duplex (FDD) system, FDD is also known as out-of-band full-duplex, or at different time slots as in the time division duplex (TDD) system, leading to degrading the SE.

On the contrary, FD allows a device to simultaneously transmit and receive signals at the same frequency, leading to better performance (potentially double) in terms of SE, throughput and end-to-end delay. Obviously, FD will not be applicable unless a rigorous self-interference cancellation (SIC) technique is applied at the FD device. SI refers to the interference imposed on the receiver of an FD device by its own transmitter, and it is depicted in a red curved line in the FD bidirectional communication model shown in Fig.1.3. Moreover, in this figure, the desired signals are represented as straight black lines, while the transmit and receive antennas of an FD device are denoted as Tx and Rx respectively.

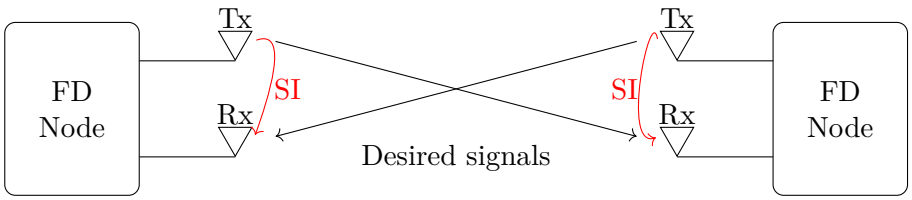

Figure 1.3 – A model of full-duplex peer to peer communication.

To highlight the impact of SI, let us consider the following FD femtocell scenario from [28] where the FD Femto BS transmit power is assumed 20dBm and the noise floor power is -100dBm. Moreover, a 15dB isolation is assumed between the BS's transmitter and receiver [28]. Hence, as illustrated in Fig.1.4, to bring down SI to the noise level, an intensive amount of 105dB self-interference mitigation is required. Fortunately, the recent advancements in antenna designs

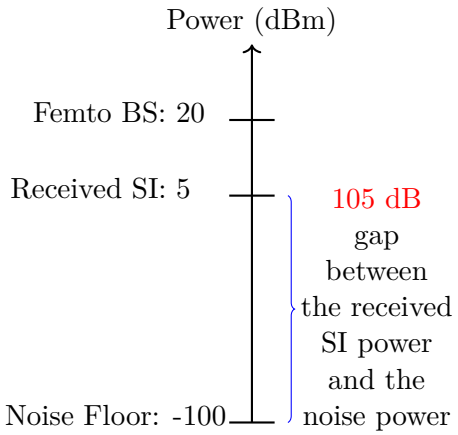

Figure 1.4 – Illustration about the required SI mitigation value assuming a FD Femto *BS* with 20 dBm transmission power.

and transmitter's architectures could achieve a high level of SIC [28–40]. For instance, the work in [34] was able to obtain 110 dB SIC which makes FD feasible for implementation in WiFi networks with 20 dB transmission power. Due to the importance of SIC in FD operation, in the sequel, we provide an overview of the proposed SIC techniques in the literature.

1.2.1 Self-interference cancellation techniques

The main idea behind FD transmission is to transmit and receive signals at the same time and on the same bandwidth. In this case, in addition to the desired signal, an FD device receives its own transmitted signal which forms the SI imposed on the device (see Fig.1.3). The power of SI can be 50-100dB larger than the desired signal [28], enforcing for an effective SIC technique. At first sight, one may suggest subtracting the transmitted signal, which is known by the device, from the received signals to cancel out all SI. This basic intuition is not totally true since in practice the transmitted signal is subjected to different non-linear distortions and noise when passing the RF chain, limiting the knowledge about the transmitted signal to only the digital domain, and consequently making the SIC a challenging task.

Literature classifies the SIC techniques into passive suppression, analog cancellation, and digital cancellation [28, 41, 42]. To ease understanding these techniques we first discuss the architecture of an FD terminal illustrated in Fig.1.5, and then we describe each SIC technique individually.

Fig.1.5(a) represents a schematic of a separated-antenna FD terminal which uses one transmit antenna (Tx) and one receive antenna (Rx) to interface with the node's transmitter chain (Tx chain) and the node's receiver chain (Rx chain) respectively. The schematic of a shared-antenna FD terminal is presented in Fig.1.5(b) in which one antenna is used to interact with the TX/RX chains. In this schematic, a duplexer is required to route the transmit signal from the transmitter to TX and to route the signal received at RX to the receiver, while isolating the RX chain from the Tx chain.

In both architectures, first, the FD terminal codes and modulates the transmit bitstream ($x[n]$), producing a digital baseband signal which is then converted to analog using a digital-to-analog converter (DAC). Thereafter, the analog signal enters the TX chain to be up-converted to the carrier frequency and amplified before being radiated at Tx. At the same time, and over the same frequency band, the FD terminal performs as a receiver. The received signal at RX goes through the Rx chain to be amplified and down-converted to a low frequency before being converted to a digital baseband signal using an analog-to-digital Converter (ADC). The resulting digital signal is then demodulated and decoded to produce the received bitstream. Fig.1.5 also shows the operation place of each SIC technique in an FD terminal.

Passive suppression

Passive suppression techniques are propagation-based methods that aim to attenuate SI before it gets into the receiver RF chain as indicated in Fig.1.5, helping the receiver to avoid dealing with large dynamic range signals. To maximize the benefits of passive suppression, different techniques are proposed including path-loss methods [30, 43–45], cross-polarization techniques [46–48];

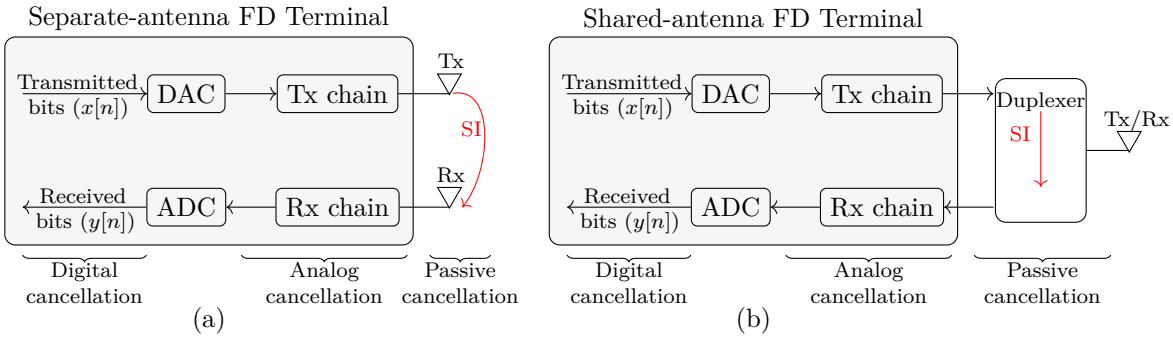

Figure 1.5 – The architectural of an (a) separate-antenna FD device and (b) shared-antenna FD device.

antenna directionality [33, 46, 48, 49]. The Path-loss-based methods basically aim to increase the transmitter to receiver separation distance which enhances the signal attenuation. The cross-polarization techniques isolate the TX and RX of an FD node electromagnetically by sending and receiving signals over orthogonal polarization. Similarly, the directional antenna methods look to electromagnetically separate the transmitted and received signals by using TX and RX antennas with minimum radiation lobes intersections. Further, several absorption materials can be placed between the antennas to help in attenuating the analog signals [46]. In case of a shared antenna model, a duplexer is needed to isolate the transmitted and received signals [50–52]. The SI reduction reported in the literature varies between 45 dB and 70 dB, showing that it is insufficient for a real FD operation. Moreover, the main drawback of these techniques is that it is constrained by the node size: the smaller the device becomes, the harder the high passive SI-reduction becomes to achieve.

Analog cancellation

Analog cancellation aims to cancel SI before it enters the analog to digital conversion process as shown in Fig.1.5 (a)-(b). In literature, two analog cancellation strategies exist and they are independent of the FD architecture [28, 53]. The first strategy cancels SI by taking a reference signal from the transmit antenna feed, applying analog processing using delay and variable attenuators to emulate a replica version of this signal and then subtracting it from the received signal at the receiver antenna feed [29, 32, 54, 55]. We denote this approach as RF-to-RF-analog-based SIC (RF2RF) and it is illustrated in Fig.1.6(a). The second approach applies some digital operations on a reference digital signal to create a replica of the SI, and then converts it to the analog domain to subtract it from the received signal at the receiver antenna feed [28, 30, 31, 34]. This is mainly because digitally adjusting the signal is much easier than analog processing. We called this process digital-to-RF-analog based SIC (Dig2RF) and it is shown in Fig.1.6(b). These analog techniques are environmentally sensitive, i.e., they are affected by the reflection and refraction of the signal that is normally unpredictable. Moreover,

in these schemes, channel estimation and tracking are required to correctly predict the SI channel. For these reasons, Digital cancellation becomes inevitable.

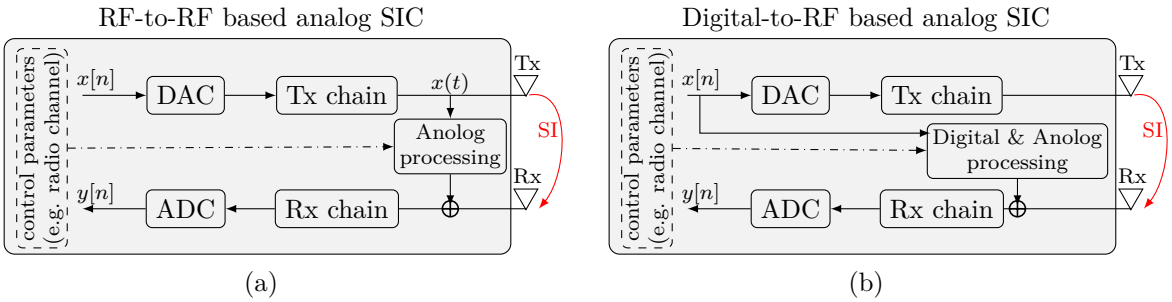

Figure 1.6 – The analog SIC approaches, where (a) illustrates the RF to RF cancellation technique and (b) represents the digital to RF analog cancellation scheme.

Digital cancellation

The digital cancellation schemes are the last defense line against the SI, and they seek to cancel the remaining SI in the received signal after passing the ADC process. Similarly to the analog techniques, the digital SIC schemes take a reference signal from the transmitter, apply the necessary phase and delay adjustments to emulate SI, and then subtracts it from the received digital signal. As illustrated in Fig.1.7, two digital SIC approaches exist. The first approach takes a copy from the transmitted signal in the digital domain to predict SI and subtracts it from the received digital signal [29, 31, 56–60]. We denote this approach as digital-to-digital-based SIC, and it is abbreviated as Dig2Dig for ease of notation. The second approach called RF-to-digital-based SIC (RF2dig) taps a copy of the transmitted signal from the transmitter feed, applies the necessary operations to mimic SI, and finally subtracts it from the received digital signal [61–63]. The main challenge of these schemes is the dynamic range problem of the ADC which limits the amount of SI reduction that can be achieved and that is why passive and analog cancellation is needed. Thus, for a practical FD application, a concatenated passive and active cancellation is imperative. Recently, several promising prototypes of FD terminals adopting hybrid SIC schemes could achieve up to 110 dB SI reduction in a low transmission power scenario, proving the feasibility of FD operation [29, 30, 35–40].

To achieve the highest possible SI mitigation value, usually, the above SIC techniques got combined. Table 1.1 shows a list of the recent FD terminal prototypes and their SIC techniques.

Although the aforementioned FD techniques could achieve a high level of SIC, in practice it is impossible to totally delete SI due to hardware impairments. This residual self-interference will highly impact the experience of an FD terminal. Besides RSI, applying the FD operation in a cellular network will introduce additional interference, which in turn can question the

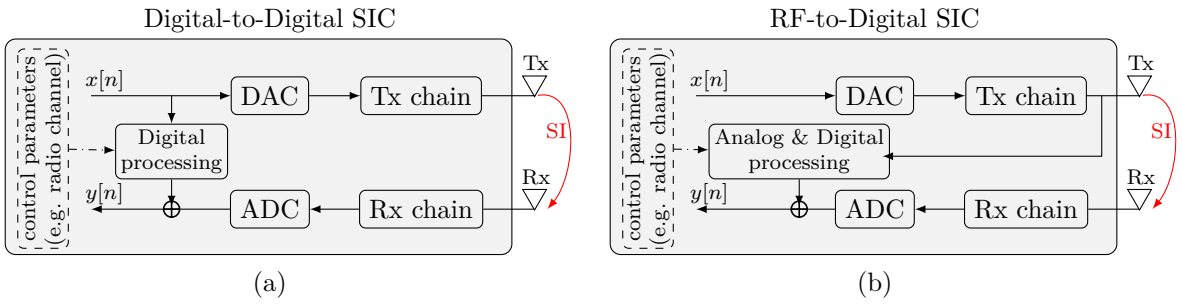

Figure 1.7 – The digital SIC approaches, where (a) illustrates the digital to digital cancellation technique and (b) represents the RF to digital cancellation scheme.

Table 1.1 – A list of the recent FD prototypes

Prototype	Year	Architecture	Passive cancellation	Analog cancellation	Digital cancellation	Total SIC
[30]	2010	Separate-antenna	Antenna separation	Dig2RF	Dig2Dig	80 dB
[29]	2013	Shared- antenna	Circulator	RF2RF	Dig2Dig	110 dB
[39]	2015	Shared-antenna	Electrical balance duplexer	RF2RF	No	83 dB
[40]	2015	Shared-antenna	Circulator	RF2RF	No	54 dB
[35]	2015	Shared-antenna	cross-polorization	RF2RF	Dig2Dig	103 dB
[36]	2016	Separate-antenna	Antenna seperation	RF2RF	No	78 dB
[37]	2016	Shared-antenna	Circulator	RF2RF	Dig2Dig	88 dB
[38]	2017	Separate-antenna	Wavetraps	No	Dig2Dig	103 dB

possible FD benefits such as doubling the SE and throughput. This motivates the researcher to investigate the theoretical bounds of FD operation using abstract analysis [64–72]. For example, the works in [64–67] analyze the degrees of freedom (DoF) that can be brought by FD operation to a wireless network, while the studies in [68–71] investigate the throughput enhancement in a wireless network when FD operation is applied using stochastic geometry analysis. The authors of [72] derive the capacity gain of an FD network from a network level perspective using the *protocol model* [73] to model the interference in an FD network. Enabling FD operation in a wireless network will impose several medium access control (MAC) layer issues such as channel contention, collision, and fairness. To address these concerns many FD MAC protocols have been proposed [74–78]. Most of these analysis model the RSI as a complex Gaussian random variable with zero mean and variance ηp_{tx}, where p_{tx} is the transmission power of the FD device, $\eta\,(0{\leq}\eta{\leq}1)$ denotes the SI cancellation capability of the FD transmitter.

Thus, the power of the residual self-interference (p_{RSI}) is defined as follows:

$$p_{RSI} = \eta p_{tx}. \tag{1.1}$$

The case of $\eta = 0$ corresponds to the perfect SIC while $\eta = 1$ reflects that no SIC technique has been applied. From (1.1), it is clear that RSI is directly related to the transmit power of the FD device. This, in turn, makes FD more suitable for low transmission power network such as the *D2D* network. Thus, to further enhance the SE in wireless network recently researchers suggest integrating FD with other low power networks like the small cell, *D2D*, cognitive radio, and WiFi. In this thesis, we look to analyze the performance of FD operation in a *D2D* based cellular network, thus we provide in the next section, the state-of-the-art works that tackled the FD-D2D network.

1.3 The state-of-the-art FD-D2D works

Latterly, FD operation and *D2D* communication have emerged to be an essential part of the upcoming 5G network. The potential advantages of merging these two technologies have triggered numerous researches which in turn proposed new *D2D* applications and scenarios. From a network topology perspective, the works in FD-D2D can be categorized into: 1) bidirectional FD-D2D topology, 2) FD relay assisted *D2D* communication, and 3) *D2D* enabled FD cellular network.

Fig.1.8(a)-(c) illustrate these topologies and compare each one with its counterpart TDD-based HD system. In particular, the TDD-HD system is used to illustrate the possible end-to-end latency enhancement of the FD operation. In this figure, the dashed red lines denote the interference link, the curved dot-dashed lines represent the SI due to FD operation, and the straight black lines stand for the data links. Moreover, it is worthy to note that in Fig.1.8(a)-(c) we only consider the underlay *D2D* scenario in which the *D2D* users are sharing the uplink (UL) resources of a CU. This is mainly because the UL underlay scheme helps in enhancing the SE of the network and imposes interference on the *BS*, which is more capable in managing the interference comparing to the downlink (DL) underlay scheme. The following subsections describe each topology individually.

1.3.1 D2D enabled FD cellular network

Consider the cellular topology of Fig.1.8(a) which consists of one *BS*, two CUs denoted as CU_1 and CU_2, and two *D2D* users in the proximity of each-other D_1 and D_2. In this scenario, CU_1 has signals to be sent to the *BS* on the UL channel, and *BS* also has another independent info need to be exchanged with CU_2 on the DL bandwidth. In addition, the *D2D* user D_1 wants

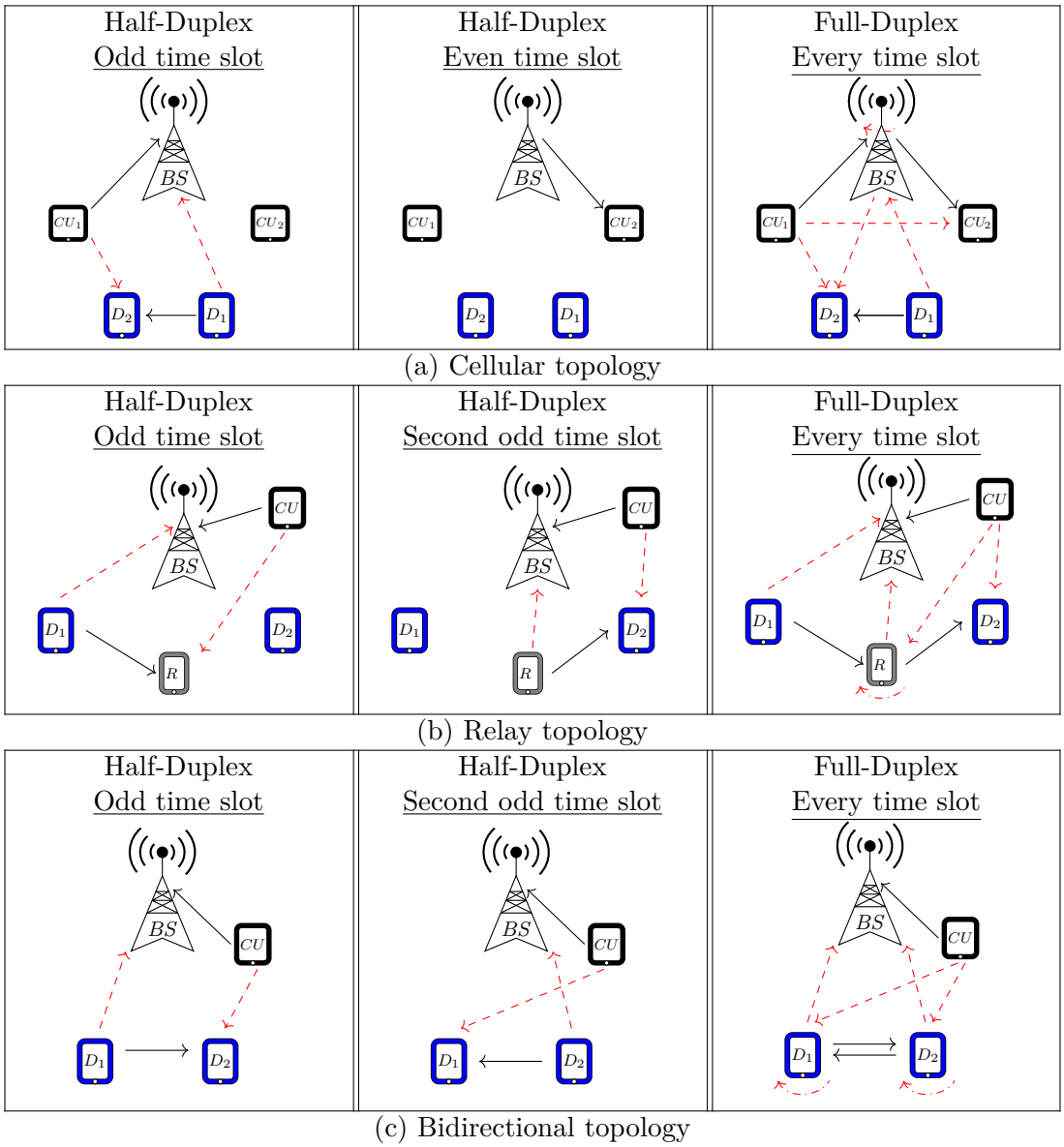

Figure 1.8 – The topology-based classification of the FD-D2D works (the straight black lines and the dashed red lines denotes the direct and interference links respectively).

to take advantage of its proximity with D_2 to send his signal via a direct *D2D* link using the UL resource of CU_1. When HD operation is applied at the *BS*, the UL and DL channels must be orthogonally separated using either TDD or FDD system. However, if *BS* can operate in FD mode, it can support simultaneous transmission and reception over the same UL or DL channel, potentially enhancing the SE at the expense of additional interference. Accordingly, a rigorous interference management technique is required to achieve the possible FD gains of this topology.

The first research which proposes this topology is the work done by Yang et. all in [79] where an optimal channel assignment using a graph coloring-based algorithm was derived assuming a fixed transmission power strategy. Similarly, within a *D2D* underlaying FD cellular network, [80] proposes a two-stage resource allocation algorithm to maximize the network throughput. The first step assigns channels to CUs using a graph coloring-based algorithm, and then a bipartite graph is constructed to select the *D2D* channels. In [81] and with the goal of maximizing the number of the served users in a limited spectrum cell, the authors propose an FD enabled *BS* which can serve both the UL and DL users using one frequency. Moreover, to control the inter-node interference of this scenario, they propose to offload the FD cellular link inducing intense interference to an outband *D2D* link. The work in [82] aims to jointly optimize the CA and PA of a *D2D* enabled FD cellular network. To that end, first, they proposed an interference-limited area based channel assignment algorithm, and then they model the PA as a Stackelberg game in which the *BS* is the leader, and the CUs and *D2D* are the followers. The main momentum behind this topology is the cost and the size factors of the *BS* which make it more capable of achieving a high level of SIC. Nevertheless, in the cellular-based topology, only the *BS* is required to be an FD device, the other communications parties are HD devices. However, based on our previous discussion in Section 1.2.1, we know that RSI is proportionally related to the transmit power. Moreover, all the proposed SIC techniques are only tested and verified in a low-transmit power scenario. Thus, this topology will be more suitable for a small-cell network such as Femto *BS*. Nonetheless, in a small cell network, the users inside the cell are more likely to be close to each other, which makes the interference issue more severe, and consequently limits the achievable FD gains.

1.3.2 FD relay assisted D2D communication

Let us consider the relay topology shown in Fig.1.8(b) in which a relay node R is relaying the transmitted data of a source node D_1 to a destination node D_2 and thus assisting the *D2D* communication between the *D2D* users D_1 and D_2. If the relay node R is operating on HD mode, the *D2D* users D_1 and D_2 need to transmit and receive over orthogonal frequencies (in FDD system) or different time slots (in TDD system). However, when FD operation is applied at the R terminal, D_2 can receive the data sent by D_1 simultaneously and using only one frequency, leading to potentially doubling the SE and decreasing the communication latency.

This scenario was first proposed by Han et.all in [83] in which they suggest an interference suppression mechanism to mitigate the interference from cellular communications to the other *D2D* party. The optimal relay selection problem for a scenario in which multiple FD relays exist with multiple HD-D2D pairs is considered in [84]. The coverage probability for an FD relay assisted *D2D* communication underlaying cellular network was derived in [85]. In the context of social aware clustering, the authors of [86] propose to take advantage of an FD relay

to increase the SE of the clustering process. The works in [87] and [88] derived the outage probability expression of an FD -Relay assisted single and multiple *D2D* links, respectively.

The main idea behind this topology is to extend the range of *D2D* communication by enabling two-hop *D2D* communication through a relay capable CU. Thus, the key point in such topology is to select the optimal relay for the *D2D* pair. Most of the works design a relay selection algorithm aiming at enhancing the network's performance in terms of throughput, power consumption, and network's coverage. However, the battery level of the relay node is ignored during the selection process. Besides, in such topology, it is natural to raise several security concerns. For example, if the selected relay node is an eavesdropper, the data sent over the *D2D* link will be vulnerable to steal.

1.3.3 Bidirectional FD-D2D topology

Consider the bidirectional topology presented in Fig.1.8(c) where two nodes D_1 and D_2 want to directly exchange data signals with each other using the CU's bandwidth. If either node D_1 or node D_2 can only operate in HD mode, then the communication flow between D_1 and D_2 and between D_2 and D_1 must be performed over orthogonal time slots as shown in the left side of Fig.1.8(c) or over orthogonal frequencies. This will reduce the SE, and also it can increase the communication delay. To avoid such problems, FD operation can be applied on both nodes D_1 and D_2, allowing them to exchange signals directly at the same time and on the same frequency.

This topology took the most attraction and triggered plenty of research works that can be classified into bidirectional FD-D2D overlay/underlay cellular network. The works in [89–91] analyze the overlay FD-D2D scenario. Specifically, the work in [89] proposed a simple protocol to improve the rate of a single FD-D2D pair which is allocated a dedicated spectrum. Moreover, in [90] a power allocation scheme is developed to maximize the ergodic bitrate of an FD-D2D pair overlay cellular network. Besides, the authors of [91] aimed to maximize the effective capacity of an FD-D2D network while satisfying the statistical delay-bound QoS requirements. However, allocating a dedicated spectrum for the FD-D2D pairs as in the overlay scenario would lead to low spectrum efficiency and diminish the gain of FD transmission. That is why the focus is more about FD-D2D underlay cellular network [6, 92–120]. Fig.1.9 grouped these works according to their tackled subjects.

The works in [92–94] are among the initial studies that aim to investigate the performance of FD-D2D underlaying cellular network. For instance, the studies in [92, 93] explore the effect of the RSI on the network performance considering a single-cell scenario in which an FD-D2D pair is sharing the UL resources of one CU. Results show that integrating FD with *D2D* can double the SE comparing to the HD network when the power of the RSI is very low. Motivated by this observation, the work in [94] considers UL underlaying scenario in which multiple FD-D2D

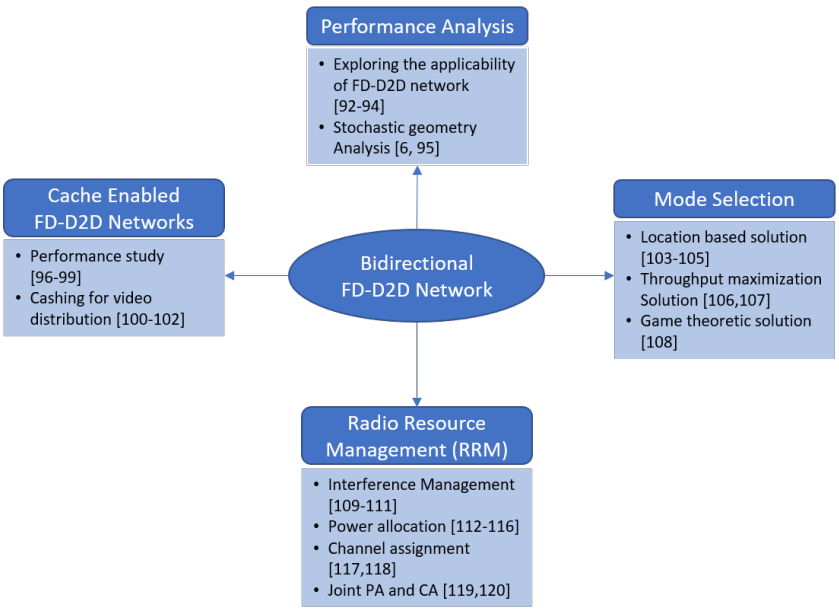

Figure 1.9 – Works classification for bidirectional FD-D2D underlaying cellular network

pairs are sharing the resources of a single CU, and tries to maximize the number of possible FD-D2D links constrained to the amount of interference imposed on the CU. Results show that the number of active FD-D2D pairs is smaller than in the traditional HD-D2D network. This is because the FD mode doubles the number of transmitting devices which in turn increases the interference on the cellular link. Moreover, results show that the mutual interference between the *D2D* pairs has negative impact on the performance of each FD-D2D link. To understand the performance of FD-D2D network in a more real-like scenario, the authors of [6, 95] conduct a multi-cell analysis using the stochastic geometry tool. Simulation results showed that an FD-D2D network has a significant gain over its counterpart HD-D2D especially when the SI is low. However, in their work, only a simple on- off power allocation was used.

The proved possible gains of FD-D2D network encouraged the researchers to exploit the FD-D2D communication inside a cache-enabled network to further improve the network performance and meet the strict 5G requirements. The works in [96–99] conduct several performance studies for such network for general cashing policies, while the researches in [100–102] explore the benefits of FD-D2D communication for cashing and distributing the videos in a cellular network.

The main result of the previous performance studies is that the FD-D2D network may not always outperform the conventional HD-D2D network due to the RSI and the additional interference on the network. Thus, a mode selection step must be studied before starting the transmission. In that direction, several solutions have been proposed as in [103–108]. The authors of [103–105] developed a duplex mode strategy based on the location relationship between the users while the studies in [106, 107] propose to select the duplex mode that yields

to better throughput. The work in [108] derived a game-theoretic-based mode selection strategy considering a fixed transmission power scheme.

To achieve the promising advantages of FD-D2D underlaying cellular network several kinds of research have been conducted in the context of radio resource management (RRM) which include interference management techniques, power allocation schemes, and channel assignment strategies. To limit the co-channel interference between the *D2D* and cellular links, the works in [109–111] proposed various versions of an interference-limited area (ILA) based channel sharing scheme which prevents the transmission of FD-D2D users that are located inside a pre-set guard area. The power control issue was the subject of the works in [112–116]. In [112] a convex optimization problem that maximizes the FD-D2D link rate while satisfying the data rate requirement of the CU was derived. Build on [112], a similar maximization problem has been developed in [113] assuming that both the *D2D* pair and *BS* are FD capable devices. Aiming to maximize the energy efficiency of an FD-D2D link, the authors of [114] proposed an energy-efficient power control algorithm for an FD-D2D network. The research in [115] assumed a dense FD-D2D scenario in which several F-D2D pairs sharing the same CU spectrum and proposed a fairness based power control strategy. A similar scenario was proposed in [116] where a PA strategy was developed to maximize the ergodic *D2D* rate while satisfying the users' requirements.

Assuming a fixed transmit power strategy the studies in [117, 118] addresses the channel assignment problem of an FD-D2D based cellular network. For instance, the authors of [117] assumed a scenario in which single FD-D2D pair coexists with multiple CUs and proposed an outage-probability based CA scheme to select the best CU to reuse its resources and increase the network throughput. Assuming a different scenario in which multiple FD-D2D pairs coexist with multiple CUs, the study in [118] tackled the problem of dynamic channel assignment of an FD-D2D network. Specifically, to deal with the unexpected arrival of *D2D* users, the work in [118] developed a greedy online matching-based algorithm which allows the *BS* to effectively assign the channels for *D2D* users without prior knowledge on future *D2D* arrivals.

The joint power allocation and channel assignment problem of an FD-D2D network when multiple FD-D2D pairs coexist with multiple CUs has been addressed in [119] and [120]. The authors of [119] aimed to maximize the sum-rate of an FD-D2D network by considering both the power allocation and the channel assignment problems. In [120] an energy-efficient resource allocation for FD-D2D based cellular network was provided. For ease of notation, in this thesis, we denote the joint power allocation and channel assignment problem by resource allocation (RA) and we will use it interchangeably.

In this dissertation, we recognize the importance of RRM techniques in improving the performance of a bidirectional FD-D2D based cellular network. In particular, we focus on proper designing PA schemes and RA strategies to realize the promises of integrating FD with a *D2D*

network. By Investigating the related works such as [112–116, 119, 120] we found that the global optimal solutions of PA and RA are not yet found. Specifically, due to the non-convexity feature of the PA and RA problems, the related works only provide a sub-optimal power allocation solution by approximating the original PA problem with a more simpler convex problem. This technique belongs to the sequential convex optimization (SCO) framework and normally it finds the first-order optimal solution of the problem as we will see in the next chapter. Nevertheless, almost all the mentioned works proposed centralized PA and RA algorithms that require the *BS* to know the channel state information (CSI) of the users at each step. Here, [113, 116] proposed two distributed on-off based PA schemes. The authors of [113] aimed at maximizing the *D2D* rate but without considering their QoS requirements. In [116], relying on stochastic geometry, the optimal transmit probability that can maximize the ergodic *D2D* rate was found assuming that the *D2D* users have the same rate requirements. Aiming at filling the gap of this related research works, this dissertation suggests using the monotonic optimization (MO) theory to achieve the optimal PA and RA schemes. Moreover, it proposes to get benefit from the game theory (GT) tools to develop an energy-efficient PA and RA algorithms. In summary, the main goals of this thesis can be summarized as follows:

1. Address the problem of PA/RA of an FD-D2D underlay cellular network with the aim to maximize the *D2D* rate, the total sum-rate, and the energy efficiency of the network.

2. Propose effective optimization algorithms to obtain the global solution by means of a suitable formulation and mathematical tools such as MO. Numerical results will be provided to demonstrate the merits of proposed algorithms in terms of both throughput maximization, energy-efficient performance and complexity.

3. Propose distributed PA algorithm by using GT that can be applied in real network and compare its performance with the derived optimal solution.

The next section provides the thesis skeleton and the adopted paths to achieve these three goals.

1.4 Thesis outline and contribution

As described earlier, the main challenge of an FD-D2D underlaying cellular network is its complex interference medium. This dissertation focuses on how to improve the performance of an FD-D2D based cellular network by means of proper design and coordination of radio resource management techniques. Specifically, we recognize the importance of power allocation and channel assignment to realize the promises of FD-D2D communication. The outline of the thesis, together with the publications supporting the contributions, is as follows.

In Chapter 2 we tackle the power allocation of an FD-D2D network that consists of a single *D2D* pair sharing the bandwidth of a CU. In the first section of the chapter, we look to derive the ergodic performance of the system to have an overview about the different parameters that may affect the network behavior. To that end, we derive the closed-form expression of the ergodic rate, and then we formulate the ergodic rate maximization problem. The formulated problem is proven to be non-convex, thus we propose a sub-optimal solution by assuming an interference-limited system and high signal-to-interference ratio region. The proposed solution directly shows the impact of the users' locations, the SIC capability, the *D2D* distance on the network performance.

In the second section, we switch our focus on the instantaneous power allocation problem which is normally used in real systems. Therein, first, we present the SCO framework that is widely used in literature to solve the non-convex PA problem. After that, we develop a geometric based optimization framework denoted as GALEN which can achieve the global optimal solution of the PA problem. In particular, GALEN takes advantage of the inherent monotonocity feature of the rate function and solve the optimization problem only on the boundary of the feasible set instead of exploring the whole set. In addition, GALEN found that the solution of the problem on the boundary belongs to a set of points whose coordinates are known and directly related to the users' channel gain, receiver noise, and SIC capability. This chapter includes part of the materials in:

- H. Chour, F. Bader, Y. Nasser, and O. Bazzi,"Galen: A Geometric Framework for Global Optimal Power Allocation in a Full-Duplex D2D Network," in Proc. IEEE Wireless Communications and Networking Conf (WCNC2019), Apr. 2019.

- H. Chour, O. Bazzi, F. Bader,and Y. Nasser, "Analytical Framework for Joint Mode Selection and Power Allocation for Full-Duplex D2D Network," in Proc. IEEE Wireless Communications and Networking Conf. (WCNC2019), Apr. 2019.

- H. Chour, Y. Nasser, O. Bazzi,and F. Bader, "Full-duplex or half-duplex D2D Mode Closed Form Expression of the Optimal Power Allocation," in Proc. 25th Int. Conf. Telecommunications (ICT), Jun.2018.

Chapter 3 addresses the joint CA and PA problem of an FD-D2D network with multiple *D2D* pairs coexisting with multiple CUs, which is a non-convex problem. Throughout this dissertation, we called the joint CA and PA problem as resource allocation (RA) problem and we use it interchangeably. After formulating the RA problem, we show that the global optimal solution can be achieved by decoupling the original RA problem into two sub-problems as PA and CA. Next, we solve the PA sub-problem by means of monotonic optimization theory (MO). Precisely, we propose a new polyblock-based algorithm, MARIO, which efficiently converges to the global solution of the PA problem. Then, based on the optimal PA solution, the CA problem reduces to an assignment problem, which can be solved by Khun-Munkers algorithm

(also known as the Hungarian algorithm). The main drawback of the MO-based solution is its high complexity, hence we propose a sub-optimal solution by solving the original RA problem in the reverse order, i.e., first assigning the channel and then allocating the power. The simulation results show the effectiveness of the proposed algorithms and provide important insights on the solution design parameters such as the proximity distance and the self-interference cancellation capability. The content of this chapter is based on:

- H. Chour, E. Jorswieck, F. Bader, Y. Nasser, and O. Bazzi, "Global Optimal Resource Allocation for Efficient FD-D2D Enabled Cellular Network," IEEE Access, Vol. 7, pp. 59690-59707, May 2019.

Chapter 4 aims at providing a distributed PA algorithm for an FD-D2D underlaying cellular network. Towards this end, first, we formulate the PA problem as a non-cooperative game in which each user decides how much power to transmit over its allocated channel to maximize its link's energy efficiency. Next, we show that this game admits a unique Nash equilibrium point which can be obtained through an iterative process. After that, we show that this iterative algorithm can be implemented in a fully distributed manner. Also, we compare our proposed distributed algorithm with the centralized PA algorithm developed in Chapter 3 and simulation results verify the importance of the proposed distributed algorithm. The content of this chapter is based on:

- H. Chour, Y. Nasser, F.Bader, and O.Bazzi, "Game-Theoretic Based Power Allocation for a Full-Duplex D2D Network" in Proc. IEEE International Workshop on Computer Aided Modeling and Design of Communication Links and Networks (CAMAD2019), Sept. 2019.

Finally, Chapter 5 concludes the thesis and summarizes the main contributions. It also points out the thesis limitations and provides a discussion about the perspective directions for future works.

Besides the aforementioned chapters, Appendix A and Appendix B detail some mathematical derivations related to Chapter 1, Appendix C describes the Hungarian algorithm which is used in Chapter 3, and Appendix D lists the publications the author has contributed to during his PhD.

Before terminating this chapter, and for ease following the manuscript, we present in Table 1.2 the tackled challenges of an FD-D2D network in this thesis, i.e., the PA and RA problems, with the adopted solutions in literature and our proposed solutions for these challenges. Moreover, we show in Table 1.2 the main issues of each solution as well as the location or references of each solution. The blue texts in Table 1.2 indicate our contributions in this field. The next chapter tackles the PA issue aiming at developing an efficient global optimal PA strategy for an FD-D2D based UL cellular network.

Table 1.2 – Tackled challenges, solutions, and issues of a bidirectional FD-D2D based cellular network.

Bidirectional FD-D2D communication underlaying UL cellular network						
Challenges	Solutions					
	Reference	Used techniques	Optimal	Centralized	Objective	Complexity
Power Allocation	[112,113]	SCO	✗	✓	Maximize D2D sum-rate	Medium
	[114]	SCO	✗	✓	Maximize GEE	Medium
	[116]	SCO	✗	✓	Maximize D2D sum-rate	Medium
	Chapter 2	The geometry structure of the feasible set	✓	✓	Maximize D2D sum-rate	Low
	Chapter 3	MO	✓	✓	Maximize WSR or GEE	High
	Chapter 4	GT	✗	✗	Maximize EE	Medium
	[113, Section II.B]	On-off-based method	✗	✗	Maximize D2D sum-rate	Low
	[116, Section IV]	On-off-based method	✗	✗	Maximize D2D ergodic rate	Low
Resource Allocation	[119]	SCO + Hungarian algorithm	✗	✓	Maximize WSR	Medium
	[120]	SCO + Hungarian algorithm	✗	✓	Maximize EE	Medium
	Chapter 3	MO + Hungarian algorithm	✓	✓	Maximize WSR or GEE	High
	Chapter 3	Heuristic solution	✗	✓	Maximize WSR or GEE	Low

Chapter 2

Power Allocation for an FD-D2D based cellular network

Contents

The previous chapter provided the general idea of the FD-D2D network and pointed out the main challenges that may arise when integrating the FD operation with *D2D* such as the self-interference and the complicated interference environment generated by the FD operation. This chapter aims to control such complex interference ambiance by controlling the transmit power of the involved users and characterize the behavior of an FD-D2D underlaying cellular network.

Towards this end, first, we provide an ergodic sum-rate analysis for the FD-D2D network in which we derive the closed-form expression of the *D2D* ergodic rate and we address the ergodic rate maximization problem. We further propose a closed-form expression PA strategy for both *D2D* and cellular users. The simulation results show the accuracy of the derived power allocation scheme and provide important insights into the separation distance between the *D2D* users and the interfering cellular user. In addition, the results provide important conditions to switch between FD and HD modes. The more related work to this part is the study in [121]. However, in [121] the power allocation scheme was not considered. Moreover, in their analysis, only a symmetric scenario, in which the *D2D* users have the same distance to the base station from one side and the cellular user has equal distance to the *D2D* users from the other side, was assumed therein. In our analysis a mathematical framework of the FD-D2D communication is developed, and advanced analysis of the impact of the *CU* location on the optimal FD-D2D rate is provided. Precisely, the derived framework covers both the symmetric and the asymmetric scenarios of the *D2D* users. Throughout this chapter, the symmetric case means that the *D2D* users are receiving the same interference power from the *CU* and they are introducing equal average interference power at the *BS*, i.e., the *CU* has equal distance to the *D2D* users and the *D2D* users have equal distance to the base station. The asymmetric case reflects the situation where one of the *D2D* users introduces more interference on the *BS* than the other, or one of the *D2D* users is receiving more interference from the *CU* than the other or both.

In a real network scenario, the power allocation needs to be applied in a short time period to mitigate the interference. Thus, later on in this chapter, we study the instantaneous rate maximization problem aiming at providing efficient PA algorithm that can be applied in a real FD-D2D scenario. In this direction, we begin our analysis by providing the most used PA technique, referred to as the SCO tool, in solving the PA problem of an FD-D2D network. Since SCO can only obtain a sub-optimal solution of the problem, we propose a novel geometric based optimization framework, named as GALEN, which can achieve the optimal solution. The proposed GALEN framework has a much lower complexity comparing to the SCO method, because it computes the closed-form expression of the optimal solution.

The remainder of this chapter is organized as follows. Section 2.1 describes the system model. Section 2.2 and Section 2.2.2 provides the ergodic rate and the instantaneous rate

analysis respectively. In Section 2.4 we discuss the simulation results, and the conclusion is drawn in Section 2.5.

2.1 System model

We consider a simple single cell FD-D2D enabled cellular network which consists of one *BS*, and one *D2D* pair reusing the uplink channel of one CU. The *D2D* pair may operate in both FD and HD mode while the *CU* in assumed to be operated only in HD mode. The coexistence between the *D2D* users and CUs creates cross interference between them. Fig. 2.1(a) and Fig. 2.1(b) illustrate the interference model for the FD-D2D and HD-D2D cases respectively. In this figures, we denote the channel gains between the different users as follows:

- $g_{c,b}$ denotes the direct channel gain between *CU* and *BS*.
- g_d stands for the direct channel gain between the *D2D* users. Here, the *D2D* channel is assumed reciprocal, since both D_1 and D_2 are using the same UL channel and they are close to each other.
- $h_{d1,b}$ and $h_{d2,b}$ respectively stand for the interference channel gains from D_1 to *BS* and from D_2 to *BS*.
- $h_{c,d1}$ and $h_{c,d2}$ denote the interference channel gains from *CU* to D_1 and D_2 respectively.
- RSI is the residual self interference due to the imperfect SI cancellation at the FD devices.

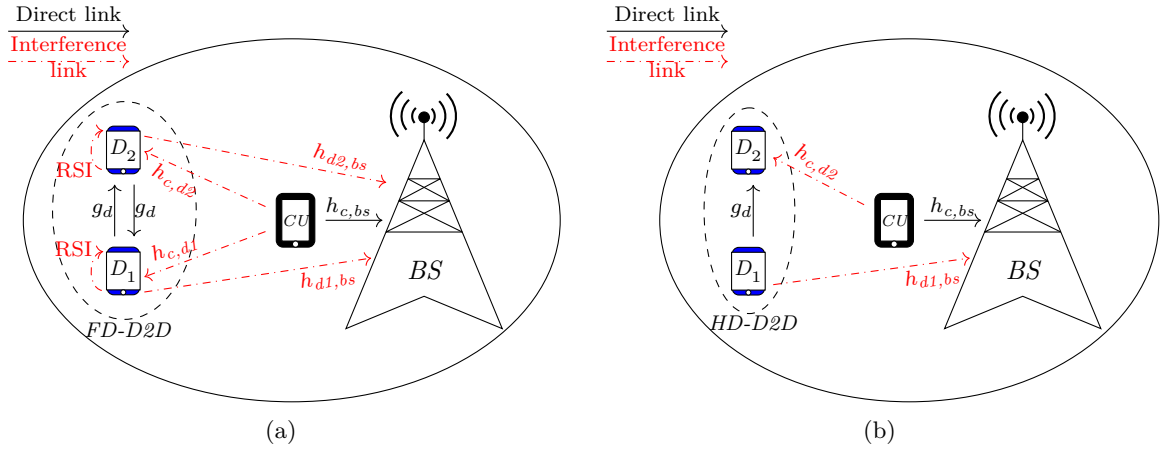

Figure 2.1 – A D2D pair shares the UL resources of one cellular user and operating on (a) the FD mode and (b) HD mode.

As we already explained in Chapter 1 Section 2, the power of the residual self-interference (P_{RSI}) is defined as follows:

$$p_{RSI} = \eta p_{tx} \tag{2.1}$$

where $\eta\,(0{\leq}\eta{\leq}1)$ is the SI mitigation coefficient which represents the effect of the advanced SIC techniques [90] [112], and p_{tx} is the local transmit power. The case of $\eta = 0$ corresponds to the perfect SIC while $\eta = 1$ reflects that no SIC technique has been applied.

Besides we assume that all involved links experience independent fast-fading due to multi-path propagation and distance-based path-loss attenuation. Thus, both direct and interference channel gains between a transmitter i and a receiver j respectively can be expressed as:

$$g_{i,j} = l_{i,j}\zeta_{i,j}, \quad h_{i,j} = l_{i,j}\zeta_{i,j} \quad i \in \{c, d1, d2\},\ j \in \{b, d2, d1\}$$

where $l_{i,j}$ denotes the path-loss attenuation and $\zeta_{i,j}$ represents the fast-fading gain. Furthermore, the path-loss attenuation can be expressed by $l_{i,j} = d_{i,j}^{-\alpha}$ where $d_{i,j}$ is the distance between the nodes i and j and α stands for the path-loss exponent.

2.1.1 Full duplex D2D link

In the FD-D2D communication mode, both D_1 and D_2 reuse the spectrum of CU to communicate with each other. Denote by σ_N^2 the power of additive white Gaussian noise (AWGN) and let p_c be the transmit power of the CU, the received signal-to-interference-plus-noise-ratio (SINR) at BS, D_1 and D_2 when $D2D$ shares the spectrum of CU can be respectively expressed as

$$\Gamma_{bs} = \frac{p_c\, g_{c,bs}}{p_{d1}\, h_{d1,bs} + p_{d2}\, h_{d2,bs} + \sigma_N^2} \tag{2.2}$$

$$\Gamma_{\mathrm{FD},d1} = \frac{p_{d2}\, g_d}{p_c\, h_{c,d1} + \eta p_{d1} + \sigma_N^2} \tag{2.3}$$

$$\Gamma_{\mathrm{FD},d2} = \frac{p_{d1}\, g_d}{p_c\, h_{c,d2} + \eta p_{d2} + \sigma_N^2} \tag{2.4}$$

Applying Shannon theorem, the normalized FD-D2D rate measured in $(bit/sec/Hz)$ is defined as the summation of the normalized D1's and D2's rates and it is given by :

$$R_{\mathrm{FD}} = \underbrace{\log_2(1 + \Gamma_{\mathrm{FD},d1})}_{R_{\mathrm{FD},D1}} + \underbrace{\log_2(1 + \Gamma_{\mathrm{FD},d2})}_{R_{\mathrm{FD},D2}} \tag{2.5}$$

where $R_{\mathrm{FD},D1}$ and $R_{\mathrm{FD},D2}$ are respectively the normalized D1's and D2's rates.

In the same manner, the ergodic FD-D2D ($\mathcal{R}_{FD}$) is defined as the summation of D1's and D2's ergodic rates, $\mathcal{R}_{D1}$ and $\mathcal{R}_{D2}$ in (2.6), and it is given by:

$$\mathcal{R}_{FD} = \mathbb{E}[R_{FD}] = \underbrace{\mathbb{E}_{\Gamma_{\mathrm{FD},d1}}[\log_2(1 + \Gamma_{\mathrm{FD},d1})]}_{\mathcal{R}_{\mathrm{FD},D1}} + \underbrace{\mathbb{E}_{\Gamma_{\mathrm{FD},d2}}[\log_2(1 + \Gamma_{\mathrm{FD},d2})]}_{\mathcal{R}_{\mathrm{FD},D2}} \tag{2.6}$$

where $\mathbb{E}(.)$ denotes the expectation operation.

2.1.2 Half duplex D2D link

For fair comparison with the FD mode, we assume that D_1 and D_2 are operating on two equally orthogonal portions of the *CU* bandwidth B during the transmission in HD mode. Thus, the received SINRs at *BS* from each couple remains the same as in the FD mode, i.e., (2.2). However, and since in HD mode the RSI no longer exists, the received SINRs at D_1 and D_2 when *D2D* is operating in HD change to the follows:

$$\Gamma_{\mathrm{HD},d1} = \frac{p_{d2}\, g_d}{p_c\, h_{c,d1} + \sigma_N^2} \tag{2.7}$$

$$\Gamma_{\mathrm{HD},d2} = \frac{p_{d1}\, g_d}{p_c\, h_{c,d2} + \sigma_N^2} \tag{2.8}$$

Again by using Shannon theorem, the normalized HD-D2D link rate of *D2D* measured in $bit/sec/Hz$ is given by

$$R_{HD}=\frac{1}{2}\log_2(1+\Gamma_{\mathrm{HD},d1}) + \frac{1}{2}\log_2(1+\Gamma_{\mathrm{HD},d2}) \tag{2.9}$$

The ergodic HD-D2D rate is defined as:

$$\mathcal{R}_{HD} = \mathbb{E}[R_{HD}] = \underbrace{\mathbb{E}_{\Gamma_{\mathrm{HD},d1}}[\log_2(1+\Gamma_{\mathrm{HD},d1})]}_{\mathcal{R}_{\mathrm{HD},D1}} + \underbrace{\mathbb{E}_{\Gamma_{\mathrm{HD},d2}}[\log_2(1+\Gamma_{\mathrm{HD},d2})]}_{\mathcal{R}_{\mathrm{HD},D2}} \tag{2.10}$$

To have a good understanding about the FD-D2D performance we provide in the next section an ergodic analysis about the FD-D2D rate. After that, we derive several instantaneous PA algorithms that can be applied in real scenarios.

2.2 Ergodic rate analysis

The goal of this section is to provide an ergodic rate analysis for an FD-D2D network to help in discovering the performance of this network in real scenario when RSI exist. Thus we first start by deriving the closed form expression of the ergodic rate $\mathcal{R}_{FD}$ under the assumption that the network links are expressing Rayleigh fading. From (2.6), in order to derive the FD ergodic capacity, the probability density function (PDF) of the *D2D* SINRs must be calculated. The following Lemma provide such PDFs.

Lemma 2.1. *The distribution of D1' SINR ($f_{\Gamma_{d_1}}$) and D2' SINR ($f_{\Gamma_{d_2}}$) are given by:*

$$f_{\Gamma_{d_i}}(s) = \frac{a_i b_i + c_i a_i + s b_i c_i}{(b_i s + a_i)^2} \quad e^{(-s\, c_i/a_i)}, \quad i \in \{1,2\} \tag{2.11}$$

where

$$\begin{aligned} a_1 &= p_{d2}\, l_d, \quad b_1 = p_c\, l_{c,d1}, \quad c_1 = \eta\, p_{d1} + \sigma_N^2, \\ a_2 &= p_{d1}\, l_d, \quad b_2 = p_c\, l_{c,d2}, \quad c_2 = \eta\, p_{d2} + \sigma_N^2. \end{aligned} \tag{2.12}$$

Proof: Observe that Γ_{d1} and Γ_{d2} share the same function structure. Thus, in the following we will only derive the PDF of Γ_{d1}. First, let us define the two following random variables: $X = a_1\, \zeta_d$ and $Y = b_1\, \zeta_{c,d1}$ and recall that the channel power gains ζ_{ij} are following the exponential distribution with unit mean. Thus, the PDF of X and Y are $f_X(x) = \frac{\exp(-x/a_1)}{a_1}$ and $f_Y(y) = \frac{\exp(-y/b_1)}{b_1}$ respectively . Next, we apply the change of variable technique as follows:

$$\begin{cases} S = \dfrac{X}{Y + c} \\ T = Y \end{cases} \iff \begin{cases} X = ST + Sc \\ Y = T \end{cases} \tag{2.13}$$

Then, the joint PDF for the couple (S, T) can be written as:

$$f_{ST}(s,t) = f_{XY}(X(s,t), y(s,t))|J(s,t)| \tag{2.14}$$

where, $|J(s,t)| \triangleq \begin{vmatrix} \frac{\partial X}{\partial S} & \frac{\partial X}{\partial T} \\ \frac{\partial Y}{\partial S} & \frac{\partial Y}{\partial T} \end{vmatrix}$ is the determinant of the Jacobian transformation matrix. The independence between the users' channels implies that the random variables X and Y are independent of each other. Thus, (2.14) will reduce to the follow:

$$\begin{aligned} f_{ST}(s,t) &= (t + c_1) f_X(st + sc_1) f_Y(t) \\ &= \frac{\exp(-sc_1/a_1)}{a_1 b_1} \left[(t + c_1) \exp\left(-t(\frac{s}{a_1} + \frac{1}{b_1}) \right) \right] \end{aligned} \tag{2.15}$$

Now, to obtain the PDF of γ_{d1} we integrate (2.15) w.r.t to t as follows:

$$\begin{aligned} f_{\Gamma_{d1}}(s) &= \frac{\exp(-sc_1/a_1)}{a_1 b_1} \left[\int_0^\infty (t + c_1) \exp\left(-t(\frac{s}{a_1} + \frac{1}{b_1}) \right) dt \right] \\ &= \frac{a_1 b_1 + c_1 a_1 + s b_1 c_1}{(b_1 s + a_1)^2} \exp(-sc_1/a_1) \end{aligned} \tag{2.16}$$

Similar procedure can be done to obtain the PDF of γ_{d2} and complete the proof. ■

Using Lemma 2.1, the closed form expression of the FD-D2D ergodic rate can be derived as shown in Theorem 1.

Theorem 2.1. *The full-duplex D2D ergodic rate $\mathcal{R}_{FD}$ and the half-duplex ergodic rate $\mathcal{R}_{HD}$ are given by:*

$$\mathcal{R}_{FD} = \underbrace{\frac{E_1\left(\frac{\eta p_{d1}+\sigma_N^2}{p_c l_{c,d_1}}\right) e^{\frac{\eta p_{d1}+\sigma_N^2}{p_c l_{c,d1}}} - E_1\left(\frac{\eta p_{d1}+\sigma_N^2}{p_{d2} l_d}\right) e^{\frac{\eta p_{d1}+\sigma_N^2}{p_{d2} l_d}}}{\frac{p_c l_{c,d_1}}{p_{d2} l_d} - 1}}_{\mathcal{R}_{FD,D1}} + \underbrace{\frac{E_1\left(\frac{\eta p_{d2}+\sigma_N^2}{p_c l_{c,d2}}\right) e^{\frac{\eta p_{d2}+\sigma_N^2}{p_c l_{c,d2}}} - E_1\left(\frac{\eta p_{d2}+\sigma_N^2}{p_{d1} l_d}\right) e^{\frac{\eta p_{d2}+\sigma_N^2}{p_{d1} l_d}}}{\frac{p_c l_{c,d_2}}{p_{d1} l_d} - 1}}_{\mathcal{R}_{FD,D2}} \tag{2.17}$$

$$\mathcal{R}_{HD} = \frac{1}{2}\underbrace{\frac{E_1\left(\frac{\sigma_N^2}{p_c l_{c,d_1}}\right) e^{\frac{\sigma_N^2}{p_c l_{c,d1}}} - E_1\left(\frac{\sigma_N^2}{p_{d2} l_d}\right) e^{\frac{\sigma_N^2}{p_{d2} l_d}}}{\frac{p_c l_{c,d_1}}{p_{d2} l_d} - 1}}_{\mathcal{R}_{D1}^{HD}} + \frac{1}{2}\underbrace{\frac{E_1\left(\frac{\sigma_N^2}{p_c l_{c,d2}}\right) e^{\frac{\sigma_N^2}{p_c l_{c,d2}}} - E_1\left(\frac{\sigma_N^2}{p_{d1} l_d}\right) e^{\frac{\sigma_N^2}{p_{d1} l_d}}}{\frac{p_c l_{c,d_2}}{p_{d1} l_d} - 1}}_{\mathcal{R}_{D2}^{HD}} \tag{2.18}$$

with $E_1(z) = \int_z^\infty \frac{e^{-t}}{t} dt$ being the first order exponential integral.

Proof: First note that both $\mathcal{R}_{FD}$ and $\mathcal{R}_{HD}$ share the same function structure. Thus, in the following we focus only on deriving the closed form expression of $\mathcal{R}_{FD}$. We start our proof by computing $R_{FD,D1}$ and $R_{FD,D2}$ through applying the D1 and D2 SINRs distributions derived in Lemma 2.1 in (2.6) and integrating the result over the SINR as follows:

$$\begin{aligned} \mathcal{R}_{FD,Di} &= \mathbb{E}_{\Gamma_{FD,di}}[\log_2(1+\Gamma_{FD,di})], \quad i \in \{1,2\} \\ &= \int_0^\infty \log_2(1+s) \frac{a_i b_i + c_i a_i + s b_i c_i}{(b_i s + a_i)^2} \exp\left(-s c_i/a_i\right) \quad ds \\ &= \frac{E_1(c_i/b_i)e^{c_i/b_i} - E_1(c_i/a_i)e^{c_i/a_i}}{b_i/a_i - 1}. \end{aligned} \tag{2.19}$$

Next, to complete the proof, it is sufficient to substitute a_i, b_i, and c_i with $i \in \{1,2\}$ as defined in (2.12) and sum $R_{FD,D1}$ and $R_{FD,D2}$. ∎

Note that the function

$$h(x) \triangleq \exp\left(\frac{1}{x}\right) E_1\left(\frac{1}{x}\right) \tag{2.20}$$

is a monotonically increasing function with x [122]. Accordingly, for a positive c_i and $a_i > b_i$ (a_i and b_i are arbitrarily positive numbers)

$$\exp\left(\frac{c_i}{a_i}\right) E_1\left(\frac{c_i}{a_i}\right) > \exp\left(\frac{c_i}{b_i}\right) E_1\left(\frac{c_i}{b_i}\right) \tag{2.21}$$

then we have

$$\frac{b_i}{a_i - b_i}\left[e^{\frac{c_i}{a_i}} E_1\left(\frac{c_i}{a_i}\right) - e^{\frac{c_i}{b_i}} E_1\left(\frac{c_i}{b_i}\right)\right] > 0 \tag{2.22}$$

The same result can be obtained for $a<b$. Thus, R_{D1} and R_{D2} are always positive which in turn verifies that the ergodic FD rate derived in Theorem 1 is always positive.

2.2.1 Problem formulation

The aim of this section is to maximize the FD-D2D capacity while satisfying the QoS requirement of the interferer *CU* by finding the optimal power allocation scheme. Thus, the maximization problem denoted by ***P1*** can be formulated as,

$$\begin{aligned}
\textbf{\textit{P1}}: \max_{\mathbf{p}} \quad & \mathcal{R}_{FD}(\mathbf{p}) = \mathcal{R}_{D1} + \mathcal{R}_{D2} && (2.23)\\
\text{s.t.} \quad & \mathbb{E}_{g_{c,bs},h_{d1,bs},h_{d2,bs}}[\Gamma_{bs}] \geq \overline{\gamma}_{\min} && (2.23a)\\
& 0 < p_c \leq P^{c}_{\max}, \quad 0 \leq p_{d1} \leq P^{d1}_{\max}, \quad 0 \leq p_{d2} \leq P^{d2}_{\max} && (2.24)
\end{aligned}$$

where, $\mathbf{p} = [p_{d1}, p_{d2}, p_c]$ is the power variable vector, $\mathbb{E}[\Gamma_{bs}]$ is the expected CU's SINR at the *BS*, and $\overline{\gamma}_{\min}$ denotes the average minimum CU's SINR to maintain the data rate requirement of the CU. The powers $P^{d1}_{\max}, P^{d2}_{\max}$, $P^{c}_{\max}$ represent the maximum power of D_1, D_2, and *CU* respectively. The utility function in (2.23) is the FD-D2D capacity presented in (2.17), while the constraint in (2.24) keeps the CU's SINR at a certain level and thus it reflects the QoS of the CU. Constraint (2.24) ensures that none of the users is violating the maximum power limit. To obtain the optimal power allocation scheme, it is highly desirable that ***P1*** is a concave optimization problem. However, this is not the case here because R_{FD} is a summation of two non-linear fractional functions and thus it is non-convex function. Moreover, $\mathbb{E}[\Gamma_{bs}]$ is also a non-concave function. To have a suitable solution, we assume an interference-limited scenario, and we relax ***P1*** to the following:

$$\begin{aligned}
\textbf{\textit{P2}}: \max_{x,y} \quad & \overline{R_{FD}}(x,y) = \overline{R_{D1}} + \overline{R_{D2}} && (2.25)\\
\text{s.t.} \quad & x\, l_{d1,bs} + y\, l_{d2,bs} \leq l_{c,bs}\overline{\gamma}_{\min} && (2.25a)\\
& 0 \leq x \leq M_x \triangleq \frac{l_{c,bs}\overline{\gamma}_{\min}}{l_{d1,bs}}, \quad 0 \leq x \leq M_y \triangleq \frac{l_{c,bs}\overline{\gamma}_{\min}}{l_{d2,bs}}, && (2.26)
\end{aligned}$$

where $x = \frac{p_{d_1}}{p_c}, y = \frac{p_{d_2}}{p_c}$ are the power ratio variables. M_x and M_y are defined as the maximum power ratio constraints and they are deduced from the relaxed QoS constraint in (2.25a). The

rates $\overline{\mathcal{R}_{FD}}$, $\overline{\mathcal{R}_{D1}}$, and $\overline{\mathcal{R}_{D2}}$ are respectively the upper bounds of $\mathcal{R}_{FD}$, $\mathcal{R}_{FD,D1}$, and $\mathcal{R}_{FD,D2}$ when neglecting the effect of σ_N^2 and they are given by:

$$\overline{\mathcal{R}_{FD}} = \underbrace{\frac{E_1\left(\frac{\eta\, x}{l_{c,d_1}}\right) e^{\frac{\eta\, x}{l_{c,d_1}}} - E_1\left(\frac{\eta\, x}{l_d\, y}\right) e^{\frac{\eta\, x}{l_d\, y}}}{\frac{l_{c,d_1}}{l_d\, y} - 1}}_{\overline{\mathcal{R}_{FD,D1}}} + \underbrace{\frac{E_1\left(\frac{\eta\, y}{l_{c,d_2}}\right) e^{\frac{\eta\, y}{l_{c,d_2}}} - E_1\left(\frac{\eta\, y}{l_d\, x}\right) e^{\frac{\eta\, y}{l_d\, x}}}{\frac{l_{c,d_2}}{l_d\, x} - 1}}_{\overline{\mathcal{R}_{FD,D2}}} \tag{2.27}$$

The QoS constraint in 2.25a was obtained by computing the first order Taylor expansion of $\mathbb{E}[\Gamma_{bs}]$ as showing in 2.28 assuming an interference limited scenario.

$$\mathbb{E}[\Gamma_{bs}] \overset{(i)}{\approx} \frac{\mathbb{E}[p_c g_{c,bs}]}{\mathbb{E}[p_{d1} h_{d1,bs} + p_{d2} h_{d2,bs}]} = \frac{p_c l_{c,bs}}{p_{d1} l_{d1,bs} + p_{d2} l_{d2,bs}}. \tag{2.28}$$

The proof of the (i) step in (2.28) is provided in Appendix A. This approximation makes the QoS constraint a linear function. However, The upper bound $\overline{\mathcal{R}_{FD}}$ is still non-concave function because it is a summation of two non-linear fractional functions as the original $\mathcal{R}_{FD}$, and thus the **P2** is still non-concave problem. To overcome this issue, $\overline{\mathcal{R}_{FD}}$ is relaxed to a concave function as shown in the next subsection.

Problem relaxation

From (2.27), $\overline{\mathcal{R}_{FD}}$ is defined if $y \neq \frac{l_{c,d_1}}{l_d}$ and $x \neq \frac{l_{c,d_2}}{l_d}$. Accordingly, the FD rate is defined over four regions $\mathcal{R}_1 = \{y < \frac{l_{c,d_1}}{l_d}, x > \frac{l_{c,d_2}}{l_d}\}$, $\mathcal{R}_2 = \{y > \frac{l_{c,d_1}}{l_d}, x < \frac{l_{c,d_2}}{l_d}\}$, $\mathcal{R}_3 = \{y < \frac{l_{c,d_1}}{l_d}, x < \frac{l_{c,d_2}}{l_d}\}$ and $\mathcal{R}_4 = \{y > \frac{l_{c,d_1}}{l_d}, x > \frac{l_{c,d_2}}{l_d}\}$. However, the main FD gain can only be achievable in $\mathcal{R}_4$ as shown in Appendix B. Otherwise, the FD gain will be less than $1bit/s/Hz$. Intuitively, the FD gain is considerable in $\mathcal{R}_4$ where the average power of the useful signal is greater than the average interference power.

To further reduce the problem complexity, we consider a sub-region of $\mathcal{R}_4$ in which the average interference power is much lower than the average received power, i.e., $y >> l_{c,d_1}/l_d$ and $x >> l_{c,d_2}/l_d$. Moreover, we use the properties of $E_1(z)$ given in [123], to approximate the function $E_1(z)\exp(z)$ by $\frac{2}{3}\ln(1+\frac{3}{2}\frac{1}{z})$, and rewrite $\overline{\mathcal{R}_{FD}}$ as follows:

$$\overline{\mathcal{R}_{FD}} \approx \underbrace{\frac{2}{3}\ln\left(1+\frac{3}{2}\frac{l_d\, y}{\eta\, x}\right)}_{I_1} - \underbrace{\frac{2}{3}\ln\left(1+\frac{3}{2}\frac{l_{c,d_1}}{\eta\, x}\right)}_{I_2} + \underbrace{\frac{2}{3}\ln\left(1+\frac{3}{2}\frac{l_d\, x}{\eta\, y}\right)}_{I_3} - \underbrace{\frac{2}{3}\ln\left(1+\frac{3}{2}\frac{l_{c,d_2}}{\eta\, y}\right)}_{I_4} \tag{2.29}$$

Now, by investigating **P2**, it is easy to see that the maximum *D2D* rate occurs when the interference power of the *D2D* is at the maximum level, i.e. the equality case in (2.25a). As a

result, the problem shrinks down to study the concavity of the following equation.

$$\overline{R_{FD}} \approx \underbrace{\frac{2}{3}\ln\left(1+\frac{3}{2}\frac{l_d\left(l_{c,bs}\overline{\gamma}_{\min}-l_{d1,bs}x\right)}{\eta\, l_{d2,bs}\, x}\right)}_{I_1} - \underbrace{\frac{2}{3}\ln\left(1+\frac{3}{2}\frac{l_{c,d_1}}{\eta\, x}\right)}_{I_2} + \underbrace{\frac{2}{3}\ln\left(1+\frac{3}{2}\frac{l_d l_{d2,bs}\, x}{\eta\left(l_{c,bs}\overline{\gamma}_{\min}-l_{d1,bs}x\right)}\right)}_{I_3} - \underbrace{\frac{2}{3}\ln\left(1+\frac{3}{2}\frac{l_{c,d_2} l_{d2,bs}}{\eta\left(l_{c,bs}\overline{\gamma}_{\min}-l_{d1,bs}x\right)}\right)}_{I_4} \tag{2.30}$$

The concavity of the above approximation is established in the following Lemma.

Lemma 2.2. *The approximated function of* $\overline{R_{FD}}$ *in* (2.30) *is concave when the power ratio* x *is non-less than a minimum value* $x_{\min}$ *given by:*

$$x \geq x_{\min} \triangleq \max\left(\frac{l_{c,bs}\,\eta + l_{c,d2}\, l_{d2,bs}}{\eta\, l_{d1,bs}}, \frac{l_{c,bs}\ \left(2\,\eta\, l_{d1,bs} - l_d\, l_{d2,bs}\right)}{2 l_{d1,bs}\ \left(\eta\, l_{d1,bs} - l_d\, l_{d2,bs}\right)}\right) \tag{2.31}$$

Proof: From [124], the summation of convex functions is a convex function. Hence, analyzing the convexity of (2.30) is equivalent to analyzing the convexity of I_1, I_2, I_3 and I_4. To that end, we show in the following the second derivatives of I_1, I_2, I_3 and I_4 w.r.t. x.

$$I_1''(x) = \frac{\left(-2\,x\, l_{d1,bs}\, l_d + l_{c,bs}\, l_d l_d + 2\,x\,\eta\, l_{d2,bs}\right) l_{c,bs}\, l_d}{\left(\left(-x l_{d1,bs} + l_{c,bs}\right) l_d + \eta\, x l_{d2,bs}\right)^2 x^2} \tag{2.32}$$

$$I_2''(x) = \frac{2\, l_{c,d1}\left(\eta\, x + l_{c,d1}\right)}{x^2\left(\eta\, x + 2 l_{c,d1}\right)^2} \tag{2.32a}$$

$$I_3''(x) = -2\,\frac{l_{d2,bs}\, l_{c,bs}\, l_d\left(\eta\, x {l_{d1,bs}}^2 - \left(x l_d\, l_{d2,bs} + l_{c,bs}\,\eta\right) l_{d1,bs} + \frac{1}{2}\, l_d\, l_{d2,bs}\, l_{c,bs}\right)}{\left(\eta\, l_{d1,bs}\, x - x l_d\, l_{d2,bs} - l_{c,bs}\,\eta\right)^2 \left(x l_{d1,bs} - l_{c,bs}\right)^2} \tag{2.32b}$$

$$I_4''(x) = -2\,\frac{l_{d2,bs}\ \left(\eta\, l_{d1,bs}\, x - l_{c,bs}\,\eta - \ l_{c,d2}\, l_{d2,bs}\right) l_{c,d2}\, {l_{d1,bs}}^2}{\left(\eta\, l_{d1,bs}\, x - l_{c,bs}\,\eta - 2 l_{c,d2}\, l_{d2,bs}\right)^2 \left(x l_{d1,bs} - l_{c,bs}\right)^2} \tag{2.32c}$$

Now, solving the above derivatives w.r.t. x leads to the concavity condition given in (2.31). ■

Observe that the value of $x_{\min}$ is affected by the SIC capability of the *D2D* devices, and the positions of the users which in turn provide some insights about the different parameters that may affect the performance of an FD-D2D network.

Now, under this assumptions and relaxation, the solution of (2.30) can be easily found by solving its first derivative. However, to propose a general solution and understand the impact of the users position on the FD-D2D rate, we consider two users setup scenarios for which we solved (2.30). The first is denoted as symmetric scenario, and it represents the case where the *D2D* users have equal distance from the *BS* (i.e, $l_{d_1,bs} = l_{d_2,bs}$) and the *CU* has equal distance from the *D2D* users (i.e, $l_{c,d_1} = l_{c,d_2}$) (refer to Fig. 2.2(a)). The second is called the asymmetric

scenario and it covers all the remaining possible users locations (see Fig. 2.2(b)). The next section will find the optimal solution for these two scenarios assuming Lemma 2.2 is satisfied. After that, and based on the solution of the symmetric and asymmetric scenario, we propose a closed-form PA strategy for the general case where Lemma 2.2 is not satisfied and the $\mathcal{R}_4$ conditions are not fulfilled.

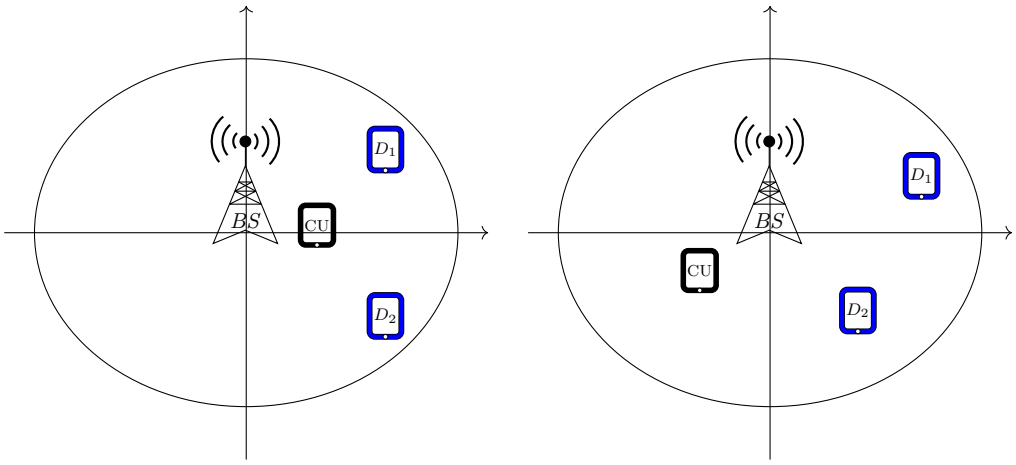

Figure 2.2 – Illustration about the (a) Symmetric scenario where $d_{d1,bs} = d_{d2,bs}$ & $d_{c,d1} = d_{c,d2}$ and (b) the asymmetric scenario in which $d_{d1,bs} \neq d_{d2,bs}$ or $d_{c,d1} \neq d_{c,d2}$.

2.2.2 Optimal power ratio allocation

In this section we first provide the solution of (2.30) for both the symmetric and asymmetric setups assuming that Lemma 2.2 is holding true. After that, and based on the solution of these two scenarios, we propose a general solution when Lemma 2.2 is not satisfied.

Power allocation in the symmetric case

Denote by $\overline{x}^{\star}_{sym}$ the optimal value of (2.30) in the symmetric scenario, and assume that Lemma 2.2 is satisfied. Then, $\overline{x}^{\star}_{sym}$ can be directly obtained by solving the first derivative of (2.30) as follows:

$$\begin{aligned} \overline{x}^{\star}_{sym} &= \frac{l_{c,bs}}{2l_{d_1,bs}} \\ \overline{y}^{\star}_{sym} &= \frac{l_{c,bs}}{l_{d2,bs}} - \frac{l_{d1,bs}}{l_{d2,bs}} x^{\star}_{sym} = \frac{l_{c,bs}}{2l_{d_1,bs}} \end{aligned} \tag{2.33}$$

Physically speaking, (2.33) means that when the *D2D* users are receiving the same interference power from *CU* and introducing equal interference power at the *BS*, the optima can be obtained by allocating half the maximum power for each *D2D* user.

Power allocation in the asymmetric case

Let $\overline{x}^{\star}_{asym}$ and $\overline{y}^{\star}_{asym}$ be the optimal power ratio value of (2.30) in the asymmetric scenario when Lemma 2 is satisfied. Then, by solving the first derivative of (2.30), $\overline{x}^{\star}_{asym}$ and $\overline{y}^{\star}_{asym}$ can be calculated as follows:

$$
\begin{aligned}
&x^{\star}_{asym} = \\
&\frac{\left(8bcrM_y{}^2+\left(12r^2+12\right)cM_y+18r^2+18\right)a-18M_ycr-\left(8M_ycr+12r\right)a^2}{\pm\sqrt{\left(-2M_yc+2ar-3\right)\left(4M_yac+6a-9r\right)\left(-2M_yb+2a-3r\right)\left(4M_yab+6ar-9\right)}-27r} \\
&\qquad\qquad \left(-8cr^2+8br\right)a^2+\left(\left(8br^2-8b\right)cM_y-12\left(r^2+1\right)\left(-cr+b\right)\right)a+18r\left(-cr+b\right) \\
&y^{\star}_{asym} = M_y - \frac{l_{d1,bs}}{l_{d2,bs}}\,x^{\star}_{asym}
\end{aligned}
\tag{2.34}
$$

where $a \triangleq \frac{\eta}{l_d}$, $b \triangleq \frac{\eta}{l_{c,d1}}$, $c \triangleq \frac{\eta}{l_{c,d2}}$, and $r \triangleq \frac{l_{d1,bs}}{l_{d2,bs}}$.

The proposed power allocation for the general case

The obtained optima in (2.33) and (2.34) are for two particular cases. For the general case where the SI factor can be any number and the users are in random positions the optima can not be mathematically derived. However, after analyzing (2.34) we found that when *CU* is relatively far from the *D2D* pair the optima will be achieved by allocating more power to the *D2D* user who is introducing less interference power to the base station. And, when the *CU* is relatively near to the *D2D* pair, more power should be allocated to the *D2D* user who is suffering more from the *CU* interference power. Based on this analysis and the previous results we propose the following power allocation technique which yields the optimum results in both the symmetric and asymmetric case when Lemma 2.2 and for a sub-optimal solution in the general case.

$$
\begin{aligned}
x^{\star} &= \max\left(0, \min\left(M_x, e^{\frac{\eta M_x}{l_d}}\frac{M_x}{2}\left[1+\frac{l_{c,d_1}-l_{c,d_2}}{l_d+l_{c,d_1}+l_{c,d_2}}\right]\right)\right) \\
y^{\star} &= \frac{l_{c,bs}-l_{d1.bs}x^{\star}}{l_{d_2,bs}}
\end{aligned}
\tag{2.35}
$$

The max(.) and min(.) operators in (2.35) are used to ensure that our approximated optima do not violate the power ratio constraints, i.e., the minimum power ratio 0 and the maximum power ratio M_x. The exponential term reflects the effect of the SIC techniques, more precisely when η

goes to zero the effect of SI will disappear while when η goes to one the SI will highly affect the optima solution. The fraction term in (2.35) will be positive or negative w.r.t the *CU* location and thus more power will be allocated to D_1 if it is suffering more from the *CU* interference and vice versa. Accordingly, depending on the *CU* location the value of the optima will tend to either $(M_x, 0)$ or $(0, M_y)$ which represent the HD-D2D mode for D_1 and D_2 respectively. In other word, the *CU* location highly affects the transmission mode for the *D2D* pair.

The equation in (2.35) presents the proposed power ratio relation between *CU*, D_1, and D_2. To extract the transmit power of each user, first, we employ a truncated channel inversion power control strategy on *CU* to deal with the average channel variation between *CU* and *BS*, i.e., we set the transmit power of *CU* to $p_c^* = \frac{1}{l_{c,bs}}$. Next, the proposed transmit powers of the users are calculated based on (2.35) as follows:

$$\begin{aligned} p_{d1}^* &= \max(0, \min(P_{\max}^{d1}, \frac{1}{l_{d1,bs}}, e^{\frac{\eta l_{c,bs}}{l_{d-d1,bs}}} \frac{1}{2l_{d1,bs}}[1 + \frac{l_{c,d_1} - l_{c,d_2}}{l_d + l_{c,d_1} + l_{c,d_2}}])) \\ p_{d2}^* &= \max(0, \min(P_{\max}^{d2}, \frac{1 - l_{d1.bs} p_{d1}^*}{l_{d_2,bs}}). \end{aligned} \tag{2.36}$$

This power control scheme is unable to achieve the optimal value, but it will correctly present the general behaviour of the FD-D2D network as we will see in the numerical simulation section. This, in turn, will allow us to understand more the performance of the network with the variation of the different parameters, such as the SIC factor η and the users locations, and build on this knowledge to investigate the derived optimal PA strategy in the next section and the following chapters. Besides, in a real network an instantaneous solution needs to be applied every short period of time such as the Transmission Time Interval (TTI) interval in LTE network. To resolve these shortcomings, in the next section, we shift our focus on solving the maximization problem of the instantaneous FD-D2D rate and HD-D2D rate defined in (2.5) and (2.9) respectively.

2.3 Instantaneous full-duplex rate analysis

Assuming that the *BS* has all information about the instantaneous CSI of the users, in this section we tackle the PA problem of an FD-D2D network. In general, the complex interference nature of an FD-D2D network generates a non-convex PA problem for which the optimal solution is hard to find. Thus, most of the related research provide a sub-optimal PA strategy by maximizing a convex lower bound of the original non-convex PA problem. The root of this solving approach is the SCO framework which can achieve a first-order optimal solution as described later on in this section. Our goal here is to efficiently obtain the optimal PA scheme in an FD-D2D network. In this direction, we developed a novel optimization framework for an FD-D2D underlaying cellular network by exploiting the geometric structure of the PA

problem's feasible set. For the sake of readability, we named this approach GALEN (Geometrical framework Approach for gLobal optimal powEr allocatioN). Besides the global PA solution, GALEN provides a closed-form expression for the optimal PA strategy, which in turn makes it very efficient in terms of complexity. We start our analysis by formulating the PA problem as shown in the following.

2.3.1 Instantaneous PA problem formulation

The main goal of *D2D* technology is to offload a portion of the data traffic from the cellular network. Thus, in this chapter, we aim to maximize the total D2D capacity while satisfying the QoS of the cellular users. Since each *D2D* pair may operate either in HD or FD mode, two maximization problem must be studied.

Let $R_{\min}$ be the minimum data rate for the CU, and denote by $\mathbf{p} = (p_{d1}, p_{d2}, p_c)$ the transmission power vector of the couple $(D2D, CU)$, the D2D rate maximization problem in the HD and the FD modes can be respectively formulated as follows:

$$\boldsymbol{PA}_{HD} : \max_{\mathbf{p}} R_{HD} = R_{HD,D1} + R_{HD,D2} \text{ s.t. } \mathbf{p} \in \Phi \tag{2.37}$$

$$\boldsymbol{PA}_{FD} : \max_{\mathbf{p}} R_{FD} = R_{FD,D1} + R_{FD,D2} \text{ s.t. } \mathbf{p} \in \Phi \tag{2.38}$$

$$\Phi = \{\Gamma_{bs} \geq \gamma_{\min} = 2^{R_{\min}} - 1, \tag{2.39}$$

$$0 \leq p_i \leq P^i_{\max}, i \in \{d1, d2, c\}\} \tag{2.40}$$

where $P^i_{\max}$ is the maximum transmission power of a transmitter i. Solving $\boldsymbol{PA}_{FD}$ and $\boldsymbol{PA}_{HD}$ is the target of the following sections.

2.3.2 Sequential convex optimization solution

Here we solve the optimization problem defined in $\boldsymbol{PA}_{FD}$ by using the sequential convex optimization method (SCO). The SCO technique is an iterative algorithm which finds local optima of a non-convex maximization problem with objective f, by solving a sequence of simpler problems with convex objectives $\{f_i\}_i$. Moreover, SCO is guaranteed to converge to a first-order optimal solution of the optimization problem when at each iteration i the following three properties are satisfied [125, Section IV].

- $f_i(x) \leq f(x), \forall x$;
- $f_i(x^*_{i-1}) = f(x^*_{i-1})$;
- $\nabla f_i(x^*_{i-1}) = \nabla f(x^*_{i-1})$;

where x^*_{i-1} is the maximizer of f_{i-1}. Hence,the key point in SCO is to find a simpler objective $\{f_i\}_i$ which fulfills the above three properties. In the following we show how to apply SCO in $\boldsymbol{PA}_{FD}$ and $\boldsymbol{PA}_{HD}$.

Since both R_{FD} and R_{HD} have the same function structure we will demonstrate how to derive the first-order optimal solution only for the FD mode. Now, using the logarithm properties R_{FD} is reshaped as follows:

$$\begin{aligned} R_{FD}=&B\Big[\log_2(p_c h_{c,d1}+\eta p_{d1}+\sigma_N^2+p_{d2}g_d)+\log_2(p_c h_{c,d2}+\eta p_{d2}+\sigma_N^2+p_{d1}g_d)\\ &-\log_2(p_c h_{c,d1}+\eta p_{d1}+\sigma_N^2)-\log_2(p_c h_{c,d2}+\eta p_{d2}+\sigma_N^2)\Big]\\ =&r^+_{fd}(\mathbf{p})-r^-_{fd}(\mathbf{p}) \end{aligned} \tag{2.41}$$

observe that r^+_{fd} and r^-_{fd} are concave functions and recall that any concave function is upper bounded by its first-order Taylor expansion at any point. Therefore, for any given power vector $\mathbf{p}^t$ we can approximate (2.41) as follows:

$$R_{FD}\geq r^+_{fd}(\mathbf{p})-\left[r^-_{fd}(\mathbf{p}^t)+\left(\nabla_{\mathbf{p}} r^-_{fd}|_{\mathbf{p}=\mathbf{p}^t}\right)^T(\mathbf{p}-\mathbf{p}^t)\right] \tag{2.42}$$

Hence, (2.42) is lower bound of the utility in (2.41). Moreover, since the lower bound in (2.41) is tight when evaluated in $\mathbf{p}^t$, (2.42) is equal to (2.41) for $\mathbf{p}=\mathbf{p}^t$. Next, by using the linearity property of the gradient it is easily verified that $\nabla\left((2.41)\right)=\nabla\left((2.42)\right)|_{\mathbf{p}=\mathbf{p}^t}$. Thus, all the above requirements are satisfied and by using this relaxation the convergence of SCO to the first order optimal solution is guaranteed.

Similarly, the approximation of R_{HD} can be derived as:

$$R_{HD}\geq r^+_{hd}(\mathbf{p})-\left[r^-_{hd}(\mathbf{p}^t)+\left(\nabla_{\mathbf{p}} r^-_{hd}|_{\mathbf{p}=\mathbf{p}^t}\right)^T(\mathbf{p}-\mathbf{p}^t)\right] \tag{2.43}$$

wherein $r^+_{hd}=\frac{1}{2}B(\log_2(p_c h_{c,d1}+\sigma_N^2+p_{d2}g_{d2,d1})+\log_2(p_c h_{c,d2}+\sigma_N^2+p_{d1}g_{d1,d2})$ and $r^-_{hd}=\frac{1}{2}B(\log_2(p_c h_{c,d1}+\sigma_N^2)+\log_2(p_c h_{c,d2}+\sigma_N^2))$.

Note that both (2.42) and (2.43) are convex function (since they are summation of concave and linear functions), and thus the solutions of the power allocation problems $\mathbf{PA}_{FD}$ and $\mathbf{PA}_{HD}$ can be easily found by using any convex optimization tools such as CVX [126]. Since SCO is an iterative based solution and it requires solving an approximated convex problem at each iteration, in the next section we look to provide a closed-form optimal solution.

2.3.3 GALEN's framework

Despite the interest of the SCO theory, the latter does not provide a closed-form analytical expression for the optimal power allocation and also may require high iteration numbers in some

situation. In this section, we provide a mathematical framework named GALEN which efficiently finds the optimal solutions of $\boldsymbol{PA}_{HD}$ and $\boldsymbol{PA}_{FD}$ defined in (2.37) and (2.38) respectively, by analyzing the geometric structure of the feasible set Φ.

Geometric representation of Φ

The feasible set Φ of each couple $(D2D, CU)$ can be rewritten as follows:

$$\Phi = \{p_c\, g_{c,bs} - \gamma_{\min}(p_{d1}\, h_{d1,bs} + p_{d2}\, h_{d2,bs} + \sigma_N^2) \geq 0 \tag{2.44}$$

$$0 \leq p_i \leq P_{\max}^i, i \in \{d1, d2, c\}\} \tag{2.45}$$

Equations (2.44) and (2.45) respectively represent the QoS constraint of a CU and the power constraints of the couple $(D2D, CU)$. Denote by $\mathcal{P}_c$ the equality case of (2.44), i.e., the QoS plane. Moreover, let $\mathcal{P}_i^{\max}$ ($\mathcal{P}_i^0$) be the maximum (minimum) power planes, i.e., $P_i = P_{\max}^i (P_i = 0)$ where $i \in \{c, d1, d2\}$. Hence, in the three dimensional space (p_{d1}, p_{d2}, p_c), Φ can be represented as the intersection of $\mathcal{P}_c$ with $\mathcal{P}_i^0$ and $\mathcal{P}_i^{\max}$, where $i = \{c, d1, d2\}$.

It can be observed that $\mathcal{P}_i^{\max}$ ($\mathcal{P}_i^0$) with $i \in \{d1, d2, c\}$, are fixed in the 3D-space and they form a cuboid shape as shown in Fig.2.3(a)-2.3(e). However, the plane $\mathcal{P}_c$ varies according to the channel situation of $(D2D, CU)$ and the required rate of CU. Thus, Φ may have different possible shapes as shown in Fig.2.3(a)-2.3(e).

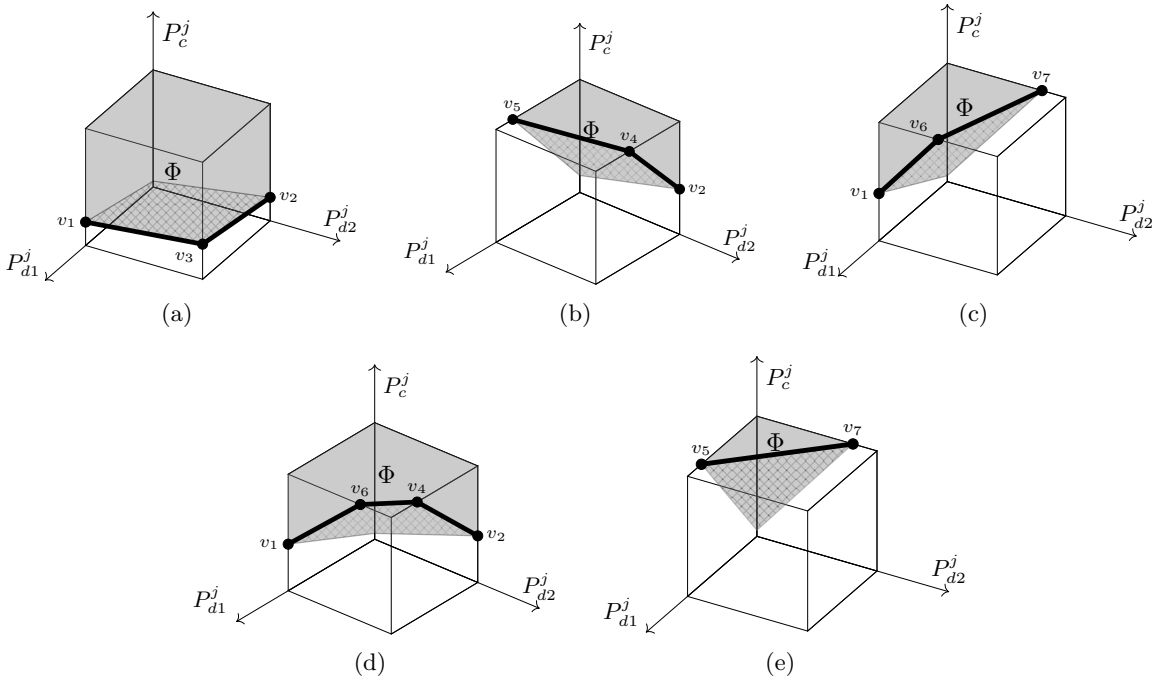

Figure 2.3 – The possible shapes of the feasible set Φ. ($\mathscr{P}_c$ ▨)

Fig.2.3(a)-2.3(c) shows the cases where $\mathscr{P}_c$ has intersection with two maximum power planes and two minimum power planes. Fig.2.3(d) shows the case where $\mathcal{P}_c$ intersects all the maximum and the minimum power planes, while Fig.2.3(e) shows the case where $\mathscr{P}_c$ intersects the plane $\mathcal{P}_c^{\max}$, $\mathcal{P}_{d1}^0$ and $\mathcal{P}_{d2}^0$. The thick lines in the above figures represent the intersection lines of $\mathcal{P}_c$ with the maximum power planes. The corner of these lines are denoted as v_i with $i = \{1, 2, ..., 7\}$. Moreover, we define the following points: $v_1 \triangleq \mathcal{P}_c \cap \mathcal{P}_{d1}^{\max} \cap \mathcal{P}_{d2}^0$; $v_2 \triangleq \mathcal{P}_c \cap \mathcal{P}_{d2}^{\max} \cap \mathcal{P}_{d1}^0$; $v_3 \triangleq \mathcal{P}_c \cap \mathcal{P}_{d1}^{\max} \cap \mathcal{P}_{d2}^{\max}$; $v_4 \triangleq \mathcal{P}_c \cap \mathcal{P}_{d2}^{\max} \cap \mathcal{P}_c^{\max}$; $v_5 \triangleq \mathcal{P}_c \cap \mathcal{P}_c^{\max} \cap \mathcal{P}_{d2}^0$; $v_6 \triangleq \mathcal{P}_c \cap \mathcal{P}_{d1}^{\max} \cap \mathcal{P}_c^{\max}$; and $v_7 \triangleq \mathcal{P}_c \cap \mathcal{P}_c^{\max} \cap \mathcal{P}_{d1}^0$.

Thus the coordinate of these vertices can be expressed as follows:

$$
\begin{aligned}
v_1&=\left(P_{max}^{d1};\ 0;\ (P_{\max}^{d1}h_{d1,bs}+\sigma_N^2)\gamma_{\min}/g_{c,bs}\right)\\
v_2&=\left(0;\ P_{max}^{d2};\ (P_{\max}^{d2}h_{d2,bs}+\sigma_N^2)\gamma_{\min}/g_{c,bs}\right)\\
v_3&=\left(P_{max}^{d1};\ P_{max}^{d2};\ (P_{\max}^{d1}h_{d1,bs}+P_{\max}^{d2}h_{d2,bs}+\sigma_N^2)\gamma_{\min}/g_{c,bs}\right)\\
v_4&=\left(\left(P_{max}^{c}g_{c,bs}/\gamma_{\min}-P_{max}^{d2}h_{d2,bs}-\sigma_N^2\right)/h_{d1,bs};\ P_{max}^{d2};\ P_{max}^{c}\right)\\
v_5&=\left(\left(P_{max}^{c}g_{c,bs}/\gamma_{\min}-\sigma_N^2\right)/h_{d1,bs};\ 0;\ P_{max}^{c}\right)\\
v_6&=\left(P_{max}^{d1};\ \left(P_{max}^{c}g_{c,bs}/\gamma_{\min}-P_{max}^{d1}h_{d1,bs}-\sigma_N^2\right)/h_{d2,bs};\ P_{max}^{c}\right)\\
v_7&=\left(0;\ \left(P_{max}^{c}g_{c,bs}/\gamma_{\min}-\sigma_N^2\right)/h_{d2,bs};\ P_{max}^{c}\right)
\end{aligned}
$$

Optimal power allocation

Denote by $\Omega = \{\overline{v_1v_3};\ \overline{v_2v_3};\ \overline{v_4v_5};\ \overline{v_6v_7};\overline{v_4v_6};\overline{v_5v_7}\}$ the set of the intersection lines between $\mathcal{P}_c$ and the maximum power planes. The following lemma shows that the optima can be searched only in Ω instead of Φ. Here it is worthy mentioning that Ω is an exclusive set, i.e., not all its members occurs at the same time as shown in Fig.2.3(a)-2.3(e).

Lemma 2.3. *Let $\mathbf{p}_{FD}^{\star}$ and $\mathbf{p}_{HD}^{\star}$ be the optimal power vectors for the FD and HD modes respectively. Then $\mathbf{p}_{FD}^{\star}$ and $\mathbf{p}_{HD}^{\star}$ have at least one power bounded by the maximum power constraint and it lies on the QoS plane $\mathcal{P}_c$.*

Proof: For any scaling parameter $\beta > 1$ and a power vector $\mathbf{p} = (p_{d1}, p_{d2}, p_c) \in \Phi$ we have:

$$
R_{FD}(\beta\mathbf{p})=\log_2\left[(1+\frac{p_{d2}g_d}{p_cg_{c,d1}+\eta p_{d1}+\sigma_N^2/\beta})\times(1+\frac{p_{d1}g_d}{p_cg_{c,d2}+\eta p_{d2}+\sigma_N^2/\beta})\right] > R_{FD}(\mathbf{p}) \quad (2.46)
$$

$$
R_{HD}(\beta\mathbf{p})=\log_2\left[(1+\frac{p_{d2}g_d}{p_cg_{c,d1}+\sigma_N^2/\beta})\times(1+\frac{p_{d1}g_d}{p_cg_{c,d2}+\sigma_N^2/\beta})\right] > R_{HD}(\mathbf{p}) \quad (2.47)
$$

The power constraints defined in (2.45) imply that the maximum βp_i is $P_{\max}^i$, $i \in \{d1, d2, c\}$ (due to inequality in (2.46)). Hence, the optimal transmission strategy in FD mode or HD mode

can be achieved only if at least one user is transmitting with the maximum allowed power. On the other hand, since R_{FD} and R_{HD} monotonically decrease with p_c, the maximum R_{FD} or R_{HD} occur when CU transmits with the minimum required power. Thus, $\mathbf{p}^{\star}_{FD}$ and $\mathbf{p}^{\star}_{HD}$ must reside on the plane $\mathcal{P}_c$. As a result, the optimal points must reside in Ω. ■

Lemma 2.3 reduces the feasible set Φ to Ω, and thus the optimal point for the FD and HD modes can be obtained by solving the power allocation problems defined in (2.38) and (2.37) respectively over the different points of Ω. Since R_{FD} and R_{HD} have the same function' structure in the following we solve the PA problem only for the FD mode.

Before starting the solving process we note that due to the monotocinity property of $\log_2$ maximizing $R_{FD} \triangleq \log_2(Q_{FD}) = \log_2[(1+\Gamma_{FD,d1})(1+\Gamma_{FD,d2})]$ is equivalent to maximizing Q_{FD}. Now, being on $\overline{v_1v_3}$ (see Fig.2.3(a)) or $\overline{v_1v_6}$ (see Fig.2.3(d) and Fig.2.3(b)) implies that $p_{d1} = P^{d1}_{\max}$ and $p_c = (P^{d1}_{\max}h_{d1,bs} + p_{d2}h_{d2,bs} + \sigma^2_N)\frac{\gamma_{\min}}{g_{c,bs}}$. In such case, Q_{FD} reduces to

$$Q_{FD}(\mathbf{p}) = \left(1 + \frac{p_{d2}}{p_{d2}\hat{a}_1 + \hat{a}_2}\right)\left(1 + \frac{P^{d1}_{\max}}{p_{d2}\hat{a}_3 + \hat{a}_4}\right), \tag{2.48}$$

where the constant coefficients in the above equation are defined as

$$\begin{aligned}
\hat{a}_1 &= \frac{\gamma_{\min}h_{d2,bs}h_{c,d1}}{g_{c,bs}g_d}; \quad \hat{a}_2 = \frac{P^{d1}_{\max}}{g_d}\left(\eta + \frac{\gamma_{\min}h_{d1,bs}h_{c,d1}}{g_{c,bs}}\right) + \frac{\sigma^2_N}{g_d}\left(1 + \frac{\gamma_{\min}h_{c,d1}}{g_{c,bs}}\right); \\
\hat{a}_3 &= \frac{\eta g_{c,bs} + \gamma_{\min}h_{d2,bs}h_{c,d2}}{g_{c,bs}g_d}; \quad \hat{a}_4 = \frac{\gamma_{\min}P^{d1}_{\max}h_{d1,bs}h_{c,d2}}{g_{c,bs}g_d} + \frac{\sigma^2_N}{g_d}\left(1 + \frac{\gamma_{\min}h_{c,d2}}{g_{c,bs}}\right).
\end{aligned} \tag{2.49}$$

Taking the first derivative of (2.48) w.r.t p_{d2} leads to the following:

$$\frac{\partial Q_{FD}}{\partial p_{d2}} = \frac{\hat{A}_1 {p_{d2}}^2 + 2\hat{B}_1 p_{d2} + \hat{C}_1}{\hat{K}_1} \tag{2.50}$$

where the constants $\hat{A}_1$, $\hat{B}_1$, $\hat{C}_1$ and $\hat{K}_1$ are given as follows:

$$\begin{aligned}
\hat{A}_1 &= \left(\hat{a}_3^2\hat{a}_2 - P^{d1}_{\max}\hat{a}_1\hat{a}_3\left(\hat{a}_1 + 1\right)\right); \quad \hat{B}_1 = -\left(P^{d1}_{\max}\hat{a}_1 - \hat{a}_4\right)\hat{a}_3\hat{a}_2; \\
\hat{C}_1 &= P^{d1}_{\max}(\hat{a}_2\hat{a}_4 - \hat{a}_2^2\hat{a}_3) + \hat{a}_2\hat{a}_4^2; \quad \hat{K}_1 = (p_{d2}\hat{a}_1 + \hat{a}_2)^2(p_{d2}\hat{a}_3 + \hat{a}_4)^2.
\end{aligned}$$

Since $\hat{K}_1$ is always positive, a possible optima of (2.48) would be the solution of $\hat{A}_1{p_{d2}}^2 + 2\hat{B}_1 p_{d2} + \hat{C}_1$. Denote such optima point as e_1, the coordinates of e_1 are given by:

$$e_1 = \left(P^{d1}_{\max}; \quad \frac{1}{\hat{A}_1}\left(-\hat{B}_1 \pm \sqrt{\hat{B}_1^2 - \hat{A}_1\hat{C}_1}\right); \quad \frac{\gamma_{\min}}{g_{c,bs}}\left(P^{d1}_{\max}h_{d1,bs} + P_{d2,e_1}h_{d2,bs} + \sigma^2_N\right)\right), \tag{2.51}$$

with P_{d2,e_1} being the p_{d2} abscissa of e_1.

The above solution does not always provide a global maxima of (2.48), since there is no guarantee that the second derivative is always negative. Moreover, e_1 may not be always a feasible point (since it may lie outside $\overline{v_1v_3}$ or $\overline{v_1v_6}$, or it might be an imaginary point). Accordingly, the global maxima of (2.48) would be either one of the corner points of the line $\overline{v_1v_3}$ ($\overline{v_1v_6}$), i.e., v_1 or v_3 (v_6), or the extreme point e_1 (if e_1 is feasible).

In the same manner, the optimal point of (2.38) on the line $\overline{v_2v_3}$ as in Fig.2.3(a) (or $\overline{v_2v_4}$ as in Fig.2.3(d) and Fig.2.3(c)) is either one of the corner points v_2 or v_3 (v_4) or an extreme point e_2 which lies on $\overline{v_2v_3}$ ($\overline{v_2v_4}$) and has the following coordinate:

$$e_2=\left(\frac{1}{\hat{A}_2}\left(-\hat{B}_2\pm\sqrt{\hat{B}_2^2-\hat{A}_2\hat{C}_2}\right);\quad P_{\max}^{d2};\quad \frac{\gamma_{\min}}{g_{c,bs}}\left(P_{d1,e_2}h_{d1,bs}+P_{\max}^{d2}h_{d2,bs}+\sigma_N^2\right)\right),\quad (2.52)$$

where the constants $\hat{A}_2$, $\hat{B}_2$, and $\hat{C}_2$ are given by

$$\hat{A}_2=\left(\hat{b}_3^2\hat{b}_2-P_{\max}^{d2}\hat{b}_0\hat{b}_3\left(\hat{b}_0+1\right)\right);\quad \hat{B}_2=\left(\hat{b}_4-P_{\max}^{d2}\hat{b}_0\right)\hat{b}_3\hat{b}_2;\quad \hat{C}_2=P_{\max}^{d1}(\hat{b}_2\hat{b}_4-\hat{b}_2^2\hat{b}_3)+\hat{b}_2\hat{b}_4^2,$$

and the constant coefficients $\hat{b}_0$, $\hat{b}_2$, $\hat{b}_3$, and $\hat{b}_4$ are given by

$$\hat{b}_0=\frac{\gamma_{\min}h_{d1,bs}h_{c,d2}}{g_{c,bs}g_d};\qquad \hat{b}_2=\frac{P_{\max}^{d2}}{g_d}\left(\eta+\frac{\gamma_{\min}h_{d2,bs}h_{c,d2}}{g_{c,bs}}\right)+\frac{\sigma_N^2}{g_d}\left(1+\frac{\gamma_{\min}h_{c,d2}}{g_{c,bs}}\right)$$
$$\hat{b}_3=\frac{\eta g_{c,bs}+\gamma_{\min}h_{d1,bs}h_{c,d1}}{g_{c,bs}g_d};\quad \hat{b}_4=\frac{\gamma_{\min}P_{\max}^{d2}h_{d2,bs}h_{c,d1}}{g_{c,bs}g_d}+\frac{\sigma_N^2}{g_d}\left(1+\frac{\gamma_{\min}}{g_{c,bs}}h_{c,d1}\right).$$

Similarly, the optimal point of (2.38) on the line $\overline{v_6v_4}$ as in Fig.2.3(c) (or $\overline{v_5v_7}$ as in Fig.2.3(e)) is either one of the corner points v_4 or v_6 (v_5 or v_7) or an extreme point e_3 which lies on $\overline{v_6v_4}$ ($\overline{v_5v_7}$) and has the following coordinate

$$e_3=\left(\frac{1}{\hat{A}_3}\left(-\hat{B}_3\pm\sqrt{\hat{B}_3^2-\hat{A}_3\hat{C}_3}\right);\quad \frac{1}{h_{d2,bs}}\left(\frac{P_{\max}^{c}g_{c,bs}}{\gamma_{\min}}-\sigma_N^2-P_{d1,e_3}h_{d1,bs}\right);\quad P_{\max}^{c}\right),\quad (2.53)$$

where the constants $\hat{A}_3$, $\hat{B}_3$, and $\hat{C}_3$ are given by

$$\hat{A}_3=\eta\hat{c}_4\left(\eta-\hat{c}_3\right)-\hat{c}_5\left(\hat{c}_5-1\right)\left(\hat{c}_1\hat{c}_3+\hat{c}_2\eta\right);\quad \hat{B}_3=\left(\left(\hat{c}_3\hat{c}_5-\hat{c}_3+\eta\right)\hat{c}_1+\eta\,\hat{c}_2\,\hat{c}_5\right)\hat{c}_4;$$
$$\hat{C}_3=\hat{c}_4\left(\hat{c}_1\left(\hat{c}_1+\hat{c}_2\right)-\left(\hat{c}_1\hat{c}_3+\hat{c}_2\eta\right)\hat{c}_4\right);$$

and the constant coefficients $\hat{c}_1$, $\hat{c}_2$, $\hat{c}_3$, $\hat{c}_4$, and $\hat{c}_5$ are given by

$$\hat{c}_1=\frac{1}{g_d}\left(P_{\max}^{c}g_{c,d1}+\sigma_N^2\right);\quad \hat{c}_2=\frac{P_{max}^{c}g_{c,bs}}{\gamma_{\min}h_{d2,bs}}-\frac{\sigma_N^2}{h_{d2,bs}};\quad \hat{c}_3=\frac{h_{d1,bs}}{h_{d2,bs}};$$
$$\hat{c}_4=\frac{P_{\max}^{c}}{g_d}\left(g_{c,d2}+\frac{\eta g_{c,bs}}{\gamma_{\min}h_{d2,bs}}\right)+\frac{\sigma_N^2}{g_d}\left(1-\frac{\eta}{h_{d2,bs}}\right);\quad \hat{c}_5=\frac{\eta h_{d1,bs}}{h_{d2,bs}g_d}.$$

Accordingly, the optimal point would be the point which gives higher rate. The following Theorem summarizes all the previous discussion.

Theorem 2.2. *The optimal power vector $\boldsymbol{p}^{\star}_{FD}$ can be searched only in the set $\mathcal{P}^{FD}_{opt}$ defined as*

$$\mathcal{P}_{opt} = \{v_1, v_2, v_3, v_4, v_5, v_6, v_7, e_1, e_2, e_3\} \tag{2.54}$$

Now to obtain the optimal power vector in HD mode, the same procedure can be applied after setting η to zero. This will lead to the following theorem.

Theorem 2.3. *The optimal power vector $\boldsymbol{p}^{\star}_{HD}$ can be searched only in the set $\mathcal{P}^{HD}_{opt}$ defined as*

$$\mathcal{P}^{HD}_{opt} = \mathcal{P}^{FD}_{opt}|_{\eta=0} \tag{2.55}$$

In Theorem 2, (2.55) means that the elements of $\mathcal{P}^{HD}_{opt}$ are the same elements of $\mathcal{P}^{FD}_{opt}$ such that $\eta = 0$. Here we should emphasize that Theorem 1 and Theorem 2 reduce the feasible set from a three dimensional shape to a set of points with known coordinates. Hence, with GALEN the global optimal point can be obtained in one iteration on contrary to SCO algorithm which requires a high number of iterations. Moreover, GALEN provides a closed form expression of the optimal solution.

2.4 Numerical Results

In this section we aim to evaluate the performance of an FD-D2D enabled cellular network. In our simulation we varied the value of the SI mitigation factor η between two realistic values $-60dB$ and $-90dB$ as discussed in Section 1.2 and reported in Table 1.1 . Moreover, we set the path-loss exponent α to 4 and the noise power σ^2_N to $-114dBm$. The maximum transmit power of the users is assumed to be $24dBm$. Besides, different users distributions are used to assist the ergodic analysis, the SCO based solution, and the derived GALEN framework as described below. The common simulation parameters between the ergodic and instantaneous simulations are summarized in Table 2.1.

Table 2.1 – Simulation parameters

Noise power (σ^2_N)	-114 dBm
Path-loss exponent (α)	4
Maximum power of *CU* and D2D users	24 dBm
SI cancellation factor (η)	-100,-90,...,-50 dB
Multiple-path fading	Exponential distribution with l_{ij} mean

2.4.1 Ergodic results

In this subsection, we conduct numerical experiments to evaluate the performance of our proposed power allocation strategy in (2.36). To that end, we set the *D2D* pair at a distance $100m$ from *BS* with inter-distance $15m$, and we moved *CU* on a chord of a circle with radius $90m$ as illustrated in Fig.2.4. In particular, we choose this setup because it allows us to assist our proposed PA strategy in the general case. Also, the selected path enables us to cover the cases when *CU* is near *BS* but far from *D2D* pair, and when *CU* is near the *D2D* pair but far from *BS*.

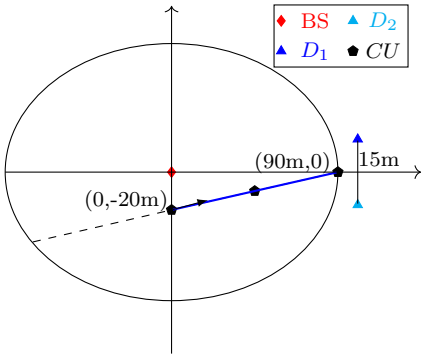

Figure 2.4 – Illustration about the used setup to assess the proposed ergodic PA scheme.

Using the setup described in Fig.2.4, in Fig. 2.5 we compare our proposed ergodic PA scheme in (2.36) with the exhaustive search method. As expected, our PA scheme fails at obtaining the optimal result, but its resulting ergodic D2D rate behaves almost the same as the one produced by the exhaustive search method. Nevertheless, the proposed PA scheme is a closed-form expression, thus it has much lower complexity than the search-based solution, which makes it an interesting tool to earn general knowledge about the FD-D2D network performance. Besides that, Fig. 2.5 provides useful insights about the impact of the SIC factor η and the users positions on the network behavior. For instance, Fig. 2.5 clearly shows that as η decreases the ergodic rate increases. The reason behind that is when η decreases the power of the residual self interference decreases and hence the average interference power decreases. Fig. 2.5 also shows that the ergodic FD rate $\mathcal{R}_{FD}$ decreases as *CU* moves toward the *D2D* pair. This is expected behavior because in such case the *D2D* users need to mitigate their transmission power in order not to violate the interference constraint at the base station. Moreover, we observe that in Fig. 2.5, the minimum rate occurs when *CU* became too close to the *D2D* pair, and after that a small improvement happened. This action implicitly declares the shortcomings of FD mode when the FD device is suffering from high *CU* interference. Specifically, the small rate enhancement happens after *CU* passed the *D2D* users and became further away from *BS*. In such case, to maintain the QoS of *CU* the *D2D* users must switch to HD mode specially when η is low.

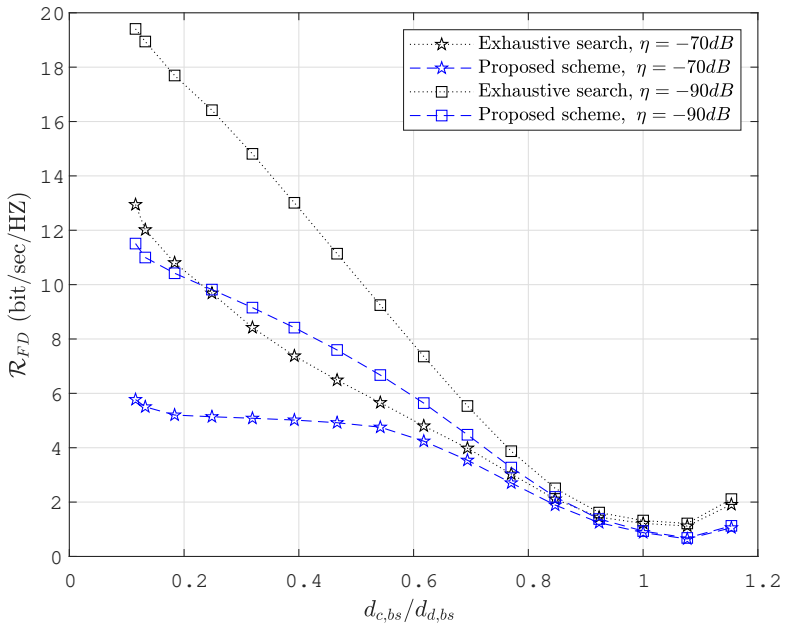

Figure 2.5 – Comparison of FD-D2D rate obtained from the exhaustive search and from the proposed power allocation scheme.

To highlight the later observation, we show in Fig. 2.6 shows the variations of the optimal power ratios with respect to the cellular user distances from the *D2D* users. In this figure, we first fix the *D2D* pair at 100m from the *BS*, then we set the *CU* at a position where $d_{c,d1} > d_{c,d2}$. After that we moved the *CU* toward $D1$ or $D2$. We repeated this scenario for different values of l_d. As expected, x^* and y^* have opposite variation w.r.t the *CU* location. For instance, when $d_{c,d1} = d_{c,d2}$ we have $x^\star = y^\star = 50$. While when the *CU* becomes too close to $D1$ (i.e., $d_{c,d1} = 5m$), $x^\star$ is almost equal to the maximum allowed power ratio and $y^\star$ is almost zero. This is because in such case $D1$ is facing high interference from *CU* while $D2$ is not. Hence, it is better to let $D1$ only send messages, i.e., it will operate in HD mode.

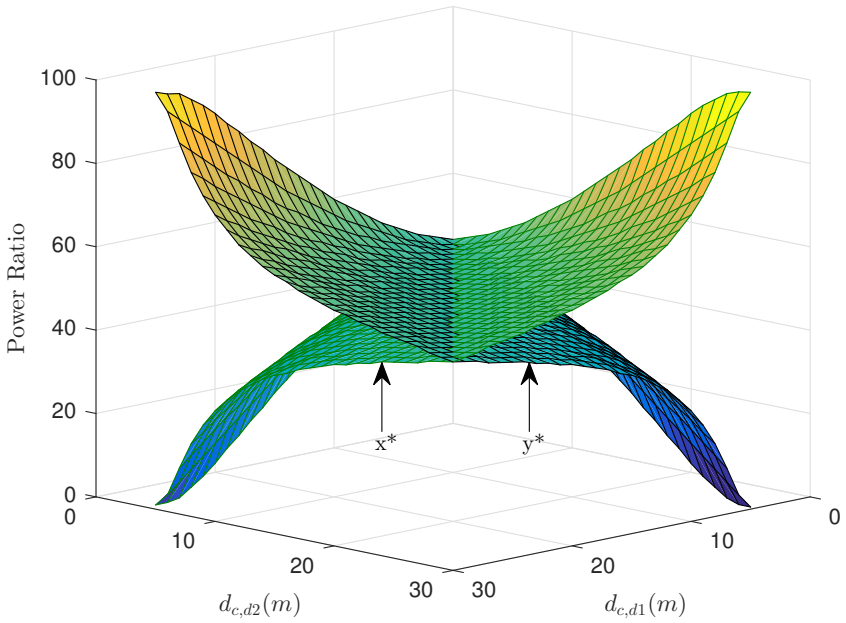

Figure 2.6 – The optimal power ratios variation w.r.t to *CU* location (η=$-70dB$)

.

Now, based on this knowledge, we show in the next sections further investigations about the impact of η and the positions of the users on the network performance using the PA strategies proposed in the instantaneous rate analysis section.

2.4.2 SCO and GALEN results

This subsection looks to evaluated the derived GALEN framework and compare it with the existing SCO based solution. Moreover, it also aims to further discover the effect of the *CU* location on the PA strategy and the achieved rate. To that end, the *CU* is uniformly distributed in the cell and the *D2D* pair is uniformly distributed within a randomly located cluster with radius r.

GALEN versus SCO

Here we look to investigate the impact of the SCO and GALEN on the performance of an FD-D2D network. Fig. 2.7 shows the variation of the *D2D* rate w.r.t the SI cancellation factor (η) and the *D2D* cluster radius (r). Moreover, it compares the proposed PA scheme, GALEN, with the SCO method for different cluster radius and different SI cancellation factors. In this figure we consider 5000 realizations, then we average the results over all realizations. As it can be seen, the curves almost perfectly match in all cases which in turn validates the proposed GALEN framework. Moreover, Fig. 2.7 clearly shows that as the cluster radius r increases, the

average rate decreases. As expected, we can see that the average rate increases as the SI factor decreases.

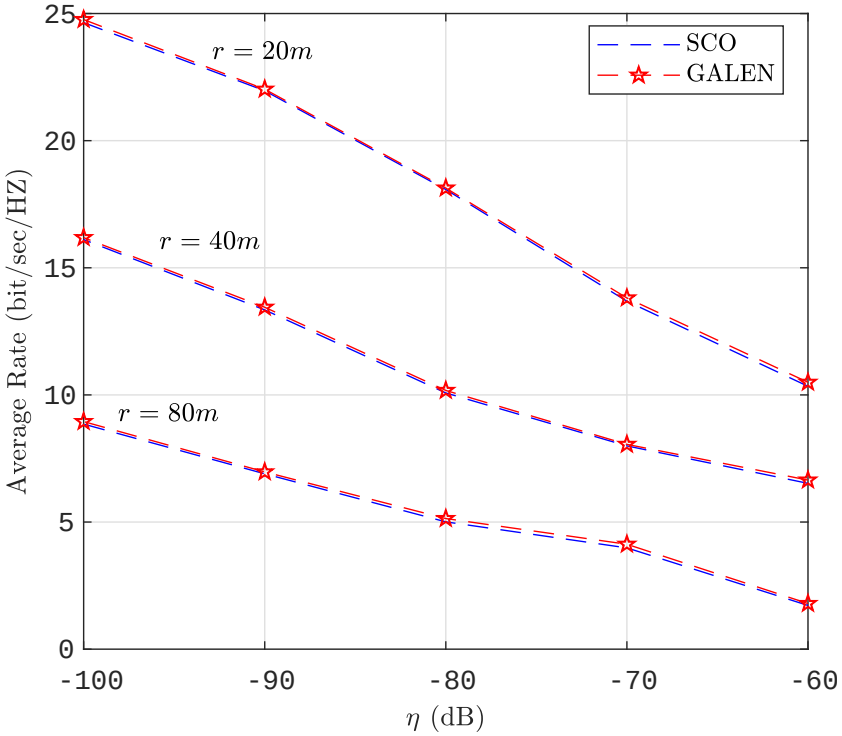

Figure 2.7 – Comparison of FD-D2D rate obtained from the SCO-based method and the proposed GALEN framework.

Moreover, to highlight the importance of GALEN, we report in Table 2.2 the complexity of SCO in terms of the required number of iterations to achieve the solution. As it can be seen, on average SCO requires three to five iterations to obtain the solution. In addition, at each iteration SCO requires using a convex optimization solver to solve the approximated convex problem. On contrary, the proposed method can find the optimal solution with only one iteration and without using any optimization solver as indicated in Theorem 1 and Theorem 2. This low complexity feature of GALEN makes the analysis of an FD-D2D network easier and much more attractive.

FD-D2D or HD-D2D

Here we aim to investigate the performance of the FD-D2D communication, and see if it always outperforms the HD-D2D mode. In Fig.2.8 we compare the FD-D2D performance with the HD-D2D in terms of the average *D2D* rate. In particular, Fig. 2.8 shows the variation of the *D2D* rate w.r.t the SI cancellation factor and for different *D2D* cluster radius. As it can be seen, at low self interference cancellation in the FD mode, the HD mode outperforms FD. In

Table 2.2 – Average number of Iterations for the SCO method

η (dB)	Number of Iterations	
	$r = 20m$	$r = 40m$
-50	2.41	2.28
-60	2.45	2.35
-70	2.59	2.41
-80	3.34	2.88
-90	4.98	3.79
-100	6.15	5.42

addition when the separation between the *D2D* users increases the FD mode needs higher SI cancellation to outperform the HD mode. As a result, the FD gain mainly appears when the *D2D* users are close to each other and they have high SI cancellation capability. Hence, to achieve the maximum gain from the *D2D* technology, a mode selection step must always be taken into consideration when allocating the resources for the users.

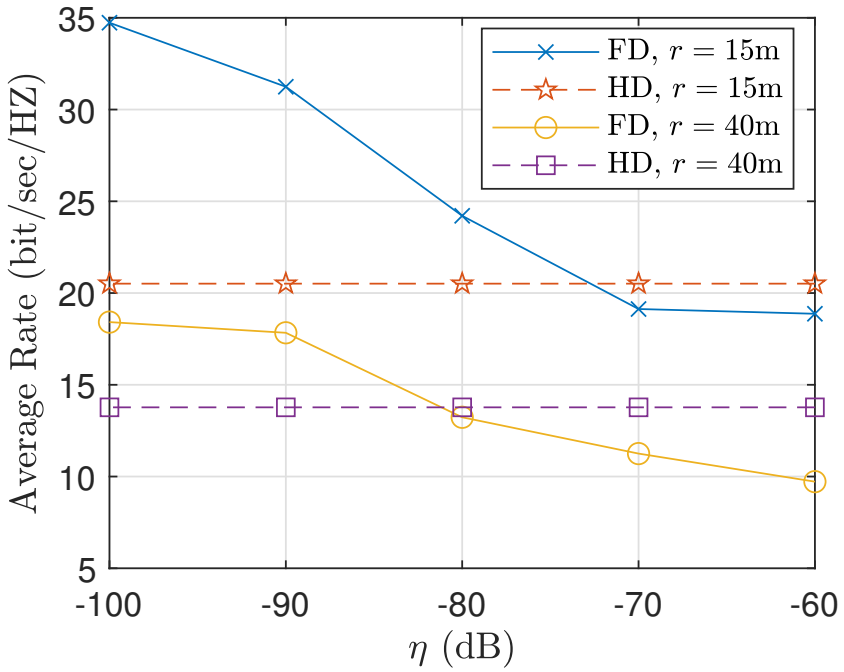

Figure 2.8 – Comparison of the FD-D2D rate and the HD-D2D rate.

To show the effect of the *CU* location on the optimal duplex mode selection we first set $D1$ and $D2$ at a distance equal to $100m$ and $140m$ from the *BS*. Then we moved the *CU* toward the *D2D* pair and at each step we computed the optimal transmission powers as shown in Fig. 2.9. From Fig. 2.9 we can see that when *CU* is near the *BS* and far from the *D2D* pair ($d_{c,BS} = 20m$) both $D1$ and $D2$ can transmit with their maximum powers. However, when the *CU* becomes close to $D1$ the transmission power of $D2$ decreases and at the point $d_{c,BS} = 70m$

only D1 must transmit to achieve the optima. This is because starting from this point $D1$ will face high interference from the CU and thus it is better to send messages rather than receiving messages. The same analogy can be applied to the case where the CU is closer to $D2$. On the other hand, p_c increases with the increasing of $d_{c,BS}$. This is because the CU has QoS constraint. As a result, the CU location highly affects the optimal mode selection.

In the same direction and to further highlight the impact of the CU location on the optimal $D2D$ transmission mode, we reset the $D2D$ users at 100m and 140m from the BS. Then, we moved the CU on a random trajectory which covers almost all the cell. At each position we computed the optimal $D2D$ transmission mode and we colored the CU's location accordingly. As expected, when the CU is far from the $D2D$ pair, the yellow area in Fig. 2.10, the optima is achieved by using the FD mode. However, when the CU is close to the $D2D$ pair, the blue sector in Fig 2.10, the optima can be achieved by switching to the HD mode which is inline with the results obtained in the previous ergodic numerical assessment section.

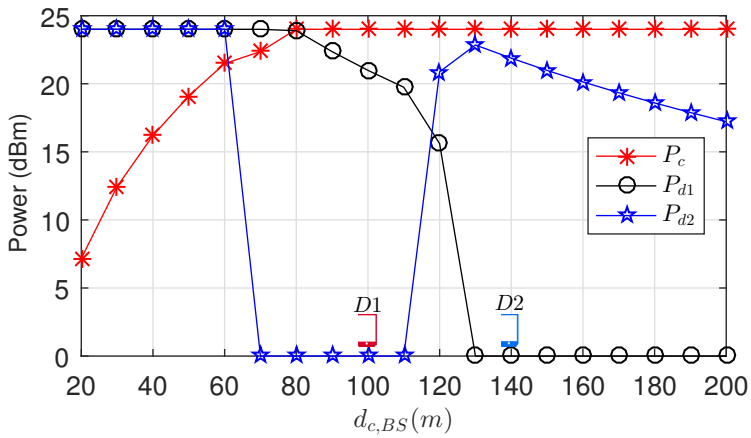

Figure 2.9 – The effect of the CU location on the optimal power ($\eta = -70dB$).

2.5 Conclusions

In this chapter, we first investigated the ergodic rate performance of an FD-D2D based cellular network. In particular, we formulated an ergodic rate optimization problem to maximize the FD-D2D ergodic rate while keeping the average $D2D$ interference at a certain level. We further proposed a closed-form expression for the optimal power-ratio allocation strategy. On contrary to the related works, the derived solution covered both the symmetric and the asymmetric scenarios. The simulation results proved the derived equation and showed that the distance from the interferer cellular user, the distance between the $D2D$ pair, and the SIC factor have a great impact on the FD-D2D ergodic capacity and the power allocation scheme. For instance, when CU is relatively far from the $D2D$ pair the optima will be achieved by allocating more

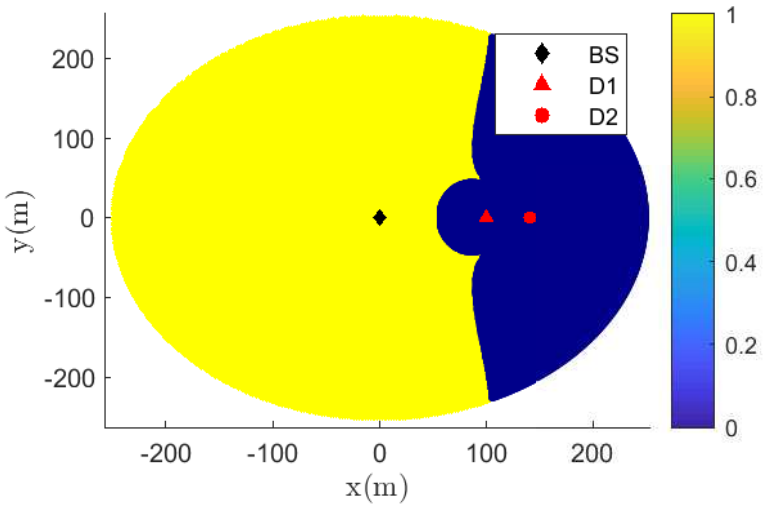

Figure 2.10 – The effect of the *CU* location on the optimal D2D transmission mode ($\eta = -70dB$).

power to the *D2D* user who is introducing less interference power to the base station. While when the *CU* is relatively near the *D2D* pair, more power should be allocated to the *D2D* user who is suffering more from the *CU* interference power. Finally, both simulation and analysis showed that the maximum FD-D2D rate occurs when the *D2D* users are sharing the spectrum of *CU* who is located near the *BS* and far away from the *D2D* pair. As a result the users location or in general the users' interference highly affects the *D2D* rate and thus it should be well treated in the resource allocation phase.

After that, we propose two frameworks to solve instantaneous rate maximization problem of an FD-D2D network. The first framework yields to a first-order optimal solution by using the SCO theory. The second framework called GALEN takes advantage of the geometric shape of the feasible set to achieve the optimal solution with low complexity. The derived approach has been validated in simulation results. Among the different results, it is important to re-highlight the impact of the *CU* location on the *D2D* transmission mode as well as the capabilities of the *D2D* devices to reduce the self-interference in the FD mode.

Although in this chapter we could obtain the optimal PA strategy, the proposed GALEN framework seems to be intractable with any changing in the considered scenario. For instance, if we assume that the *D2D* users are rate-constrained the proposed GALEN will be unable to obtain the optimal solution. This is indeed a major drawback because in a read FD-D2D application both *D2D* users look to ensure their QoS. Moreover, given the battery consumption problem or generally the network energy consumption issue, the proposed GALEN framework seems to be unable to maximize the network's energy efficiency or even the total sum-rate of the network. Besides, throughout all this chapter, only a simple scenario in which a single *D2D* pair sharing the UL spectrum of one *CU* in a single cell network was considered.

To complete this work, in the next chapter we consider an FD-D2D network in which multiple FD-D2D pairs coexist with multiple CUs, and then we address the joint channel assignment and power allocation optimization problem which aims to maximize the energy efficiency of the network, as well as the total rate, i.e., the rate of both cellular users and *D2D* users. The derived solutions therein are mathematically tractable and they achieve the global optimal solution by using the monotonic optimization theory and the fractional programming tools.

Chapter 3

Joint Power Allocation and Channel Assignment Scheme for FD-D2D Network

Contents

The former chapter established the concept of an FD-D2D network and emphasized the importance of users' power allocation and channel assignment in controlling the complex interference environment of this network. Then, we tackled the PA problem in Chapter 2 by providing several PA algorithms such as GALEN and the SCO based PA approach. Our goal in this chapter is to address the joint PA and CA problem of an FD-D2D network.

This kind of problem has been studied only in [119] and [120]. The authors of [119] aimed to maximize the sum-rate of an FD-D2D network by considering both the power allocation PA and the channel assignment (CA) problems. Besides the sum-rate, the energy consumption became an important criteria design for the 5G network. In [120] an energy-efficient resource allocation for FD-D2D based cellular network was provided. However, both works provided the sub-optimal solution of the RA optimization problem. In particular, both [119] and [120] rely on the SCO theory presented in Chapter 2 to solve the PA problem of an FD-D2D based cellular network. The latter is guaranteed to provide only the first-order optimal solution. Thus, both works did not find the global optimal gain of an FD-D2D network, and the gap to the optimal solution is still unknown.

This chapter aims to fill this blank and derive the maximum gain of an FD-D2D network by providing an efficient global optimization framework. To that end, first we present in Section 3.1 our system model, and we formulate the RA problem as a maximization problem of a general SINR based network-centric metrics such as the *WSR* and the *GEE*. Next, we show in Section 3.2 that both the *WSR* maximization problem and the *GEE* optimization problem can be decomposed into two sub-problems as PA and CA. Hence, the global solution of the original RA problem can be found by globally solving the PA and CA sub-problems sequentially. The PA sub-problem is known to be a non-convex problem in an interference limited scenario, and thus it is hard to achieve the global optimal solution. To overcome this issue, we propose in Section 3.3 to use the Monotonic Optimization theory (MO) to globally solve the PA problem. The MO theory can globally solve the optimization problems where the utility and the constraints are monotonically increasing functions of the optimization variables, even if the optimization problem is non-convex [24, 127]. In general, both WSR and GEE are non-monotone functions of the transmit power. However, they are monotone functions of SINR, and thus they exhibit hidden monotonocity structure that allows us to find the global solution by means of MO framework.

The MO problem can be solved by using the existing Outer Polyblock Approximation algorithm (OPA) at the expense of high complexity [24]. In particular, the OPA tries to approximate the outer boundary of the feasible set by a tight polyblock, and thus the global optimal point can be found by searching the set of the polyblock vertices. Using the existing OPA leads to a rapid growth in the number of vertices, and thus to high complexity. To solve this issue, we propose in Section 3.3 a new power allocation algorithm which aims to decline the complexity of the OPA by trimming down the unnecessary vertices. For the sake of

clarity, we denote this new algorithm as Polyblock vertices triMming bAsed poweR allocatIOn (MARIO). Then, based on the optimal PA solution, the CA sub-problem becomes an assignment problem which can be well addressed by Khun-Munkers algorithm (Hungarian algorithm) [128]. Appendix C provides an informal description about the Hungarian method with good example. Hence, the optimal RA solution can be obtained by finding the global optimal transmit powers by means of MO theory for all the possible couplings between the FD-D2D pairs and the CUs and then assigning the best CU reuse partner for each FD-D2D pair by means of Khun-Munkers algorithm as presented in Section 3.4. Thus, even with the proposed MARIO algorithm, the global optimal solution still has high complexity. Motivated by the need of an efficient RA solution, we propose in Section 3.5 a novel algorithm, CATPA, which first assigns the channels for the different FD-D2D pairs, and then allocates the transmit power for each FD-D2D pair and its reuse partner. In particular, we propose a new metric, denoted as *Profit*, that quantifies the profit of an FD-D2D pair when reusing the channel of a CU, and then we assign the CU reuse partner for each D2D pair based on the highest profit values. After that, we allocate the transmit power for each D2D pair and its CU reuse partner by means of the SCO framework. This new algorithm highly reduces the complexity of the solution, since it avoids solving the PA problem for all the possible couplings between the FD-D2D pairs and the CUs. Finally, we present in Section 3.6 the simulation results of the different proposed algorithms, and we conclude this chapter in Section 3.7.

An outline of the conventional RA solution adopted in [119, 120] as well as the proposed RA solutions for an FD-D2D network is depicted in Fig.3.1. In this figure, $N \times M$ counts the number of all the possible couplings between M D2D pairs that coexist with N CUs. Besides, to ease following this chapter, we show in Fig. 3.1 the sections or the references where every step is developed.

The main contribution of this chapter can be summarized as follows:

- Deriving the ultimate gain of an FD-D2D network by globally solving the RA problem of an FD-D2D based cellular network, unlike the previous related works that only provide a sub-optimal RA scheme. The global solution is found by first decomposing the original RA problem into two sub-problems as PA and CA, and then globally solving each sub-problem individually.

- Providing insights into the importance of monotonic optimization theory in globally solving the PA optimization problem for an FD-D2D networks and more generally for any wireless cellular network. To the best of our knowledge, this is the first time in which the MO theory is applied to find the global RA solution in an FD-D2D based cellular network.

- Proposing a novel algorithm, referred to as MARIO, to obtain the global optimal solution of the PA problem. The proposed algorithm is designed based on the existing OPA

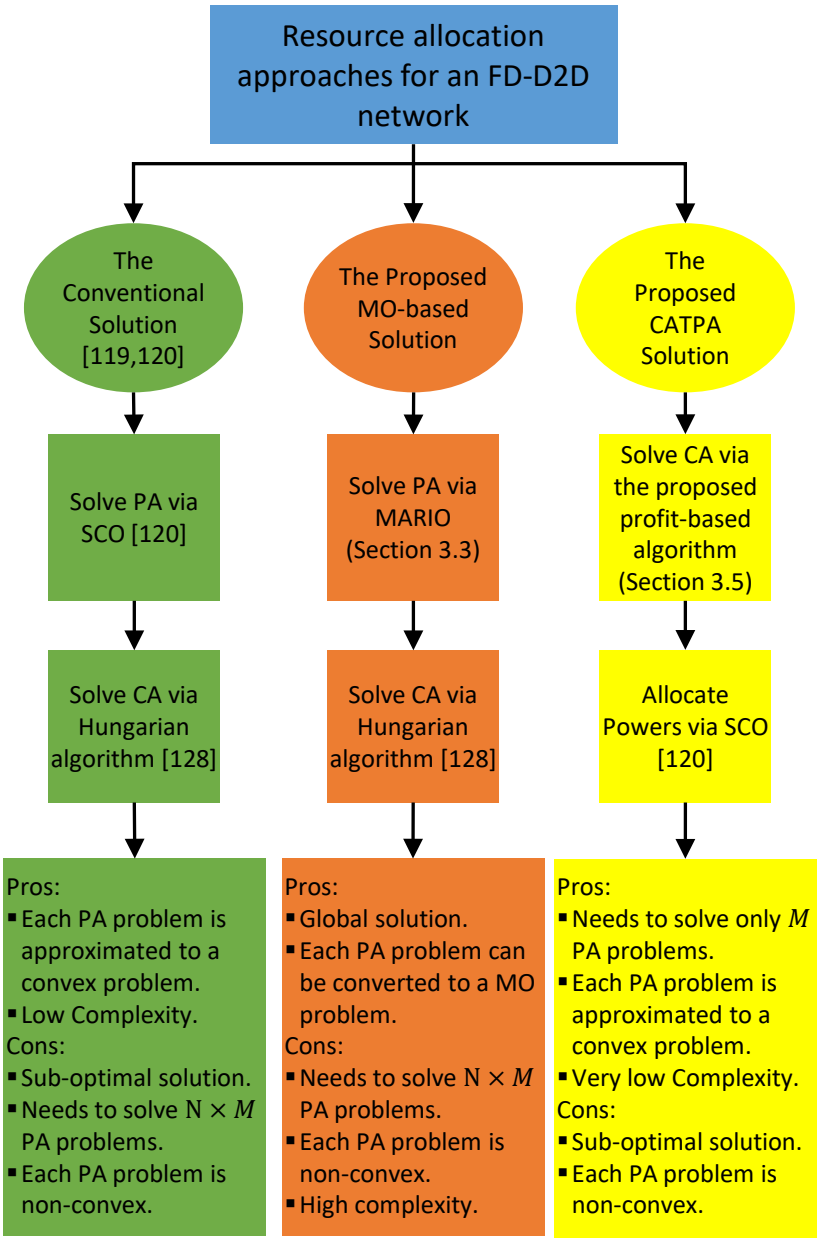

Figure 3.1 – A comparison between the existing RA solution and the proposed RA solutions for an FD-D2D network.

algorithm, and thus it obtains the solution by constructing a series of shrinking polyblocks that eventually closely approximate the boundary of the feasible set of the PA problem around the global solution. On the contrary to OPA, MARIO has a faster convergence time, since it trims down the unnecessary vertices of the generated polyblocks. The effectiveness of MARIO is validated through numerical simulation which employs OPA as

a benchmark. The results show that MARIO can achieve the same optimal point as OPA but within less number of iterations.

- Proposing an effective heuristic RA algorithm, referred to as CATPA, which first assigns the channels for the different users and then allocates the powers. We believe that this is the first work that provides such a methodology to solve the RA problem. To validate the proposed CATPA algorithm a numerical simulation is applied that employs the global optimal solution as a benchmark. Simulation results show that CATPA can achieve a solution within the 90% of the global optimal within a much lower number of iterations.
- Providing a comprehensive analysis of the FD-D2D network, by comparing the performance of the FD-D2D network with its counterpart HD-D2D network. Moreover, the effect of the different network parameters such as the QoS of the users, the maximum transmit powers of the devices, the D2D proximity distances, and the SI cancellation capability of the FD nodes, on the FD-D2D network performance have also been addressed.

3.1 System Model

As depicted in Fig. 3.2 (a), we consider an uplink resource allocation scenario where N cellular users share the uplink (UL) spectrum with M *D2D* pairs in a single cell system. In particular, uplink spectrum sharing is considered since UL resources are underutilized comparing to that of downlink [16, 129]. Furthermore, reusing UL resources in D2D links only affects the BS and incurred interference can be handled by BS coordination. The N CUs and the M D2D pairs are respectively organized in the sets $\mathcal{C} = \{CU_1, \ldots, CU_N\}$ and $\mathcal{D} = \{D2D_1, \ldots, D2D_M\}$, where CU_i and $D2D_j$ stand for the ith cellular user and the jth D2D pair respectively. Each D2D_j consists of two nearby devices denoted as D_1^j and D_2^j, and they have the capability to operate in FD mode while the CUs are assumed to operate only in HD mode.

The available UL bandwidth is composed of N orthogonal channels, and it is organized in the index set $CH = \{1, \ldots, N\}$. Without loss of generality, the ith channel is assumed to be pre-assigned to CU_i. Thus, in this chapter, we aim to allocate these channels to the M *D2D* pairs efficiently. Sharing the UL spectrum between the *D2D* users (DUs) and the CUs generates co-channel interference between the users sharing the same channel. Therefore, to limit the interference from the *D2D* pairs on the cellular links and avoid the interference between the *D2D* pairs, similar to [16, 86, 119, 120] , we require that each UL channel is allowed to be shared with at most one *D2D* pair, and each $D2D_j$ can reuse at most one UL channel.

With the above channel assignment constraints and assuming imperfect SI cancellation, the interference model when $D2D_j$ and CU_i transmit on the ith channel can be depicted as in Fig. 3.2 (b). In this Figure, we define the channel gains as follows:

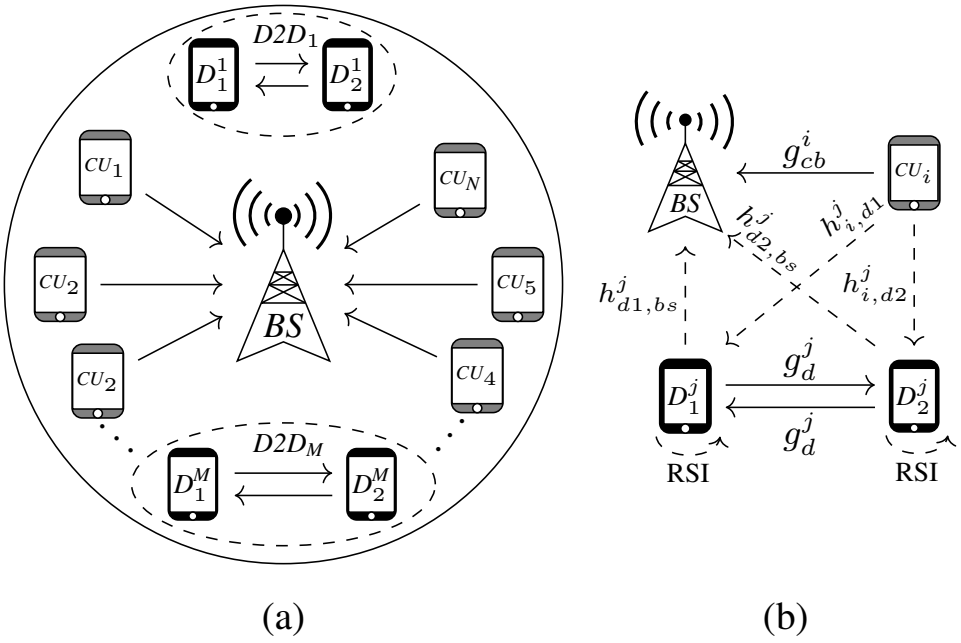

Figure 3.2 – The adopted system model in which (a) multiple FD-D2D pairs coexist with multiple cellular users, and (b) the interference model when the cellular user CU_i shares its uplink resources with $D2D_j$.

- $g^i_{\text{c,bs}}$ denotes the direct channel gain between CU_i and BS.
- g^j_d stands for the direct channel gain between the D2D users of $D2D_j$. Here, the *D2D* channel is assumed reciprocal, since both D^j_1 and D^j_2 are using the same UL channel and they are close to each other.
- $h^j_{d1,bs}$ and $h^j_{d2,bs}$ respectively stand for the interference channel gain from D^j_1 to BS and from D^j_2 to BS.
- $h^j_{i,d1}$ and $h^j_{i,d2}$ denote the interference channel gain from CU_i to D^j_1 and D^j_2 respectively.
- RSI is the residual self interference due to the imperfect SI cancellation at the FD devices.

All direct/interference channels are assumed to be zero-mean complex Gaussian random variables (i.e., channels are expressing Rayleigh fading) with variance l_{ij}, where $i \in \{c; d1; d2\}$, $j \in \{bs; d1; d2\}$, $i \neq j$, l_{ij} denotes the pathloss between the nodes i and j. The RSI can be modeled as complex Gaussian random variables with zero-mean and variance ηp_{tx} [25,90,104,106,107,112], where p_{tx} is the transmission power of the FD device, η denotes the SI cancellation capability of the FD transmitter. Without loss of generality, assuming that all *D2D* users have the same SI cancellation capability, the power of RSI at D^j_1 and D^j_2 are respectively expressed by ηp^j_{d1} and ηp^j_{d2}, with p^j_{d1}, and p^j_{d2} being respectively the transmission powers of D^j_1, and D^j_2 .

Now, denote by p_c^i the transmit power of CU_i, and let σ_N^2 represents the power of white Gaussian noise on each UL channel. Then, the SINRs of CU_i, D_1^j, and D_2^j, when CU_i shares its channel with $D2D_j$, can be respectively expressed as

$$\Gamma^i(\mathbf{p}_{ij}) = \frac{\Gamma_i^+}{\Gamma_i^-} = \frac{p_c^i g_{\mathrm{c,bs}}^i}{p_{d1}^j h_{d1,bs}^j + p_{d2}^j h_{d2,bs}^j + \sigma_N^2}, \tag{3.1}$$

$$\Gamma^{j_1}(\mathbf{p}_{ij}) = \frac{\Gamma_{j_1}^+}{\Gamma_{j_1}^-} = \frac{p_{d2}^j g_d^j}{p_c^i h_{i,d1}^j + \eta p_{d1}^j + \sigma_N^2}, \tag{3.2}$$

$$\Gamma^{j_2}(\mathbf{p}_{ij}) = \frac{\Gamma_{j_2}^+}{\Gamma_{j_2}^-} = \frac{p_{d1}^j g_d^j}{p_c^i h_{i,d2}^j + \eta p_{d2}^j + \sigma_N^2}. \tag{3.3}$$

where $\mathbf{p}_{ij} = [p_{d1}^j, p_{d2}^j, p_c^i]$ is the power allocation vector for D2D$_j$ and CU_i on the ith channel. Moreover, in the above equations, the SINR function $\Gamma^k,\ k \in \{i, j_1, j_2\}$, is expressed as a fraction of two non-negative functions denoted as $\Gamma_k^+(\mathbf{p}_{ij})$ and $\Gamma_k^-(\mathbf{p}_{ij})$. The benefits of these functions will appear later on when deriving the optimal RA scheme.

By applying Shannon's theorem, the data rates (in bits/s) of CU$_i$, D_1^j, and D_2^j can be respectively expressed as

$$\begin{aligned} R^i(\mathbf{p}_{ij}) &= B_i \log_2(1+\Gamma^i),\ i \in \{\mathcal{C}\} \\ &= B_i(\log_2(\Gamma_i^+ + \Gamma_i^-) - \log_2(\Gamma_i^-)) \\ &= r_i^+(\mathbf{p}_{ij}) - r_i^-(\mathbf{p}_{ij}) \end{aligned} \tag{3.4}$$

$$\begin{aligned} R^{j_1}(\mathbf{p}_{ij}) &= B_i \log_2(1+\Gamma^{j_2}), j \in \mathcal{D} \\ &= B_i \log_2(\Gamma_{j_1}^+ + \Gamma_{j_1}^-) - B_i \log_2(\Gamma_{j_1}^-) \\ &= r_{j_1}^+(\mathbf{p}_{ij}) - r_{j_1}^-(\mathbf{p}_{ij}) \end{aligned} \tag{3.4a}$$

$$\begin{aligned} R^{j_2}(\mathbf{p}_{ij}) &= B_i \log_2(1+\Gamma^{j_1}), j \in \mathcal{D} \\ &= B_i \log_2(\Gamma_{j_2}^+ + \Gamma_{j_2}^-) - B_i \log_2(\Gamma_{j_2}^-) \\ &= r_{j_2}^+(\mathbf{p}_{ij}) - r_{j2}^-(\mathbf{p}_{ij}) \end{aligned} \tag{3.4b}$$

where B_i is the bandwidth of the ith UL channel. Since we are assuming that all the available channels are equally shared by the active CUs, in the sequel we refer to B_i by B. Besides, in the above equations, the achievable rate $R^k, k \in \{i, j_1, j_2\}$, is expressed as the difference of two non-negative functions $r_k^+ \triangleq B\log_2(\Gamma_k^+ + \Gamma_k^-)$ and $r_k^- \triangleq B\log_2(\Gamma_k^-)$. The application of this form will appear in Section IV when deriving the optimal power allocation scheme. Now, before terminating this section and starting formulating the problem, we introduce a useful remark to be used later to derive the optimal RA scheme.

Remark 1: *The functions* $r_k^+, r_k^-, \Gamma_k^+, \Gamma_k^-, k \in \{i, j_1, j_2\}$ *are all increasing functions with* $\boldsymbol{p}_{ij}$. *However, the rate functions* $R^i(\boldsymbol{p}_{ij}), R^{j_1}(\boldsymbol{p}_{ij})$, *and* $R^{j_1}(\boldsymbol{p}_{ij})$, *and the SINRs* Γ^i, Γ^{j_1}, *and* Γ^{j_2} *are in general non-increasing functions with* $\boldsymbol{p}_{ij}$.

3.1.1 Problem formulation

In a fully loaded UL network, the FD-D2D communication can be used to accommodate more users, and thus to enhance the performance of the cellular network. However, since the *D2D* pairs are reusing the cellular spectrum, a proper RA is required to maintain the QoS of the *D2D* pairs and their reuse CUs partners and mitigate the mutual interference between the different type of links. In this chapter, we aim to maximize the rate gain that can be brought by the *D2D* communication and minimize the energy cost of the *D2D* communication. Thus, we define two objective functions to be maximized while guaranteeing the QoS of all the links and respect the maximum allowed powers. The first utility function (U_1) is the *WSR* of the admitted *D2D* pairs and their corresponding CUs reuse partners, and it is defined as

$$U_1(\rho, \mathbf{P}) = \sum_{i \in \mathcal{C}} \sum_{j \in \mathcal{D}} \varrho_{ij} [\omega_i R^i + \omega_{j_1} R^{j_1} + \omega_{j_2} R^j_{d2}]. \tag{3.5}$$

where ω_i, ω_{j_1}, and ω_{j_2} are positive weights used to control the individual rates of CU_i, D_1^j, and D_2^j respectively. ϱ_{ij} is the resource reuse indicator for D2D$_j$ and CU_i, when D2D$_j$ shares the CU$_i$'s resources $\varrho_{ij} = 1$; otherwise $\varrho_{ij} = 0$. $\mathbf{P} = [\mathbf{p}_{ij}]$ is the power allocation matrix for all CUs and DUs and $\rho = [\varrho_{ij}]$ denotes the channel assignment matrix of the *D2D* pairs.

The second utility function (U_2) is the *GEE* of the D2D pairs and their reuse partners. It is defined as the energy cost of the accepted D2D links and their corresponding cellular links, and it can be expressed as

$$U_2(\rho, \mathbf{P}) = \frac{U_1(\rho, \mathbf{P})}{\sum_{i \in \mathcal{C}} \sum_{j \in \mathcal{D}} \rho_{ij} \mu (p_c^i + p_{d1}^j + p_{d2}^j) + 3MP_{cir}}. \tag{3.6}$$

wherein $\mu \geq 1$ is the inverse of the power amplifier efficiency at each transmitter. P_{cir} denotes the fixed circuit power consumption at each device, accounting for the dissipation in analog hardware and digital signal processing [130].

Therefore, the resource allocation problem can be formulated as follows

$$P1_l : \max_{(\rho, \mathbf{P}) \in \Omega} \quad U_l(\rho, \mathbf{P}), l = 1, 2. \tag{3.7}$$

$$\Omega = \Big\{ \Gamma^i \geq \gamma_{\min}^i = 2^{r_{\min}^i} - 1, \forall i \in \mathcal{C}, \tag{3.7a}$$

$$\Gamma^{j_1} \geq \gamma_{\min}^{j_1} = 2^{r_{\min}^{j_1}} - 1, \forall j \in \mathcal{D}, \tag{3.7b}$$

$$\Gamma^{j_2} \geq \gamma_{\min}^{j_2} = 2^{r_{\min}^{j_2}} - 1, \forall j \in \mathcal{D}, \tag{3.7c}$$

$$\sum_{i} \varrho_{ij} \leq 1, \varrho_{ij} \in \{0,1\}, \forall j \in \mathcal{D}, \tag{3.7d}$$

$$\sum_{j} \varrho_{ij} \leq 1, \varrho_{ij} \in \{0,1\}, \forall i \in \mathcal{C}, \tag{3.7e}$$

$$\mathbf{0}_3 \preceq \mathbf{p}_{ij} \preceq \mathbf{p}_{\max}, \forall j \in \mathcal{D}, i \in \mathcal{C}\Big\} \tag{3.7f}$$

where Ω is the feasible set of $P1$, $\mathbf{p}_{\max} = [P_{\max}^{d1}, P_{\max}^{d2}, P_{\max}^{c}]$ is the maximum power vector for any possible pair (D2D$_j$,CU$_i$), and $\mathbf{0}_3 = [0,0,0]$ is the minimum power vector. $\gamma_{\min}^{i}$, $\gamma_{\min}^{j_1}$, $\gamma_{\min}^{j_2}$ denote the minimum required SINR to achieve the minimum rate requirements $r_{\min}^{i}$, $r_{\min}^{j_1}$, and $r_{\min}^{j_2}$ for CU_i, D_1^j, and D_2^j respectively. Hence, constraints (3.7a)-(3.7c) represent the QoS requirements (rate requirements) for CU_i, D_1^j, and D_2^j respectively. Constraint (3.7d) ensures that a *D2D* pair reuses at most the resource of one CU. Constraint (3.7e) indicates that a CU_i can share its resources with at most one *D2D* pair. Constraint (3.7f) ensures that the transmit power of any user is within the maximum limit.

3.2 Problem Decomposition

The authors of [131] have proved that the power allocation problem by itself is an NP problem in an interference limited system. The resource allocation problem (P1) defined in the previous section contains both power allocation and CA problems, and thus it is more complex than the PA problem which is already NP-hard. In this section, we show that the solution of both $P1_1$ and $P1_2$ can be found by decoupling the original problem into two sub-problems. The first one is the power allocation and the second is the channel assignment problem. The decomposition technique reduces the complexity of the original problem, but the NP-hardness of the PA still exists. In the next sections, we present efficient algorithms to globally solve the PA and the CA problems individually.

3.2.1 Decomposition of $P1_1$

Observe that in the utility function U_1 the variables ϱ_{ij} and $\mathbf{p}_{ij}$ are disjoint and thus the maximization problem $P1_1$ can be rewritten as follows:

$$P1_1 : \underset{\rho_{ij} \in \{0,1\}}{\text{maximize}} \sum_{i \in \mathcal{C}} \sum_{j \in \mathcal{D}} \varrho_{ij} \underset{\mathbf{p}_{ij}}{\text{maximize}} U_1^{ij}, \text{ s.t. } (3.7a) - (3.7f), \tag{3.8}$$

wherein $U_1^{ij} = \omega_i R_c^i + \omega_{j_1} R^{j_1} + \omega_{j_2} R_{d2}^j$ is the *WSR* of the pair $(D2D_j, CU_i)$. Accordingly, $P1_1$ can be decomposed to the following two sub-problems:

$$P2_1 : \underset{\mathbf{P}_{ij}\in\Phi, i\in\mathcal{C}, j\in\mathcal{D}}{\text{maximize}} \; U_1^{ij}, \text{ s.t. } \Phi = \{(3.7a), (3.7b), (3.7c), (3.7f)\}, \tag{3.9}$$

$$P3_1 : \underset{\rho_{ij}\in\{0,1\}}{\text{maximize}} \sum_{i\in\mathcal{C}} \sum_{j\in\mathcal{D}} \varrho_{ij} U_1^{ij\star}, \text{ s.t. } (3.7d), (3.7e), \tag{3.10}$$

where $U_1^{ij\star}$ is the optimal solution of the PA sub-problem $(P2_1)$. Thus, the optimal solution of $P1_1$ can be found by finding the optimal power allocation of all the possible pairs $(D2D_j, CU_i)$, and then selecting the optimal CU reuse partner for each D2D pair.

3.2.2 Decomposition of $P1_2$

Giving the fractional nature of the *GEE* utility function, it is clear that $P1_2$ belongs to the class of fractional programming theory. Thus, the solution of $P1_2$ can be found by means of fractional programming tools [132], such as Dinkelbach's algorithm. The latter is an iterative process which requires to solve the following auxiliary problem at iteration k:

$$\begin{aligned} &F(\lambda_k) = \\ &\underset{(\rho,\mathbf{P})\in\Omega}{\text{maximize}} \; \sum_{i\in\mathcal{C}} \sum_{j\in\mathcal{D}} \varrho_{ij}[\omega_i R_c^i + \omega_{j_1} R^{j_1} + \omega_{j_2} R_{d2}^j] \\ &\qquad - \lambda_k \left(\sum_{i\in\mathcal{C}} \sum_{j\in\mathcal{D}} \rho_{ij}\mu(p_c^i + p_{d1}^j + p_{d2}^j) + 3MP_{cir} \right) \\ =&\underset{(\rho,\mathbf{P})\in\Omega}{\text{maximize}} \sum_{i\in\mathcal{C}} \sum_{j\in\mathcal{D}} \varrho_{ij} \underbrace{\left(\begin{array}{c} \omega_i R_c^i + \omega_{j_1} R^{j_1} + \omega_{j_2} R_{d2}^j \\ - \lambda_k \mu \left(p_c^i + p_{d1}^j + p_{d2}^j \right) \end{array} \right)}_{U_2^{ij}} - P_{\text{cons}} \\ =&\underset{\rho\in\{0,1\}}{\text{maximize}} \sum_{i\in\mathcal{C}} \sum_{j\in\mathcal{D}} \varrho_{ij} \underset{\mathbf{p}_{ij}}{\text{maximize}} \, U_2^{ij}(\lambda_k, \mathbf{p}_{ij}) \end{aligned} \tag{3.11}$$

wherein $P_{\text{cons}} = \lambda_k 3MP_{cir}$. The last step in (3.11) is because the variable ϱ_{ij} is disjoint than the variables $(\lambda_k, \mathbf{p}_{ij})$, and P_{cons} is a constant. Then, and similar to $P1_1$, the maximization of *GEE* can be divided into PA and CA sub-problems. The only difference is that PA has to be iteratively solved until convergence. Mathematically, the PA and CA problems can be expressed respectively as follows.

$$P2_2 : \underset{\mathbf{P}_{ij}, i\in\mathcal{C}, j\in\mathcal{D}}{\text{maximize}} \; U_2^{ij}, \text{ s.t. } (3.7a), (3.7b), (3.7c), (3.7f), \tag{3.12}$$

$$P3_2 : \underset{\rho_{ij}\in\{0,1\}}{\text{maximize}} \sum_{i\in\mathcal{C}} \sum_{j\in\mathcal{D}} \varrho_{ij} U_2^{ij\star}, \text{ s.t. } (3.7d), (3.7e), \tag{3.13}$$

where $U_2^{ij\star}$ is the optimal power allocation of problem $P2_2$. For the reader's convenience, we report in Algorithm 1 the Dinkelbanch's algorithm which solves $P2_2$. Despite the complexity of solving $U_2^{ij}(\lambda_k, \mathbf{p}_{ij})$, the Dinkelbanch's algorithm exhibits a *super-linear* convergence rate, since λ_k is updated according to Newton's method [132]. For more detail about the fractional programming and Dinkelbach's algorithm, the reader may refer to [133]. Solving efficiently $U_2^{ij}(\lambda_k, \mathbf{p}_{ij})$ at each iteration is the target of the next section.

Remark 2: *In the first iteration of Dinkelbach's algorithm, i.e., when $\lambda_0 = 0$, Algorithm 1 finds the solution of the WSR problem. Hence, it is highly desirable to develop an algorithm which can solve both WSR and GEE problems.*

Here it is worthy to note that the PA sub-problem ($P2_l$) and the CA sub-problem ($P3_l$) must be sequentially solved to obtain the global solution of the original RA problem $P1_l$, $l \in \{1, 2\}$. As indicated in the second column of Fig.1, solving the PA sub-problem is the target of the next section while the CA is the task of Section V.

Algorithm 1 Dinkelbach's algorithm

1: Set $\epsilon > 0$, λ_0=0, and $k = 0$
2: **repeat**
3: Solve $P2_2$ defined in (3.12) and denote the optimal power vector as $\mathbf{p}_{k,ij}^{\star}$.
4: $k = k + 1$
5: $\lambda_k = \frac{\omega_i R_c^i(\mathbf{p}_{ij}^{k\star}) + \omega_{j_1} R^{j_1}(\mathbf{p}_{ij}^{k\star}) + \omega_{j_2} R_{d2}^{j}(\mathbf{p}_{ij}^{k\star})}{\mu(p_c^{i\star} + p_{d1}^{j\star} + p_{d2}^{j\star}) + 3P_{cir}}$
6: **until** $U_2^{ij}(\lambda_{k-1}, \mathbf{p}_{k-1,ij}^{\star}) \leq \epsilon$

3.3 Power allocation

The complicated interference coupling between the *D2D* pairs and their reuse partners turns the PA problem to be a non-convex problem. Thus, the global optimal solution of PA is hard to obtain because it may require examining every point in the feasible set. The monotonic optimization (MO) theory provides a guaranteed convergence to the global optimal solution and reduces the computational complexity by exploiting the monotonicity property of the utility function and the constraints to solve the optimization problem. The key idea behind MO is to search for the global solution on the outer boundary of the feasible set instead of exploring the complete feasible set of the problem. Nevertheless, we note that the complexity of MO increases exponentially with the number of optimization variables. However, it is much lower than general global optimization methods, which do not exploit the monotonocity property of the problem. Naturally, the usage of MO is limited to the problems enjoying a monotonocity structure as indicated in the following definition.

Definition 3.1. *An optimization problem belongs to the class of MO if it can be written in the following form [134]:*

$$\underset{x}{maximize}\, f(x) \;\; s.t. \;\; x \in \mathcal{H}_n \cap \mathcal{H}_c, \tag{3.14}$$

where sets $\mathcal{H}_n$ and $\mathcal{H}_c$ are respectively normal and co-normal closed sets and function, $f(x)$ is an increasing function on $\mathbb{R}_+^N$.

Recall that a function $f : \mathbb{R}^n \mapsto \mathbb{R}$ is increasing if $f(\mathbf{x}) \preceq f(\mathbf{y})$ when $0 \preceq \mathbf{x} \preceq \mathbf{y}$. A set $\mathcal{H}_n \subset \mathbb{R}^n$ is normal set, if for any point $x \in \mathcal{H}_n$, all other points x' such that $x' \leq x$ are also in set $\mathcal{H}_n$. A set $\mathcal{H}_c \subset \mathbb{R}^n$ is co-normal set, if for any point $x \in \mathcal{H}_c$, all other points x' such that $x' \geq x$ are also in set $\mathcal{H}_c$.

At a first sight and based on Definition 1 and Remark 1, the monotonic optimization theory appears to be non-applicable for $P2_1$ and $P2_2$. Thus, in an FD-D2D based cellular network, the first step to efficiently obtain an optimal PA scheme is to transform the non-convex PA problem to an MO problem as shown in Subsection 3.3.1.

3.3.1 Problem Transformation

The aim of this subsection is to convert the PA problem in an FD-D2D network to an MO problem. From **Remark 2**, we know that Dinkelbach's algorithm (Algorithm 1), which is proposed to solve the *GEE* power allocation problem, inherently solves the *WSR* problem at the first iteration when $\lambda = 0$. Hence, in this subsection, we extract the hidden monotonicity property only for $P2_2$ (the *GEE* PA problem). The monotonocity structure of $P1_1$ can be found in the same manner by setting $\lambda = 0$.

To that end, first we reshaped the objective function of $P1_2$, i.e., U_2^{ij} defined in (3.11), as follows:

$$\begin{aligned} U_2^{ij}(\mathbf{p}_{ij}, \lambda_k) &= \sum_{l \in \{i, j_1, j_2\}} \omega_l r_l^+(\mathbf{p}_{ij}) - \sum_{l \in \{i, j_1, j_2\}} \omega_l r_l^-(\mathbf{p}_{ij}) - \lambda_k \mu (p_c^i + p_{d1}^j + p_{d2}^j) \\ &= u^+(\mathbf{p}_{ij}) - u^-(\mathbf{p}_{ij}, \lambda_k) \end{aligned} \tag{3.15}$$

wherein r_l^+ and r_l^- with $l \in \{i, j_1, j_2\}$ are defined in (3.4)-(3.4b), and they are increasing functions as indicated in remark 1. The functions $u^+(\mathbf{p}_{ij})$ and $u^-(\mathbf{p}_{ij}, \lambda_k)$ are also increasing functions because each one is a summation of several increasing functions (Remark 1). Next, we introduce the slack variable $t = u^-(\mathbf{p}_{\max}, \lambda_k) - u^-(\mathbf{p}_{ij}, \lambda_k)$, and we reformulate $P2_2$ as follows:

$$\begin{aligned} \underset{(\mathbf{p}_{ij}, t) \in \Phi}{\text{maximize}} \quad & U_2^{ij}(\mathbf{p}_{ij}, t) = u^+(\mathbf{p}_{ij}) + t \\ \Phi = \Big\{ & (t, \mathbf{p}); 0 \leq t + u^-(\mathbf{p}) \leq u^-(\mathbf{p}_{\max}, \lambda_k) \end{aligned} \tag{3.16}$$

$$\underbrace{\Gamma_l^+(\mathbf{p}_{ij})}_{c_l^+(\mathbf{p}_{ij})} - \underbrace{\gamma_{\min}^l \Gamma_l^-(\mathbf{p}_{ij})}_{c_l^-(\mathbf{p}_{ij})} \geq 0, l \in \{i, j_1, j_2\} \tag{3.17}$$

$$\mathbf{0}_3 \preceq \mathbf{p}_{ij} \preceq \mathbf{p}_{\max} \forall j \in \mathcal{D}, i \in \mathcal{C}\Big\}. \tag{3.18}$$

The objective function of the above problem is now an increasing function, and thus to show that (3.16) is a monotonic optimization problem, it remains to verify that the feasible set Φ is an intersection of a normal and a co-normal set.

According to [24, 127], for any continuous increasing functions $h(x)$ and $g(x)$ on $\mathbb{R}_+^n$ the sets $\mathcal{H}_c = \{x \in \mathbb{R}_+^n | h(x) \leq 0\}$ and $\mathcal{H}_n = \{x \in \mathbb{R}_+^n | g(x) \geq 0\}$ are respectively normal and co-normal sets. Hence, to extract the hidden monotonicity property of $P2$ it only remains to verify that all the constraints in the feasible sets are continuous and increasing functions. It is easily verified that in the feasible set Φ only the QoS constraints defined in (3.17) are in general non-increasing function. By using the same technique as before, i.e., introducing a slack variable, (3.17) can be transformed to an increasing function. However, since the complexity of monotonic optimization problem exponentially increases with the number of optimization variables, we first grouped the QoS constraints defined in (3.17) under a single constraint as shown in (3.19), and then we introduce an auxiliary variable.

$$\begin{aligned}(3.17) \equiv \min_{v,l \in \{i,j_1,j_2\}} \Big[c_v^+(\mathbf{p}_{ij}) - \Big(\sum_v c_v^-(\mathbf{p}_{ij}) - \sum_{l,l \neq v} c_l^-(\mathbf{p}_{ij})\Big)\Big] = \\ \underbrace{\min_{v,l \in \{i,j_1,j_2\}} \Big[c_k^+(\mathbf{p}_{ij}) + \sum_{l,l \neq v} c_l^-(\mathbf{p}_{ij})\Big]}_{c^+(\mathbf{p}_{ij})} - \underbrace{\sum_l c_v^-(\mathbf{p}_{ij})}_{c^-(\mathbf{p}_{ij})} \geq 0\end{aligned} \tag{3.19}$$

Now, by introducing the auxiliary variable $s = c^-(\mathbf{p}_{\max}) - c^-(\mathbf{p})$ the problem defined in (3.16) can be rewritten as follows,

$$\begin{aligned} P2_{mo}: \underset{\mathbf{v}=[\mathbf{p}_{ij},t,s]}{\text{maximize}} \;\; & U_2^{ij}(\mathbf{v}) = u^+(\mathbf{p}_{ij}) + t, \text{ s.t. } \mathbf{v} \in \mathcal{S}_n \cap \mathcal{S}_c \\ \mathcal{S}_n = \Big\{ & (t, \mathbf{p}_{ij}, s) : t + u^-(\mathbf{p}_{ij}, \lambda_k) \leq u^-(\mathbf{p}_{\max}, \lambda_k), \\ & s + c^-(\mathbf{p}_{ij}) \leq c^-(\mathbf{p}_{\max}), \mathbf{p}_{ij} \preceq \mathbf{p}_{\max} \Big\} \\ \mathcal{S}_c = \Big\{ & (t, \mathbf{p}_{ij}, s) : t \geq 0, s + c^+(\mathbf{p}_{ij}) \geq c^-(\mathbf{p}_{\max}), \mathbf{p}_{ij} \succeq \mathbf{0}_3 \Big\}. \end{aligned} \tag{3.20}$$

It is clear that all the functions in $\mathcal{S}_n$ and $\mathcal{S}_c$ are increasing functions. Thus, $\mathcal{S}_n$ and $\mathcal{S}_c$ are respectively normal and co-normal sets. Therefore, $\boldsymbol{P2}_{mo}$ is an MO optimization problem, and thus by using the MO tools such that the outer Polyblock algorithm (OPA) [24, Algorithm 3], the global optimal power allocation for any pair (CU_i,D2D_j) can be obtained. However,

the OPA algorithm appears to have high complexity [24]. Moreover, in our system model, we assume that M *D2D* pairs coexist with N *CU*s, and thus OPA must be applied $N \times M$ times to calculate the global optimal power allocation for all the possible (CU_i,$\mathrm{D2D}_j$) couples. This make OPA intractable for deriving the optimal RA scheme of an FD-D2D network. To overcome this issue, we develop a new polyblock-based algorithm, referred to as MARIO, which has a much lower complexity compared to OPA. To easily understand MARIO, first, we present in the next subsection the conventional polyblock-based algorithm (OPA), then we develop in Subsection 3.3.3 the new MARIO algorithm.

3.3.2 Outer Polyblock approximation algorithm

The main idea of OPA is to construct a sequence of shrinking polyblocks that eventually closely approximate the global solution which is located on the upper boundary of the feasible region [134]. However, as mentioned earlier, OPA has high complexity feature. Thus, we propose a novel polyblock-based algorithm called MARIO. To understand MARIO the OPA concept has to be very clear for the reader. Thus, in the remaining of this subsection, the OPA process is made formal and clarified.

Definition 3.2. *(Upper boundary): A point $x \in \mathbb{R}_+^N$ is called an upper boundary point of a normal closed set $\mathcal{F}$ if $\mathcal{F} \cap \{x' \, in \mathbb{R}_+^N | x' > x\} = \emptyset$. The set of all upper boundary points of $\mathcal{F}$ is the upper boundary of $\mathcal{F}$ and it is denoted as $\partial^+\mathcal{F}$.*

Definition 3.3. *(Box): Given any two vectors $\boldsymbol{a}$ and $\boldsymbol{b} \in \mathbb{R}_+^N$, the hyper rectangle $[\boldsymbol{a}, \boldsymbol{b}] = \{x | \boldsymbol{a} \preceq \boldsymbol{x} \preceq \boldsymbol{b}\}$ is referred to as a box.*

Definition 3.4. *(Polyblock): Given any finite set $\mathcal{T} \in \mathbb{R}_+^N$ with elements v_i, the union of all the boxes $[\boldsymbol{0}, \boldsymbol{v}]$ is refereed to as a polyblock with vertex set $\mathcal{T}$. A polyblock is clearly a normal set.*

Definition 3.5. *(Proper vertices): A vertex $v \in \mathcal{T}$ is said to be proper if there is no $v' \in \mathcal{T}$ such that $v' \neq v$ and $v' \succeq v$. A vertex is said to be improper if it is not proper, and improper vertices can be removed from $\mathcal{T}$ without affecting the shape of the polyblock.*

Definition 3.6. *(Projection): Given any nonempty compact normal set $\mathcal{H}_n \subset \mathbb{R}_+^N$, and any $\boldsymbol{v} \in \mathbb{R}_+^N \setminus \mathcal{H}_n$, $\pi_{\mathcal{F}}(\boldsymbol{z})$ is a projection of $\boldsymbol{z}$ on $\mathcal{F}$ if $\pi_{\mathcal{F}}(\boldsymbol{z}) = \alpha \boldsymbol{z}$ with $\alpha = \max\{\kappa > 0 | \kappa \boldsymbol{z} \in \mathcal{F}\}$. In other words, $\pi_{\mathcal{F}}(\boldsymbol{z})$ is the unique point where the line segment joining $\boldsymbol{0}$ to $\boldsymbol{z}$ meets the upper boundary of $\mathcal{F}$.*

Remark 3: *Due to the normality of $\mathcal{H}_n$, the projection point, i.e., α, can be found by the well known bisection algorithm [24, Algorithm 1] .*

Based on the above concepts, the OPA which solves the MO problem $\boldsymbol{P2}_{mo}$ works as follows. First, a polyblock $\mathcal{P}_1$ that contains the feasible set $\mathcal{H}_n \cap \mathcal{H}_c$ of an MO problem is constructed

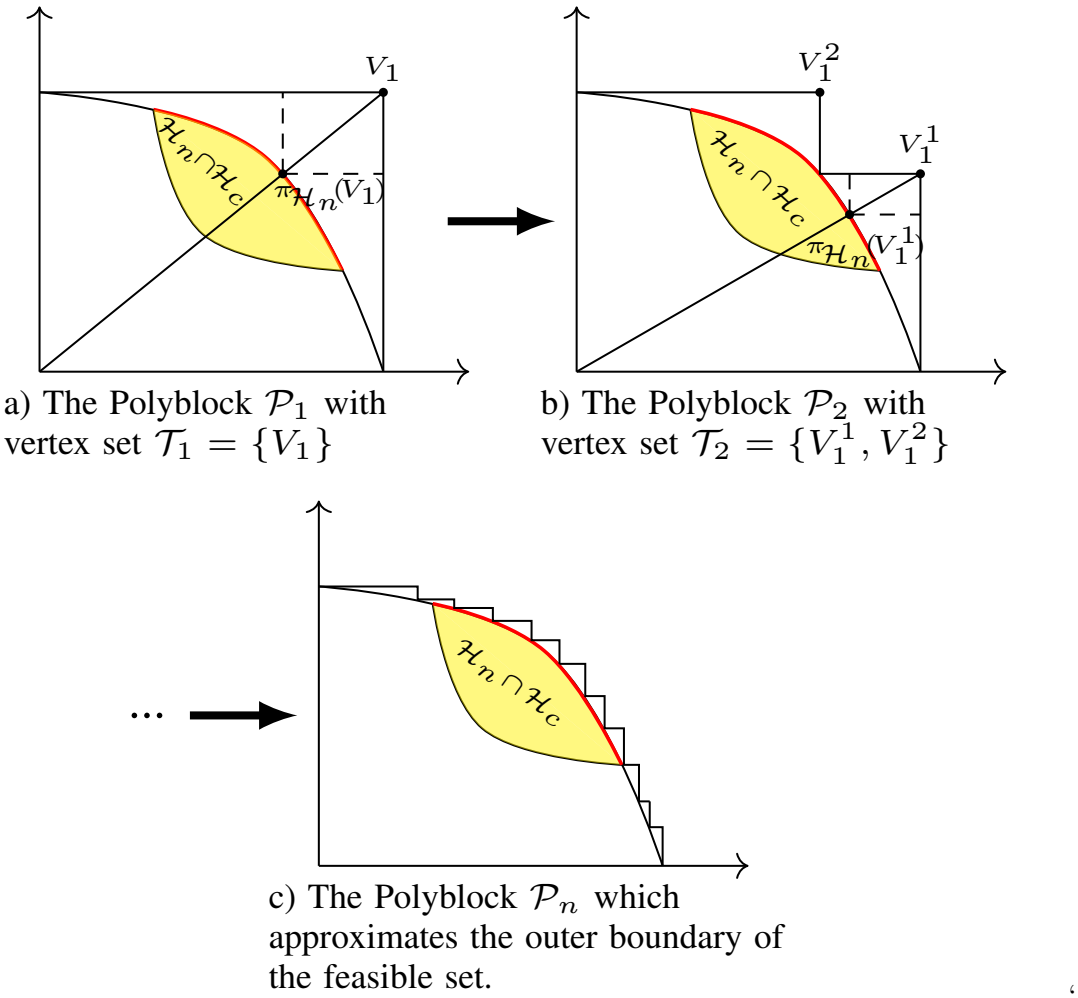

a) The Polyblock $\mathcal{P}_1$ with vertex set $\mathcal{T}_1 = \{V_1\}$

b) The Polyblock $\mathcal{P}_2$ with vertex set $\mathcal{T}_2 = \{V_1^1, V_1^2\}$

c) The Polyblock $\mathcal{P}_n$ which approximates the outer boundary of the feasible set.

Figure 3.3 – Illustration of the OPA process.

(see Fig.3.3 a). Let $\mathcal{T}_1$ be the proper vertex set of $\mathcal{P}_1$. By Proposition 2 of [24], the maximum of the utility function of an MO problem over the polyblock $\mathcal{P}_1$ occurs at some proper vertex $\mathbf{v}_1 \in \mathcal{T}_1$. If the projection of $\mathbf{v}_1$ on $\partial^+\mathcal{H}_n$ happens to reside on $\mathcal{H}_n$, i.e, $\pi_{\mathcal{H}_n}(\mathbf{v}_1) \in \mathcal{H}_n$, then $\mathbf{v}_1 = \pi_{\mathcal{H}_n}(\mathbf{v}_1)$ solve the problem and the optimal solution is equal to $\mathbf{v}_1$. Otherwise, based on Proposition 3 of [24], a smaller polyblock $\mathcal{P}_2 \subset \mathcal{P}_1$ which still contains $\mathcal{H}_n \cap \mathcal{H}_c$ but excludes $\mathbf{v}_1$ can be constructed (See Fig.3.3(b)). This is achieved by constructing the vertex set $\mathcal{T}_2$ by replacing $\mathbf{v}_1$ in $\mathcal{T}_1$ with N new vertices $\{\mathbf{v}_1^1, \ldots, \mathbf{v}_1^N\}$ and then removing the improper vertices, where $\mathbf{v}_1^j = \mathbf{v}_1 - (v_1^j - \pi\mathcal{H}_n(\mathbf{v}_1))\mathbf{e}_j$[1]. This procedure is repeated until an optimal solution is found. This leads to a sequence of polyblocks containing $\mathcal{H}_n \cap \mathcal{H}_c$:$\mathcal{P}_1 \supset \mathcal{P}_2 \supset \ldots \supset \mathcal{H}_n \cap \mathcal{H}_c$ (See Fig.3.3). The algorithm terminates at nth iteration when $\pi_{\mathcal{H}_n}(\mathbf{v}_n) \in \mathcal{H}_n$. According to [24] the OPA algorithm is guaranteed to converge to the global optimal solution *only if* the optimal solution $\mathbf{v}^\star$ has a positive lower bound $\mathbf{v}_l \succ \mathbf{0}$. Therefore, when at least one of the involved user

[1] In this chapter, $\mathbf{e}_j$ denotes the jth unit vector of $\mathbb{R}^N$.

has $\gamma_{\min} = 0$ the origin has to be shifted to the negative orthant to guarantee the convergence of the OPA.

Complexity analysis: The complexity and the convergence speed of OPA depends on the number of iterations required to search the outer boundary of the feasible set. The accuracy requirement of the bisection method for finding the projection point of the optimal vertex on the boundary of the feasible set also affects the complexity of the OPA algorithm. Another complexity key factor is the number of the optimization variables ($Nvar$), i.e., the dimensionality of the optimization problem. The latter highly affects the computational time of each iteration. Indeed, at the nth iteration, the optimal vertex over $\mathcal{P}_n$ needs to be found from $(nN_{var} - n - N_{var} + 2)$ vertices. This is because the size of the vertex set $\mathcal{T}_n$ increases by $(N_{var} - 1)$ after each iteration. Thus, the computational time of each iteration linearly increases with N_{var}. Let N_{iter} be the required number of iterations to find the optimal solution by using the OPA algorithm, the complexity for obtaining the solution is in the order of $O(N_{var}N_{iter}^2)$. The rapid growth of the size of the vertex set motivates us to develop a more efficient algorithm based on the existing OPA algorithm. For ease of notation, we denote the proposed algorithm by MARIO (Polyblock vertices triMming bAsed poweR allocatIOn).

3.3.3 MARIO algorithm

In this section, we propose the MARIO algorithm to reduce the complexity of OPA. The key idea of MARIO is to delete the unnecessary vertices that mislead the PA algorithm. Like the grass trimmer which trim down the quack grass to improve the growth of a meadow, MARIO accelerates the convergence time of PA by trimming down the hurtful vertices which slow down the PA algorithm. To make the last concept formal, first, we introduce the following proposition.

Proposition 3.1. *In the first step of Dinkelbachs' algorithm, the optimal power vector $\boldsymbol{p}_{ij}^*$ is achieved only if at least one user is transmitting with its maximum allowed power.*

Proof: For a scaling factor $\beta > 1$ and a power allocation vector $\mathbf{p}_{ij}$ satisfies the powers constraints we have the following,

$$\begin{aligned} U_1^{ij}(\beta\mathbf{p}_{ij}) = &\omega_i \log_2\left(1+\frac{p_c^i g_{c,bs}^i}{p_{d1}^j + h_{d1,bs}^j + p_{d2}^j h_{d2,bs}^j + \frac{\sigma_N^2}{\beta}}\right) \\ &+\omega_{j_1} \log_2\left(1\frac{p_{d2}^j g_d^j}{p_c^i h_{i,d1}^j + \eta p_{d1}^j + \frac{\sigma_N^2}{\beta}}\right) \\ &+\omega_{j_2} \log_2\left(1+\frac{p_{d1}^j g_d^j}{p_c^i h_{i,d2}^j + \eta p_{d2}^j + \frac{\sigma_N^2}{\beta}}\right) > U_1^{ij}(\mathbf{p}_{ij}) \end{aligned} \tag{3.21}$$

The power constraints imply that the maximum of βp_{d1}^j, βp_{d2}^j is $P_{\max}^d$ and the maximum of βp_c^i is $P_{\max}^c$. This means that the optima $\mathbf{p}_{ij}^*$ has at least one power bounded by the peak power constraint. ■

By virtue of Proposition 1.1, we know that the non-misleading vertices of a polyblock $\mathcal{P}$ are the vertices which have at least one abscissa above or equal to the maximum allowed power. Needless to say, these vertices must also satisfy the QoS of the users defined in (3.7a)-(3.7c). Observe that the extra auxiliary variables t and s defined in (3.20) may lead to a vertex which does not meet the above requirements. Hence, the misleading vertex is defined as follows.

Definition 3.7. *A vertex $\boldsymbol{v} = [v_1, v_2, \ldots, v_N]$ is said to be misleading if it does not have any power equal to or larger than the maximum power or if it cannot meet the QoS of the users or both. A misleading vertex can be deleted without affecting the PA process.*

Fig.3.4 illustrates the above concept. In this figure, x and y are the optimization variables, the lines l_1 and l_2 represent the QoS, and the shaded area denotes the feasible set. The red triangle points stand for the vertices that do not have any power at least bounded to the peak power. The blue square points are the vertices that can not meet the QoS of all users. The green diamond points are the vertices that cannot meet the QoS and do not have any user at least transmitting with the maximum allowed power. The black points represent the non-misleading vertices which can be kept to generate the new polyblock.

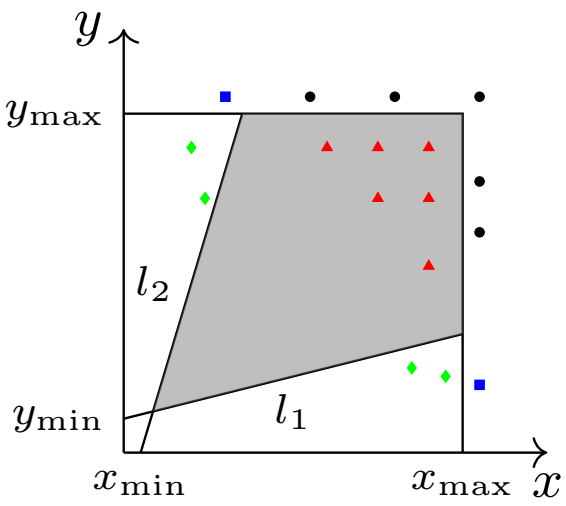

Figure 3.4 – Illustration of the misleading vertices that can be generated when auxiliary variables have been added.

The above concept is valid for the *WSR* power allocation problem. To apply it to the *GEE* power allocation problem, the maximum transmission power of the users has to be updated after each Dinkelbalch's step as indicated in the following proposition.

Proposition 3.2. *Let* $\boldsymbol{p}^{\star}_{k,ij}$ *and* $\boldsymbol{p}^{k}_{\max}$ *be the optimal transmission power and the maximum transmission power at the* k*th iteration of Dinkelbach's algorithm. The maximum transmission power in the* $k+1$*th iteration is equal to the optimal transmission power in the* k*th iteration, i.e.,* $\boldsymbol{p}^{k+1}_{\max} = \boldsymbol{p}^{\star}_{k,ij}$.

Proof: Recall that maximizing a general fraction $\frac{f(\mathbf{x})}{g(\mathbf{x})}$ by means of Dinkelback's algorithm requires to maximize $F(\lambda_k) = \max_{x\in\mathcal{S}} f(x) - \lambda_k g(x)$ at the kth iteration, with $\mathcal{S}$ being the set of constraints of the problem (in our case $\mathcal{S} = \mathcal{S} \cap \mathcal{S}_c$). Moreover, at each iteration k and for any $x \in \mathcal{S}$, $F(\lambda_k) \geq 0$. In addition, at the next iteration, the value of λ is updated as follows $\lambda_{k+1} = \frac{f(\mathbf{p}^{\star}_{k,ij})}{g(\mathbf{p}^{\star}_{k,ij})}$. Hence, at the $(k+1)$th iteration we have $F(\lambda_{k+1}) = \max_x f(x) - \frac{f(\mathbf{p}^{\star}_{k,ij})}{g(\mathbf{p}^{\star}_{k,ij})} g(x)$, which in turn implies that the maximum power at the $k+1$th iteration must be equal to the optimal power of the kth iteration. ■

Now, since the utility function of the MO problem is monotonically increasing function, the optimal point at the kth iteration will have at least one abscissa bounded to the maximum constraint. Thus, Definition 7 can also be used to reduce the complexity of globally solving the power allocation problem. This concept is illustrated in Fig.3.5, in which $\Psi_k(k \in \{1,2,3\})$ denotes the feasible set of the optimization problem at the kth iteration and the magenta star point is the optimal value. As it can be seen, the feasible set is getting smaller at each iteration and thus by updating the maximum power in PA algorithm the convergence time of PA will be significantly decreased.

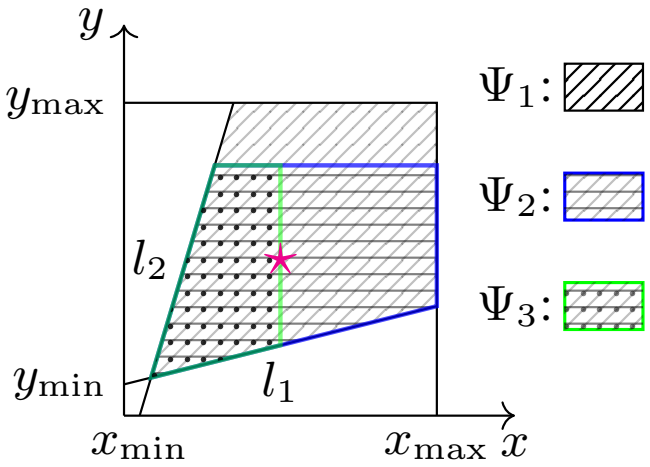

Figure 3.5 – The update process of the maximum powers.

Combining the OPA algorithm with Definition 7, Proposition 2 and Algorithm 1, the proposed MARIO algorithm can be presented as in Algorithm 2.

Now, recall that one of the work's targets is to derive the global optimal RA scheme of an FD-D2D based cellular network (see the second column of Fig.1). Up to now, we have shown

that the global RA scheme can be obtained by decomposing the original RA problem to two sub-problems as PA and CA and then globally solving each sub-problem individually. Then, we proposed MARIO to derive the global optimal PA scheme. Thus, to achieve the optimal RA scheme, it only remains to globally solve the CA sub-problem. The latter is the target of the following section.

Algorithm 2 The proposed MARIO algorithm

Input: The increasing utility function of $P2_{mo}$ defined in (3.20), the compact normal set $\mathcal{S}_n$ and the closed co-normal set $\mathcal{S}_c$ such that $\mathcal{S}_n \cap \mathcal{S}_c \neq \emptyset$.
Output: The optimal solutions of $P2_1$ and $P2_2$.
Set the accuracy of Dinkelbach's algorithm $\epsilon_1 > 0$, the counter of Dinkelback's algorithm $k = 0$, and $\lambda_0 = 0$.
while $F(\lambda_k) \geq \epsilon_1$ **do**
    Solve (3.20) as shown below:
    Initialization: Define an accuracy $\epsilon_2 > 0$, a counter $n = 0$, and an initial vertex $\mathbf{v}_0 = [\mathbf{p}^k_{\max}, s_{\max}, t_{\max}]$, with $s_{\max}$ and $t_{\max}$ being the maximum values of the introduced auxiliary variables in $P2_{mo}$. Let the initial polyblock $\mathcal{P}_1$ be box $[\mathbf{0}, \mathbf{v}_0]$ which contains $\mathcal{S}_n \cap \mathcal{S}_c$. The vertex set $\mathcal{T}_1 = \{\mathbf{v}_0\}$. Denote by $\mathbf{v}^\star_n$ the optimal vertex at the nth iteration.
    repeat
    $n = n + 1$.
    Find the best vertex $\mathbf{v}^\star_n$ in $\mathcal{P}_n$, i.e., $\mathbf{v}^\star_n = \arg\max\{f(\mathbf{v})|\mathbf{v} \in \mathcal{T}_n\}$.
    Obtain $\pi_{\mathcal{H}_n}(\mathbf{v}^\star_n)$, the projection of $\mathbf{v}^\star_n$ on the upper boundary of $\mathcal{H}_n$.
    if $\pi_{\mathcal{H}_n}(\mathbf{v}^\star_n) = \mathbf{v}^\star_n$, i.e., $v^\star_n \in \mathcal{H}_n$ **then**
        $\mathbf{v}^\star = \mathbf{v}^\star_n$, **break**.
    else
        Replace $\mathbf{v}^\star_n$ with N new vertices $\{\mathbf{v}_{11}, \ldots, \mathbf{v}_{1N}\}$.
        Delete the improper and the misleading vertices.
    end if
    until $|f(\mathbf{v}^\star_n) - f(\pi_{\mathcal{H}_n}(\mathbf{v}^\star_n))| \leq \epsilon_2$
    $\mathbf{v}^\star_n$=$\mathbf{v}^\star$=$[\mathbf{p}^\star_{k,ij}, s^\star, t^\star]$
    $k = k + 1$
    set $\mathbf{p}^k_{\max} = \mathbf{p}^\star_{k-1,ij}$
    update $\lambda_k = \frac{\omega_i R^i_c(\mathbf{p}^{k\star}_{ij}) + \omega_{j_1} R^{j_1}(\mathbf{p}^{k\star}_{ij}) + \omega_{j_2} R^j_{d2}(\mathbf{p}^{k\star}_{ij})}{\mu(p^{i\star}_c + p^{j\star}_{d1} + p^{j\star}_{d2}) + 3P_{cir}}$.
end while

3.4 Channel Assignment

So far, we find the global optimal power allocation for all the possible pairs (D2D$_j$,UE$_i$). In this section, we aim at finding the optimal reuse candidate for each pair D2D$_j$, i.e., solving the channel assignment problems $P3_1$ and $P3_2$ defined in (3.10) and (3.13) respectively. Both problems $P3_1$ and $P3_2$ consist only of the channel reuse indicator variable ϱ_{ij}. Moreover, according to the channel assignment constraints defined in (3.7d) and (3.7e), the *D2D* pairs can

share at most one CU's resources and the resources of a CU can be allocated at most to one *D2D* pair. Therefore, the channel assignment problems $P3_l$ and $P3_2$ can be seen as a maximum weight bipartite matching problem. Fig.3.6 illustrates the maximum weight bipartite problem in $P3_1$ and $P3_2$, where the set of *D2D* pairs $\mathcal{D}$, and the set of the cellular users $\mathcal{C}$ are assumed to be the two disjoint groups of vertices in the bipartite graph. The pair (D2D$_j$,UE$_i$) is joined by an edge ij when CU$_i$ is a reuse candidate of D2D$_j$. The weight of edge ij is assumed to be the optimal objective function of $P3_l$, and it is denoted by $U_l^{ij\star}$ with $l \in \{1, 2\}$. The well known Khun-Munkres algorithm (Hungarian algorithm) [128] can be used to solve such assignment problems.

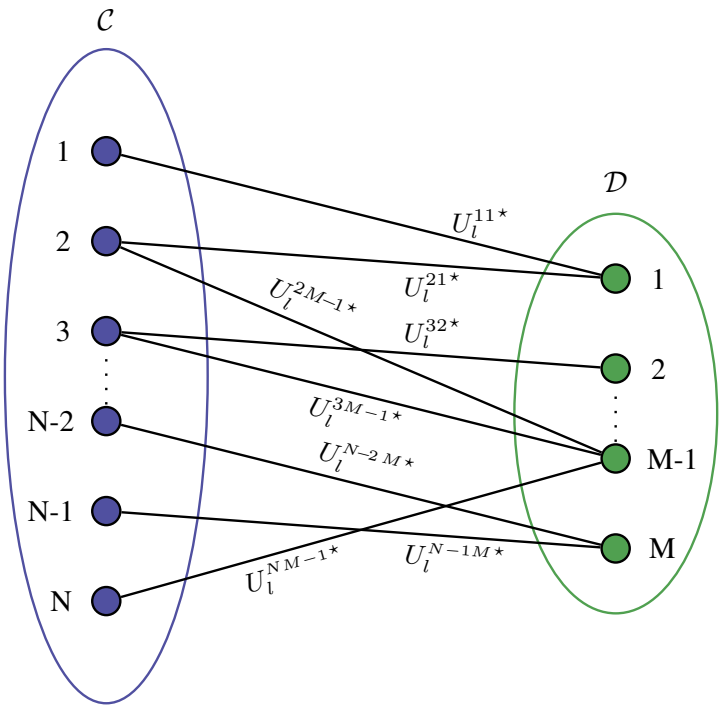

Figure 3.6 – The bipartite graph representation of the channel assignment problem.

3.4.1 Resource allocation in HD-D2D network

As a complement, we introduce the resource allocation problem in an HD-D2D network. For a fair comparison with the FD-D2D network, we assume that when $D2D_j$ reuses the bandwidth of CU_i (B_i), the users D_1^j and D_2^j will operate on two equally orthogonal portions of the bandwidth B_i. Hence, when $D2D_j$ shares the resources of CU_i in HD mode, the SINR of the CU_i will remain the same as in (3.1). However, the SINRs of D_1^j and D_2^j do not longer contain the self interference part. Consequently, the solution of the resource allocation problem of an HD-D2D based cellular network is similar to the FD-D2D network, with the only difference

that in HD mode we have $\eta = 0$ and the bandwidth of D_1^j and D_2^j is equal to half of the CU_i bandwidth.

The optimal solution of both FD-D2D and HD-D2D resource allocation problem is reported in Algorithm 3.

Algorithm 3 Optimal Resource allocation algorithm

$\mathcal{C}$: The set of existing cellular users
$\mathcal{D}$: The set of D2D pairs
$U_l(\rho, \mathbf{P})$: The function to be maximized
if HD mode **then**
    Set $\eta = 0$
    Set the bandwidth of D_1^j and D_2^j to $B/2$
end if
Step 1: Power Control
for all $j \in \mathcal{D}$ and $i \in \mathcal{C}$ **do**
    Solve $P2_l$ for the pair $(\text{D2D}_j, \text{CU}_i)$ by using MARIO algorithm.
end for
Step 2: Channel Assignment
Get the optimal CU_i for each D2D_j by using Khun-Munkres algorithm

3.4.2 Complexity analysis

As shown earlier, solving the resource allocation problem requires sequentially solving the power allocation problem ($\mathbf{P2}_l$) and the channel assignment ($\mathbf{P3}_l$) problems, with $l \in \{1, 2\}$. Hence, the complexity of Algorithm 3 depends on the complexity of the power allocation problem and the complexity of the channel assignment problem. The complexity of finding the global optimal power allocation for one couple $(D2D_j, CU_i)$ has been derived in the previous section, and it is in the order of $\mathcal{O}(N_{iter}^2 N_{var})$. Since we have M *D2D* pairs and N CUs, the total number of possible couples is MN, and thus the complexity of ($\mathbf{P2}_l$) is in the order of $MN\mathcal{O}(N_{iter}^2 N_{var})$. On the other hand, the Khun-Munkres algorithm [128] requires at most $\max^3(M, N)$ iterations to finish the assignment problem. Therefore, the overall complexity of the resource allocation problem can be described as $MN\mathcal{O}(N_{iter}^2 N_{var}) + \mathcal{O}(\max^3\{M, N\})$. Due to the high complexity of this problem, in the following, we present a heuristic algorithm to efficiently solve the resource allocation problem. The proposed algorithm follows a reverse path, i.e., first, it assigns the channels to the different *D2D* pairs and then it allocates the power for the different couples $(D2D_j, CU_i)$. We denote this algorithm by channel allocation then power allocation (CATPA) and it is described thereafter.

3.5 The proposed CATPA algorithm

From the above description, the global optimal solution of the resource allocation problem can be found by first deriving the optimal power allocation for all the possible couples $(D2D_j, CU_i)$ and then assigning the channels to the users by using the well known Hungarian algorithm. In the considered scenario, this will lead to solve $N \times M$ PA problems via the proposed MARIO algorithm and then apply the Hungarian algorithm, with $N \times M$ being the number of all the possible couplings between the M *D2D* pairs that coexist with the N CUs. The conventional RA sub-optimal solutions presented in [119, 120] have the same structure of the proposed MO based solution, and thus they also require solving $N \times M$ PA problems (refer to the first column of Fig. 3.1). Hence, both the conventional sub-optimal solution and the MO based solution will be inapplicable for deriving the optimal RA scheme in a real FD-D2D network especially when N or M increases.

To reduce the complexity we develop in this section, the CATPA algorithm that first assigns the channels to the D2D pairs and then allocates the powers for all the involved users as shown in the third column of Fig. 3.1. Hence, by using CATPA we will only need to solve M instead of $N \times M$ PA problems to achieve a solution for the RA problem.

First focusing on the channel assignment step, we propose to assign the available channels for the *D2D* pairs that are expressing good channel conditions. To that end, we define a profit for each possible couple $(D2D_j, CU_i)$ as shown below:

$$\begin{aligned} Profit^{ij} &= \frac{g^i_{c,bs} + g^j_d + g^j_d}{I_i + I_{j_1} + I_{j_2}} \\ I_i &= \gamma^i_{\min}(h^j_{d1,bs} + h^j_{d2,bs} + \sigma^2_N) \\ I_{j_1} &= \gamma^{j_1}_{\min}(h^j_{i,d1} + \eta + \sigma^2_N), \text{ and } I_{j_2} = \gamma^{j_2}_{\min}(h^j_{i,d2} + \eta + \sigma^2_N). \end{aligned} \tag{3.22}$$

The numerator of (3.22) can be seen as a measure of the possible gain when allocating the channel CH_i to $D2D_j$ while the denominator of (3.22) can be observed as the cost of reusing the bandwidth of CU_i. Hence, $Profit^{ij}$ is a metric that quantifies the profit of each couple $(D2D_j, CU_i)$. Since we are assuming that the BS has full-knowledge about the channel state information of the users, the $Profit^{ij}$ of all the possible couples $(D2D_j, CU_i)$ can be easily computed at the BS. Having the profit table of all the possible couples in the network, we propose to allocate the channels to the couples with high profits. Moreover, to respect the channel allocation constraints defined in (3.7a)- (3.7c), we first assign the ith channel to the *D2D* pair that has the highest profit, and then we remove the assigned channel and the assigned *D2D* pair after each assignment. The following example clearly explains the proposed channel assignment method.

Assume a cellular network with 4 CUs and 4 *D2D* pairs with a profit table as shown in Fig.3.7(a). From this figure, it is clear that the $Profit^{1,3}$ is the highest value. Thus we assign the third channel to the first *D2D* pair and then we remove the first row and the third column. After this deletion, the profit table will reduce to the matrix shown in Fig.3.7(b). We repeat this process until all the *D2D* pairs get assigned channel (See Fig.3.7(a)-(d)). It is clear that by following this process each channel will be assigned to only one*D2D* pair, and each *D2D* pair will reuse the channel of only one *CU*.

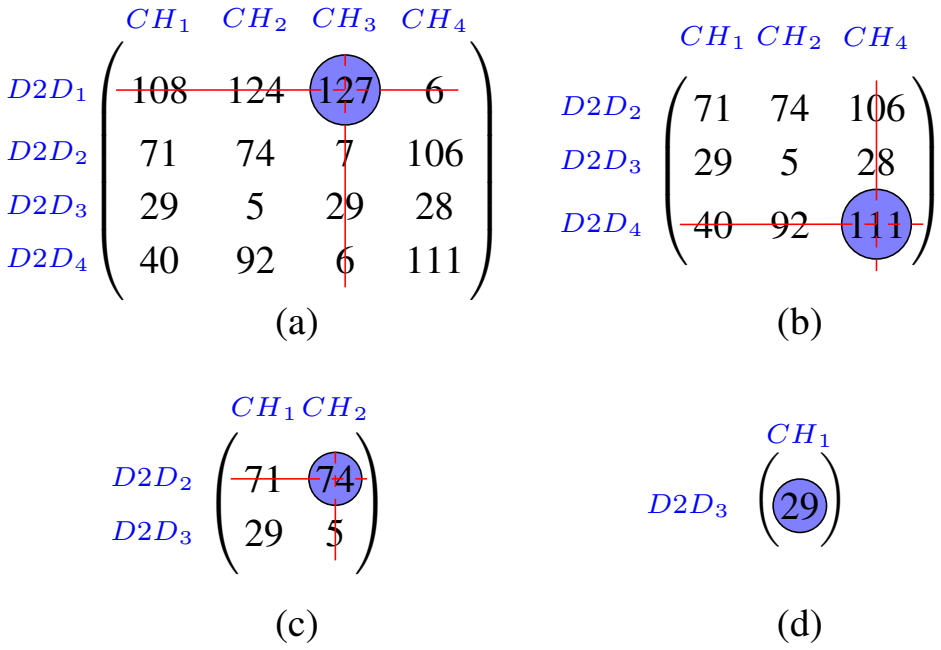

Figure 3.7 – The process of the proposed CA .

The proposed algorithm requires at most $min\{M, N\}$ iterations to finish the assignment problem, and thus it reduces the assignment complexity by $1/min\{M, N\}$ comparing to the Hungarian algorithm. In addition, for that specific profit function, both the Hungarian algorithm and the proposed CA algorithm lead to the same value as shown in the next proposition.

Proposition 3.3. *For pairwise different profits, the proposed CA algorithm leads to the global optimal assignment solution.*

Proof: First recall that the Hungarian algorithm achieves the best assignment problem for a maximum-weight bipartite matching problem. In particular, The Hungarian algorithm assigns the channel to the users who give the higher *WSR* or *GEE* . Now, assume that all the weights of the assignment problem are different. Then, the best assignment will be achieved by finding the maximum weights that are locating in different rows and different columns. This is exactly the objective of our proposed CA algorithm. ■

By examining the profit equation defined in (3.22), we see that two profit values are identical only when the related *D2D* pairs and the CUs are locating at the same locations. Hence, in practice, the proposed CA algorithm leads to the optimal assignment solution as shown in the following Remark.

Remark 4: *In a real network, each node occupies a specific area in the cell, and thus two nodes cannot reside at the same point which in turns implies that all the profit values are different. Thus, the proposed CA algorithm will lead to an optimal assignment solution.*

Now, after assigning the channels for all the *D2D* pairs, the power allocation problem can be solved using the SCO method presented in [119, 120]. Algorithm 4 summarizes all the previous discussion and shows the different steps of CATPA.

Algorithm 4 The proposed CATPA algorithm

1: $\mathcal{C}$: The set of existing cellular users
2: $\mathcal{D}$: The set of *D2D* pairs
3: Step 1: Channel Assignment
4: **for all** $j \in \mathcal{D}$ and $i \in \mathcal{C}$ **do**
5: Compute $Profit_{i,j}$ by using (3.22).
6: **end for**
7: **for** $j = 1 : min\{M, N\}$ **do**
8: Find the highest $Profit_{i,j}$ element.
9: Let I^j_{row} and I^j_{col} be the indices of the row and the column of the highest element at the jth iteration respectively.
10: Allow the I^j_{row}th *D2D* pair to reuse the channel of the I^j_{col}th CU.
11: Delete the I^j_{row}th row and the I^j_{col}th column of the profit table.
12: **end for**
13: Step 2: Power Control
14: Allocate the power for each $(D2D_j, CU_i)$ bu using the SCO theory.

3.6 Numerical assessment

We consider a single cell network, where *CU*s are uniformly distributed in the cell. The D2D users are usually within a short distance, and thus we distribute them in the cell according to the cluster distribution model [135]. In particular, the D2D users are uniformly distributed within a randomly located cluster. Moreover, in our simulation, we assume different D2D pairs are within different clusters. The *CU*s are assumed to share the total bandwidth equally. In addition, in our simulation, we only focused on the egalitarian solution, i.e., we set the weights ω_i, ω_{j_1}, and ω_{j_2} to one. Table 3.1 summarizes our simulation parameters.

Table 3.1 – Simulation parameters

Cell radius (R)	0.5 Km
D2D cluster radius (r)	20, 30, 40, ..., 100 (m)
Uplink channel bandwidth	180 KHz
Noise power (σ_N^2)	-114 dBm
Path-loss exponent (α)	4
Maximum Tx power	24 dBm
Multiple-path fading	Exponential distribution with unit mean
Egaleterian Solution	$\omega_i = \omega_{j1} = \omega_{j_2} = 1, \forall i \in \mathcal{C}, j \in \mathcal{D}$

3.6.1 MARIO vs OPA

The aim of this subsection is to compare the complexity of the proposed MARIO algorithm and the complexity of the traditional OPA algorithm. To that end, we consider a simple scenario in which a single D2D pair coexists with one *CU* . The center of the D2D cluster is located at $300m$ from the *BS* , and the *CU* is located at $100m$ from the *BS* .

Giving this scenario, Fig.3.8 shows the behavior of both MARIO and OPA algorithms in the last iteration of Dinkelbach's algorithm, i.e., when λ_k equals the optimal *GEE* value. The y-axis of this figure is the difference between the *GEE* values of the best vertex point ($\mathbf{v}_n^\star$) and its projection point ($\pi_{\mathcal{G}}(\mathbf{v}_n^\star)$), i.e., the line 17 in Algorithm 2. As can be seen in Fig.3.8, in both algorithms, the difference between the *GEE* values of $\mathbf{v}_n^\star$ and $\pi_{\mathcal{G}}(\mathbf{v}_n^\star)$ reaches zero after several numbers of iterations which in turn validates that both algorithms have already converged to the global maximum point. Fig.3.8 also shows the typical bounding behavior of the polyblock based algorithm [136]. For instance, both algorithms quickly find a feasible solution within a relatively small difference between the *GEE* values of $\mathbf{v}_n^\star$ and $\pi_{\mathcal{G}}(\mathbf{v}_n^\star)$, but many more iterations are required to squeeze the difference to zero. In addition, Fig.3.8 clearly shows the superiority of MARIO in term of the required number of iterations to achieve the optimal *GEE* value. For instance, the proposed MARIO algorithm achieved the optimal *GEE* value after 2.2×10^4 iterations while the regular OPA algorithm required five-times more iterations (11×10^4) to obtain the optimal *GEE* value. A similar behavior is obtained at the first iteration of Dinkelback's algorithm, i.e., when maximizing *WSR* , but it is omitted for sake of clarity.

This is because MARIO deletes the misleading vertices that delay the convergence time. To illustrate this concept, we show in Fig. 3.9 the generated vertices of both algorithms after 400 iterations, in the first iteration of Dinkelbach's algorithm. As illustrated in Fig. 3.9(a)-(b), MARIO generates a much lower number of vertices compared to the regular OPA algorithm, and thus it has faster convergence time.

To emphasize the superiority of MARIO, we compare in Table 3.2 the complexity of both OPA and MARIO algorithms in terms of the average number of iterations and the average

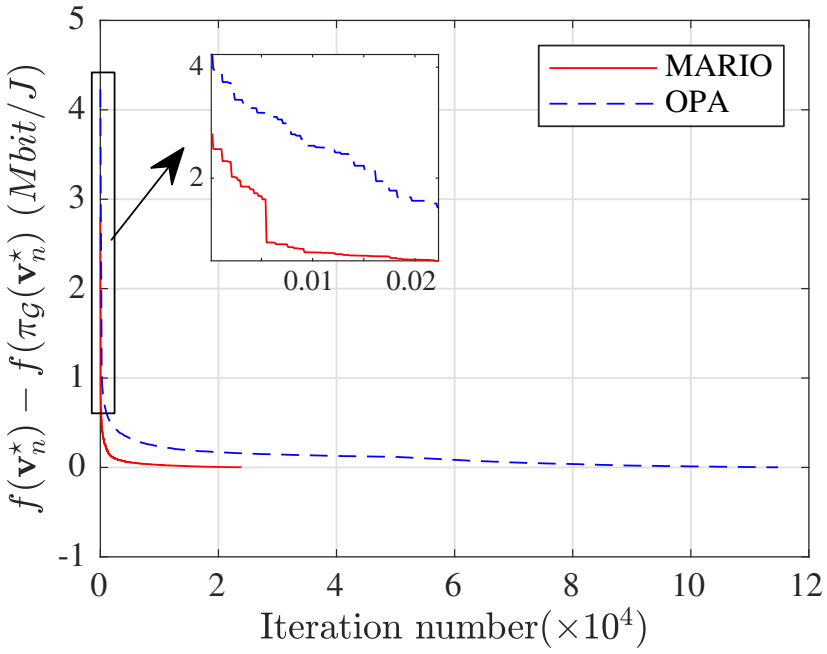

Figure 3.8 – Convergence behavior of the proposed MARIO algorithm and the regular OPA algorithm, in the last iteration of Dinkelbach's algorithm. The behavior shows the convergence to the global *GEE* optimal solution and illustrates the superiority of the proposed MARIO algorithm.

number of vertices to achieve the optimal *GEE* value for different cluster radii. As expected, MARIO requires less number of iterations and generate less number of vertices to attain the optimal *GEE* value.

Table 3.2 – The average number of iterations and vertices for the proposed MARIO algorithm and the regular OPA algorithm.

r (m)	Number of Iterations		Number of vertices	
	MARIO	OPA	MARIO	OPA
10	80990	100000	388.0699	1253
20	74604	980000	413.4425	1258.9
40	77263	950000	400.2299	871.4
80	68395	100000	632.9584	800

3.6.2 The optimality gap

As mentioned in the introduction, all the related RA works ([119, 120]) provide the solution of the RA problem by using the sequential convex optimization theory (SCO). The latter guarantees only a first-order optimal solution, and up to now the optimality gap of the SCO method in the RA problem of an FD-D2D network is not identified yet. Fig.3.10(a) and Fig.3.10(b) compare the achieved *GEE* and the achieved rate using the MO theory with that

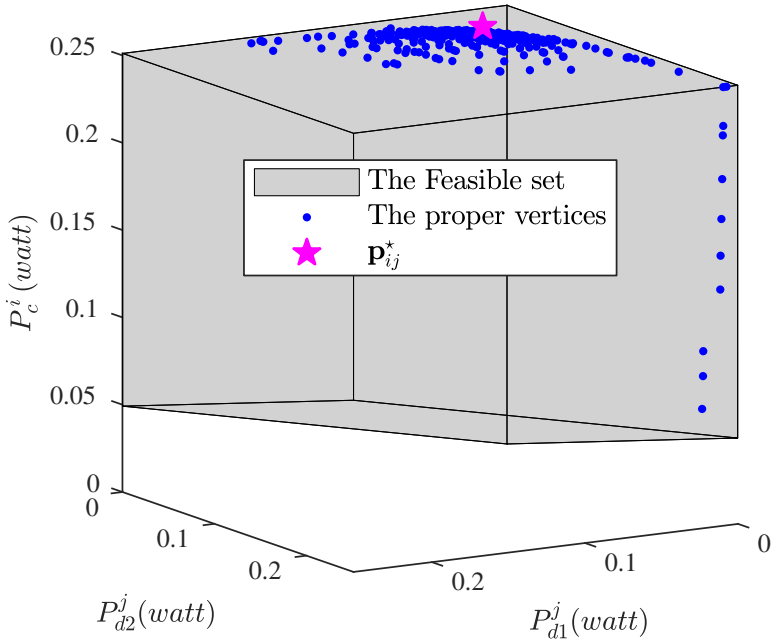

(a) The proposed MARIO algorithm

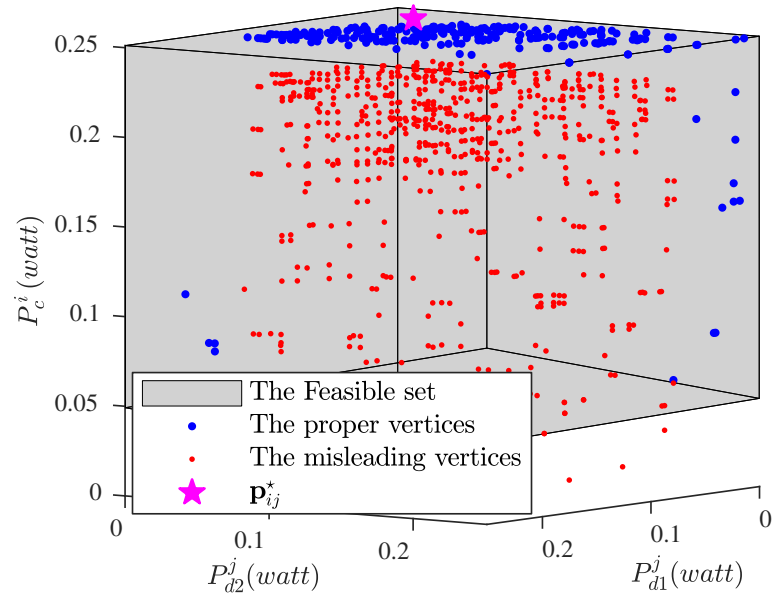

(b) The regular OPA algorithm

Figure 3.9 – The feasible set and the generated vertices of (a) the proposed MARIO algorithm and (b) the regular OPA algorithm after 400 iterations.

achieved by using the SCO for different self-interference cancellation factor (η). As can be seen, the optimality gap is less than 1%. This result is inline with the works in [24, 125]. Another remarkable observation is that both the achieved *GEE* and the achieved rate increase with the

decline of the SI cancellation factor. This is expected because when η decreases the RSI power decreases and thus the total interference will also decrease.

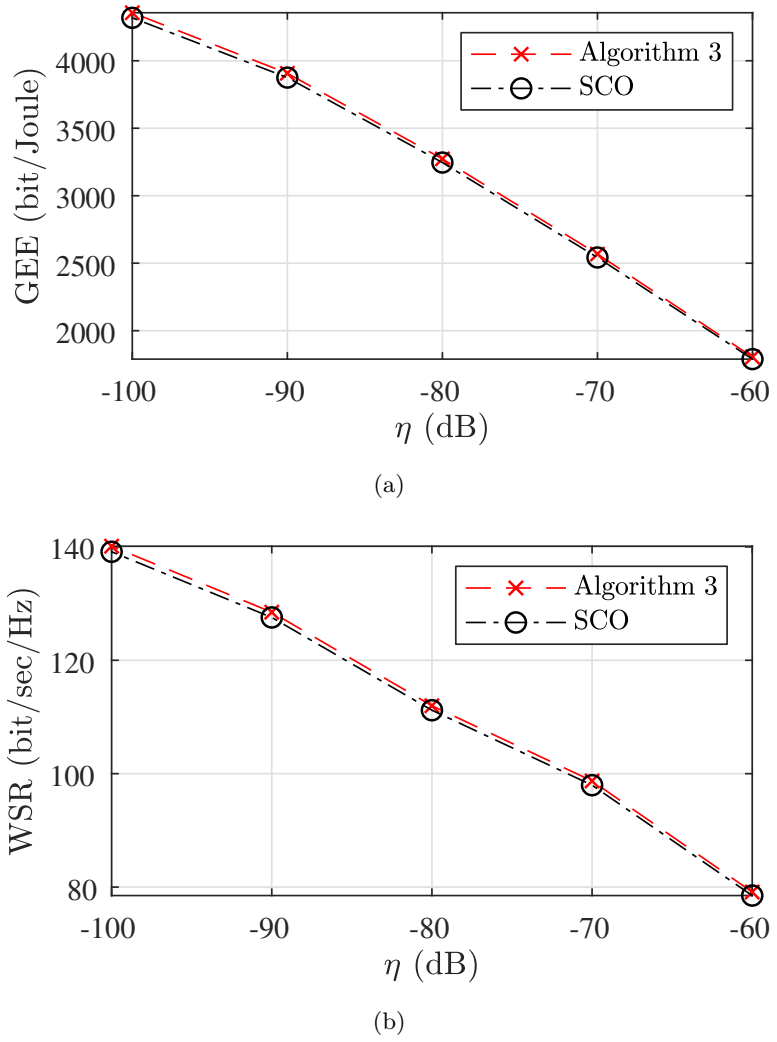

Figure 3.10 – Achieved *GEE* versus SI cancellation factor, using 1) the proposed method, 2) SCO method ([119, 120]). ($r = 20m, \gamma^{i}_{\min} = \gamma^{j_1}_{\min} = \gamma^{j_2}_{\min} = 3dB$)

While in the above figure we have shown the optimality gap in terms of the achieved rate or the achieved *GEE* , in Table 3.3 we present the average number of iterations to achieve both the global optimal solution (MO based method) and the sub-optimal solution (SCO based method). As can be seen, the global optimal solution can be achieved at the price of a high number of iterations. Hence, given the low optimality gap of the SCO method and the high complexity of the MO based method, the SCO method is an interesting candidate to analyze the FD-D2D network while the MO-based method is an interesting tool to benchmark the results. Thus, in the next sub-section, we will analyze the performance of our proposed sub-optimal RA

algorithm, CAPTA, in the FD-D2D network as compared to the SCO optimization method applied in [119] and [120].

Table 3.3 – The average number of iterations for the proposed MARIO algorithm and SCO algorithm.

η (dB)	Number of Iterations	
	SCO	MARIO
-60	63.2	77378
-70	51.65	76628
-80	46.9	75828
-90	41.29	74721
-100	34.26	72934

3.6.3 The performance of the sub-optimal resource allocation CATPA algorithm

Here we aim to identify the performance of the proposed CATPA algorithm. To that end, we assume a single cell network where $M = 4$ D2D pairs coexist with $N = 4$ *CUs* . The *CUs* are uniformly distributed in the cell, and the D2D users are uniformly distributed within a randomly located cluster. To cover all the possible location, we generate the D2D users and the *CUs* 500 times, and then we averaged the results. Fig. 3.11(a) and 3.11(b) respectively compare the achieved *GEE* and *WSR* values of the FD-D2D network with the achieved *GEE* and *WSR* values of the HD-D2D network. The *GEE* and the *WSR* values of the FD-D2D network are obtained through the proposed CATPA algorithm and the SCO method adopted in [119, 120]. Fig. 3.11 shows that the *GEE* and *WSR* values of both FD-D2D and HD-D2D networks decline as the cluster radii increases. This is expected, since when r increases the proximity distance between the *D2D* users also increases, and thus more power is needed to maintain the same QOS. However, increasing the power also increases the interference, and thus the total rate and the *GEE* decrease. In addition, Fig. 3.11 also shows that the *GEE* and the *WSR* values of the FD-D2D network decline with the increasing of η which in turn re-validate the result of the previous sub-section. Hence, the FD-D2D network's performance highly depends on both the SI cancellation capability and the proximity distance of the D2D users. For instance, the HD-D2D network outperforms the FD-D2D network when $\eta = -60dB$ and the *D2D* users are within a $10m$ distance from each other. Thus, to achieve the maximum gain of a *D2D* based cellular network, the transmission mode must always alternate between HD and FD based on the channel situation, the SIC factor, and the proximity distance. In addition, Fig. 3.11(a)-(b) clearly indicates that the proposed CATPA algorithm can achieve *GEE* and *WSR* values that are within the $91\% - 98\%$ of the optimal value obtained by SCO method which in turn validates the accuracy of the proposed CATPA algorithm. Now, to shed the light on the low complexity feature of the proposed CATPA algorithm, we present in Table 3.4 the required number of

iterations to obtain the optimal *GEE* value for both CATPA and the SCO algorithm for different SIC cancellation factors and different cluster radii values. As expected, the proposed CATPA solution decreases the number of iterations by at least $min\{M, N\}$. This is because CATPA does not compute the optimal power allocation for all the possible couples $(D2D_j, CU_i)$ as in the global optimal solution.

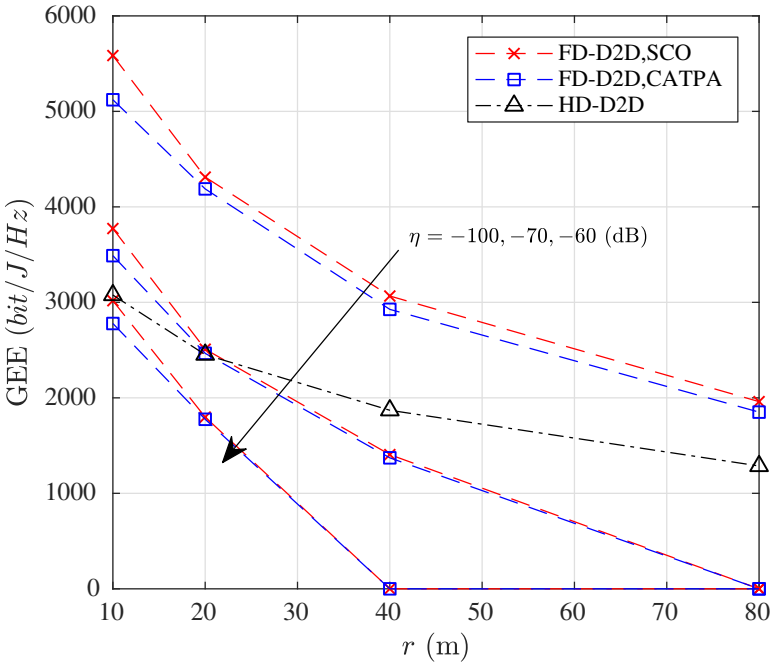

(a)

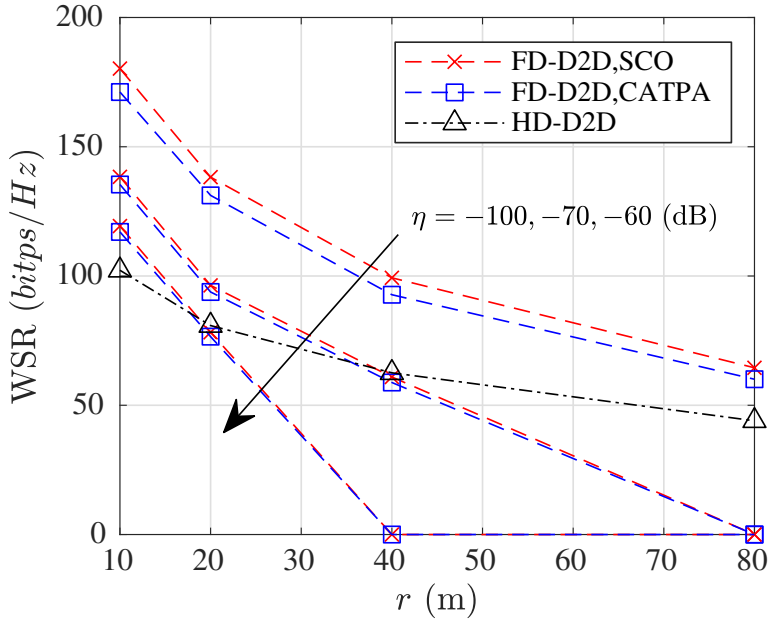

(b)

Figure 3.11 – Comparison between the performance of FD-D2D network and the HD-D2D network when applying the proposed CATPA algorithm or the SCO solution adopted in [119, 120] for (a) maximizing *GEE* , and (b) maximizing *WSR* . ($\gamma^{i}_{\min} = \gamma^{j_1}_{\min} = \gamma^{j_2}_{\min} = 3dB$)

For instance, the adopted scenario in Table 3.4 contains 4 D2D pairs and 4 *CU*s , and thus CATPA will lead to at least a 4-fold decrease in the number of iterations as shown in Table 3.4.

Table 3.4 – The number of iterations for the proposed CATPA algorithm and SCO algorithm.

$\eta\,(dB)$	$r = 10\,(m)$		$r = 20\,(m)$		$r = 40\,(m)$	
	CATPA	SCO	CATPA	SCO	CATPA	SCO
-60	108.6	425.9	121.64	481.8	52	216
-70	95.63	362.7	116.43	444.6	119.6	472.9
-80	74.38	279.19	96.39	360.3	106.9	410.6
-90	53.05	203.8	68.58	257.9	78.6	302.1
-100	38.48	153.06	46.03	182.7	55.1	220.8

3.6.4 Performance analysis of the FD-D2D network

In the previous subsections, we saw the effect of the RSI power and the *D2D* cluster radius on the performance of the FD-D2D network. Moreover, we observed that the FD-D2D network requires a small *D2D* proximity distance and high SI cancellation capability to achieve its ultimate gain. Hence, in this subsection, we aim to analyze the effect of the remaining network's parameters, such as the maximum transmission power and the required QoS, on the performance of the FD-D2D network by assuming $\eta = -100dB$ and $r = 20m$.

Fig. 3.12 presents the effect of the maximum allowed power on the achieved *GEE* value considering three power allocation strategies:1) the obtained powers when maximizing *GEE* ; 2) the obtained optimal powers when maximizing *WSR* ; 3) the maximum allowed powers. In this figure, $P^d_{\max}$ denotes the maximum power of D^j_1 and D^j_2 with $j \in \mathcal{D}$. From Fig. 3.12(a) it is seen that the *GEE* obtained by *GEE* maximizing first increases by the increasing of $\mathbf{p}_{\max}$ and then it saturates at large $\mathbf{p}_{\max}$. This is because when $\mathbf{p}_{\max}$ is large enough to allow achieving the optimal *GEE* value, the excess power is no longer utilized. However, the *GEE* attained by *WSR* maximizing first increased by the increase of $\mathbf{p}_{\max}$ until $\mathbf{p}_{\max} = -30$dBw, and then it started to decline for larger $\mathbf{p}_{\max}$. This indicates that the global optimal *GEE* value can be achieved if at least one user is transmitting at -30dBw. This result also confirms our proposed MARIO algorithm in which we update the maximum power level at each step on Dinkelbach's algorithm. In addition, transmitting with full power at all users highly degrades the *GEE* performance. Now, looking at Fig. 3.12(b), it can be observed that the achieved *WSR* when maximizing *WSR* increases as the maximum power increases. This result confirms our observation that the maximum achieved rate can be obtained only if at least one of the users is transmitting with the maximum allowed power. However, the achieved *WSR* when maximizing *GEE* saturate at large $\mathbf{p}_{\max}$ which is inline with the results of Fig.3.12(a). In addition, Fig. 3.12 also confirms

that the full power transmission strategy is not suitable for the FD-D2D network since it failed to achieve good *WSR* or *GEE* values.

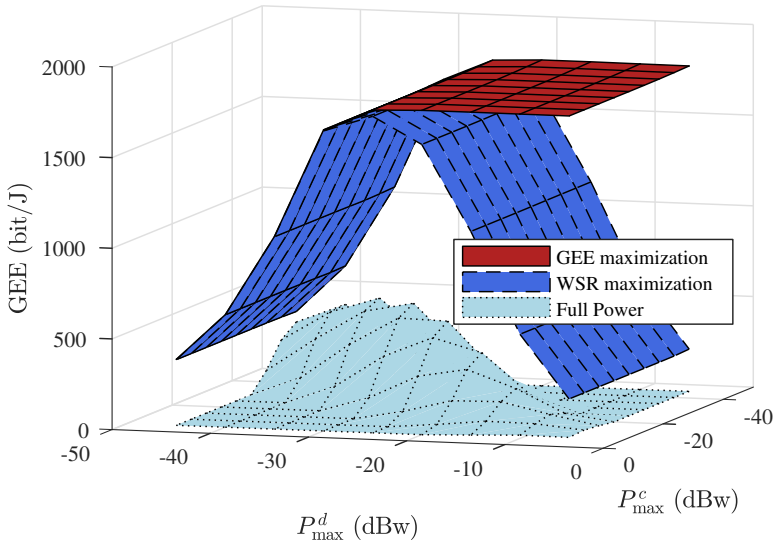

(a)

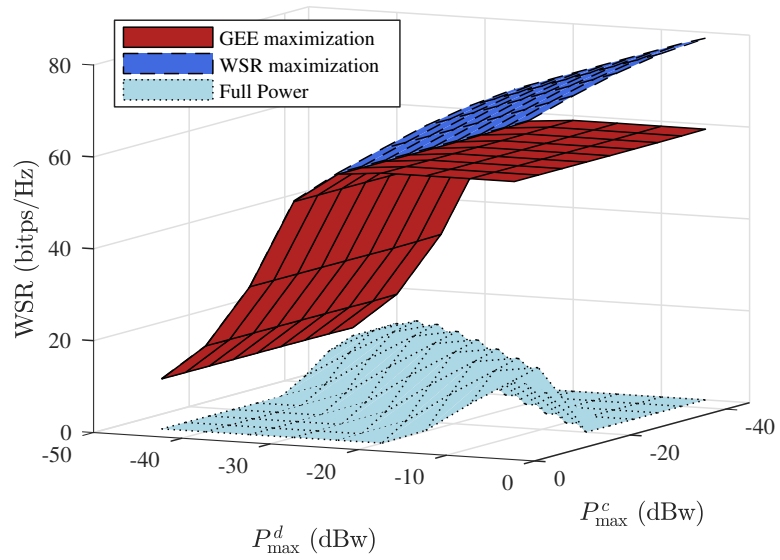

(b)

Figure 3.12 – The effect of the maximum transmission power on the (a) achieved *GEE* value and (b) achieved *WSR* value considering three power allocation strategies: 1) the obtained powers when maximizing *GEE* ; 2) the obtained optimal powers when maximizing *WSR* ; 3) the maximum allowed powers. $(r = 20m, \gamma^i_{\min} = \gamma^{j_1}_{\min} = \gamma^{j_2}_{\min} = 3dB)$

Another interesting observation can be extracted from Fig.3.12 is that the difference between the achieved *WSR* when maximizing *GEE* or maximizing *WSR* is relatively smaller than the

difference between the obtained *GEE* when maximizing *GEE* or maximizing *WSR* . Giving this result, in a resource allocation problem, maximizing the *GEE* is much attractive than maximizing the overall rate.

Next, to see the effect of the QOS on the performance of FD-D2D network, we set the maximum transmit power $\mathbf{p}_{max} = [-6, -6, -6](dBw)$, and then we draw in Fig. 3.13(a)-(b) the variation of the achieved *GEE* and *WSR* w.r.t $\gamma^{c}_{\min}$ and $\gamma^{d}_{\min}$ with $\gamma^{d}_{\min}$ being equal to $\gamma^{d1}_{\min}$ and $\gamma^{d2}_{\min}$. Since the maximum power allocation strategy is not suitable for FD-D2D network (see Fig.3.12-(b)), in this figure we only consider the remaining two power allocation schemes: 1) the obtained powers when maximizing *GEE* ; 2) the achieved powers when maximizing *WSR* . As expected the achieved *GEE* and *WSR* decline with the increase of the minimum required SINR for all power allocation strategies since at large SINR requirement less number of FD-D2D pairs can be admitted. In addition, Fig. 3.13 confirms the previous results obtained in Fig. 3.12 which says that in a FD-D2D network maximizing *GEE* will be more attractive than maximizing the overall rate. This is because the gap between the achieved *GEE* when maximizing *GEE* and maximizing *WSR* (see Fig. 3.13(a)) is much larger than the gap between the achieved *WSR* when maximizing *GEE* and maximizing *WSR* (see Fig. 3.13(b)). To have full knowledge of the performance of an FD-D2D network when maximizing *GEE* or maximizing *WSR* a joint optimization framework must be developed which is left for future work.

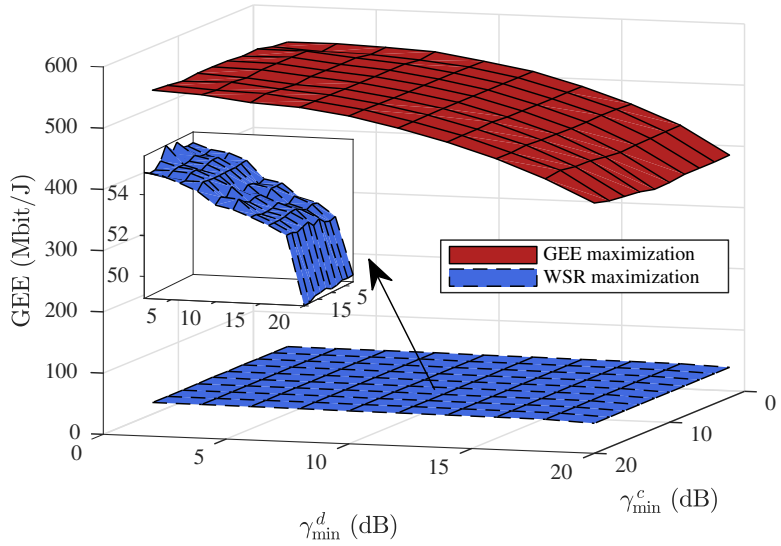

(a)

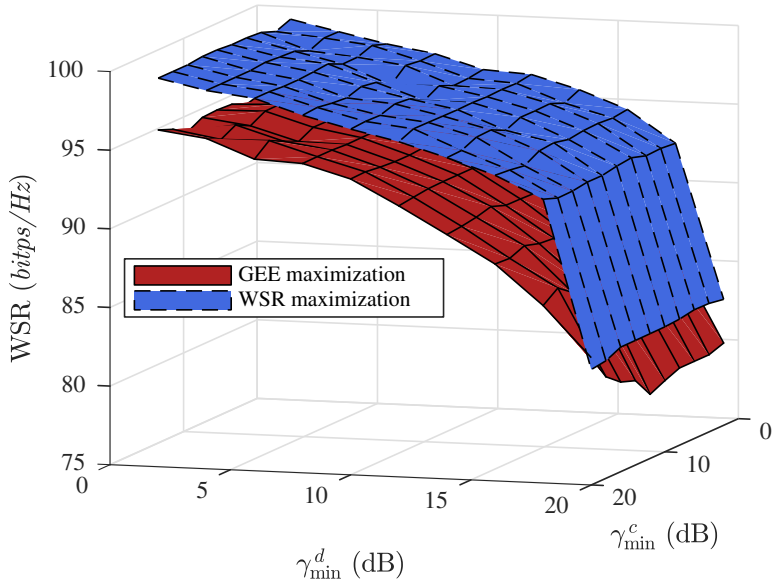

(b)

Figure 3.13 – The effect of the QoS requirement (a) achieved *GEE* value and (b) achieved *WSR* value considering two power allocation strategies: 1) the obtained powers when maximizing *GEE* ; 2) the obtained optimal powers when maximizing *WSR* . ($r = 10m, \mathbf{p}_{max} = [-6, -6, -6](dBw)$)

3.7 Conclusions

In this chapter, we have investigated the resource allocation problem for a full duplex *D2D* communication underlaying cellular network. To maximize the overall throughput and the

energy efficiency while guaranteeing the data rate requirement of both *D2D* users and *CU*s, first we formulate the resource allocation optimization problem, and then we find the global optimal solution through two steps: power control for all the possible couples $(D2D_j, CU_i)$; maximum weight matching to obtain the optimal cellular user for each *D2D* pair. By means of monotonic optimization theory, we proposed a new polyblock-based algorithm denoted as MARIO that can efficiently find the global optimal power control for the involved users. The Khun-Munkers algorithm is used to solve the matching problem. Due to the high complexity of the global optimal solution, we proposed the CATPA algorithm that can find an efficient sub-optimal solution by first assigning the channels and then controlling the users' powers. Simulation results verified the proposed algorithms and showed that the performance of the FD-D2D network highly depends on the self-interference capability and the proximity distance.

All the proposed RA algorithms in this chapter, as well as the PA algorithms of Chapter 2, are centralized algorithms in which the BS needs to know all the channel state information for all users at each step. This in turn questions the implementation feasibility of these algorithms in a real cellular network. To address this issue, the next chapter leverages the Game Theory analysis to propose a decentralized PA algorithm in which each user aim to maximize its EE individually. In particular, Chapter 4 models the PA problem as a non-cooperative game in which each user decides how much power to transmit over its allocated channel to maximize its link's EE. Moreover, chapter 4 finds the unique Nash Equilibrium solution of this game and proposes a distributed algorithm that finds this equilibrium point.

Chapter 4

Decentralized Resource Allocation Scheme for an FD-D2D Network

Contents

The previous two chapters thoroughly investigate the issues pointed out when reviewing the current state of the FD-D2D network in Chapter 1. In particular, Chapter 2 addresses the PA issue of an FD-D2D network and proposes a geometric based optimal PA scheme denoted as GALEN. Moreover, Chapter 3 achieves the optimal RA strategy of an FD-D2D network by using the powerful MO tool. However, all algorithms proposed in these two chapters are centralized and they assume that the BS has knowledge about the users' CSI at each step. Thus, in practice, the centralized approach will be unfeasible in term of implementation and a decentralized PA solution is required. In this context, the works in [113, 116] proposed two versions of an on-off based PA solution that can be implemented in a distributed manner. The work in [113] finds the optimal power of the *D2D* pairs neglecting the effects of the *CU* interference and also they did not consider the QoS constraints for the D2D users. The authors in [116] modeled the *D2D* locations as homogeneous spatial Poisson point process (PPP) and uniformly distributed the *CU* in the cell. After that, they derived the coverage probability for both cellular and *D2D* links, and with some mathematical approximations, they derived the closed-form analytical expression of the *D2D* users' optimal transmit probability which maximizes the ergodic *D2D* rate. However, in their work they assumed that the *D2D* users have the same rate constraints. The results in Chapter 3 shows that maximizing the network *GEE* is more interesting than maximizing the total sum-rate, and thus in this chapter we aim to design an energy-efficient distributed PA algorithm taking into account the QoS of all the users.

In the centralized scenarios, the resources for all the network components are optimized to maximize a system-wide utility function such as sum-rate or *GEE*. On the contrary, in a decentralized approach, each network node aims to optimize its own utility function by allocating its own resources. Thus, in the decentralized scenario, the network nodes act competitively and in a self-organizing way. Mathematically speaking, the Game theory (GT) framework is the most convenient tool to model and analyze this competitive behavior between the network nodes [133].

To the best of our knowledge, GT has not been used to provide a decentralized PA or RA in the context of FD-D2D based cellular network. Fortunately, there is abundant literature on the application of GT for distributed PA and RA in wireless communication networks and HD-D2D based cellular networks. For example, the authors of [137, 138] developed a general non-cooperative game framework to provide an energy-efficient PA mechanism for a general wireless network. Motivated by the works in [137, 138], we propose in this chapter a decentralized PA algorithm based on GT analysis for *EE* maximization in an FD-D2D underlaying cellular network. In particular, we model each user in the network as a rational player who engages in a non-cooperative game to allocate the transmission power over its assigned channel. After that, we mathematically prove that this non-cooperative game has a unique optimal point that can be obtained via an iterative distributed process. The effectiveness of our distributed algorithm

is verified through a numerical simulation which employs the centralized PA scheme proposed in our previous work [139] as a benchmark.

The main contributions of this chapter are as follows:

- Pointing out to the issue of the distributed implementation of the PA algorithm in an FD-D2D network.
- Providing a distributed PA algorithm based on Game theory for maximizing the *EE* of an FD-D2D network. We believe that this is the first work that propose a decentralized PA scheme for an FD-D2D network. To validate the proposed distributed PA algorithm a numerical assessment is conducted which adopts the centralized PA scheme proposed in [139] as a benchmark.
- Emphasizing the influence of the SI cancellation technique and the *D2D* proximity distance on the performance of the FD-D2D network.

The rest of this chapter is structured as follows. Section 4.1 provides the system model and develops the optimization problem. Section 4.2 solves the optimization problem using the Game theory analysis and Section 4.3 proposes a distributed iterative algorithm to reach the optimal PA scheme. Section 4.4 shows the simulation results, and Section 4.5 concludes this chapter.

4.1 System model and problem formulation

We consider an FD-D2D based cellular network where M half-duplex (HD) *CU*s coexist with M FD-D2D pairs. Each FD-D2D pair $D2D_j$ contains two *D2D* devices D_1^j and D_2^j that are in proximity of each other and they are reusing the j-th uplink channel assigned to CU_j. In this work, the uplink (UL) bandwidth reusing scenario is assumed because in this case, the *D2D* links only impact the BS which is more capable in interference management than the CU. Furthermore, we assume that the *CU*s are assigned orthogonal UL channels and thus there is no interference between *CU*s.

Fig. 4.1 shows an example of this network in which two *CU*s coexist with two FD-D2D pairs. In this figure, $g_{c,bs}^j$ denotes the channel gain between CU_j and BS while g_d stands for the channel gain between D_1^j and D_2^j and between D_2^j and D_1^j. Moreover, $h_{d1,bs}^j$ and $h_{d2,bs}^j$ respectively denote the interference channel gains from D_1^j and D_2^j to BS. $h_{c,d1}^j$ and $h_{c,d2}^j$ respectively represent the interference channel gains from CU_j to D_1^j and D_2^j. Besides, we assume that all channels are zero-mean complex Gaussian random variables. Thus, both direct and interference channels are facing Rayleigh fading with variance $l_{ij}^{-\alpha}$, where $i \in \{d1; d2; c\}$, $j \in \{d1; d2; bs\}$, $i \neq j$, l_{ij} is the distance between the nodes i and j, and α represents the path-loss exponent. Similar to the previous chapters, RSI denotes the residual self-interference

due to imperfect SIC at the FD devices and its power (P_{RSI}) is defined as ηp_t, with p_t being the transmit power of the node, as we already explained and discussed in Chapter 1 Section 1.2.1.

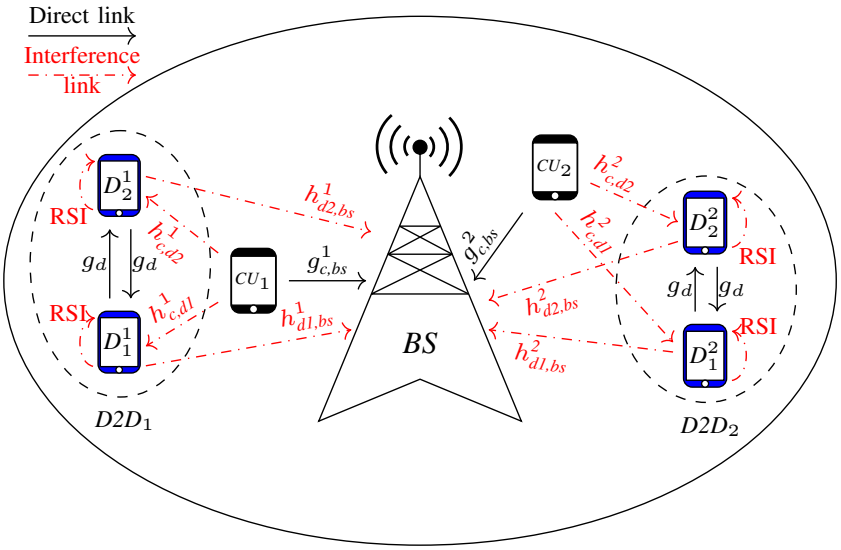

Figure 4.1 – Two full-duplex D2D pairs reusing the UL bandwidths of two *CU*s.

4.1.1 Problem Formulation

Let σ_N^2 be the power of the additive white Gaussian noise, and denote by p_c^j the transmission power of CU^j. Then, when $D2D_j$ reuses the spectrum of CU_j, the signal to interference plus noise ratio (SINR) at the intended receiver of CU_j, D_1^j, D_2^j (i.e., at BS, D_2^j and D_1^j), can be respectively expressed as

$$\Gamma_{c,rx}^j = \frac{p_c^j g_{c,bs}^j}{I_{-c} + \sigma_N^2} = \frac{p_c^j g_{c,bs}^j}{p_{d1}^j h_{d1,bs}^j + p_{d2}^j h_{d2,bs}^j + \sigma_N^2} \tag{4.1}$$

$$\Gamma_{d1,rx}^j = \frac{p_{d1}^j g_d^j}{I_{-d2} + \sigma_N^2} = \frac{p_{d1}^j g_d^j}{p_c^j h_{c,d2}^j + \eta p_{d2}^j + \sigma_N^2} \tag{4.2}$$

$$\Gamma_{d2,rx}^j = \frac{p_{d2}^j g_d^j}{I_{-d1} + \sigma_N^2} = \frac{p_{d2}^j g_d^j}{p_c^j h_{c,d1}^j + \eta p_{d1}^j + \sigma_N^2} \tag{4.3}$$

where $j \in \{1, 2, ..., M\}$, and I_{-k} stands for the interference on the intended receiver of the k-th transmitter with $k \in \{c, d1, d2\}$.

Now, using Shannon theorem, the rate (in bits/sec/Hz) of the j-th $D2D$ links and the j-th cellular link are given by:

$$R_k^j(p_k^j, \mathbf{p}_{-k}^j) = \log_2(1 + \Gamma_{k,\mathrm{rx}}^j), k \in \{c, d1, d2\}, j \in \{1, ..., M\} \tag{4.4}$$

with p_k^j being the transmission power of node k on the j-th channel and $\mathbf{p}_{-k}^j$ being the interference power vector at node k's intended receiver on the j-th channel containing all powers except user k's.

The energy efficiency (EE) of the above links measured in (bit/Joule/Hz) is defined as the energy cost of the communication link, and it is expressed as:

$$EE_k^j(p_k^j, \mathbf{p}_{-k}^j) = \frac{R_k^j(p_k^j, \mathbf{p}_{-k}^j)}{\mu p_k^j + P_{cir}}, \quad k \in \{c, d1, d2\}, j \in \{1, ..., M\} \tag{4.5}$$

where P_{cir} represents the wasted circuit power during the transmission at any mobile device, and μ denotes the inverse of the power amplifier efficiency at each node.

Considering the energy cost of the *D2D* and cellular links and the QoS constraints of the users, we aim in this chapter to propose an EE distributed PA scheme for an FD-D2D network. From a mathematical prospective, this can be done by jointly solving the following EE maximization problems:

$$arg \max_{p_k^j \in \mathcal{A}_k} \quad EE_k^j \left(p_k^j, \mathbf{p}_{-k}^j\right), \forall k \in \{c, d1, d2\}, j \in \{1, ..., M\} \tag{4.6}$$

$$\mathcal{A}_k^j = \{p_k^j \in \mathbb{R}_+ : p_k^j \leq P_{\max}^k, \Gamma_{k,rx}^j \geq \gamma_{\min}^{k,j}\} \tag{4.7}$$

with $\mathcal{A}_k^j$, being the feasible set of the kth user transmitting on the j-th channel. $P_{\max}^k$ is the transmitter k's maximum transmission power, and $\gamma_{\min}^{k,j}$ is the minimum required SINR level to fulfill the QoS of the kth user who is operating on the j-th channel. Solving these coupled maximization problems is the goal of the next section.

4.2 Game Theory based Power Allocation Algorithm

The aim of this section is to reformulate the optimization problems defined in (4.6) as game using the game theory, and to show that this game admits a unique solution which can be obtained through an iterative process. For ease of notation, and since the couples $(D2D_j, CU_j)$ with $j = \{1, 2, ..., M\}$ are independent of each others, in the sequel we remove the j-th superscript from our analysis, i.e., we solve the optimization problem of a generic $D2D$ pair that is reusing the uplink resource of an CU.

4.2.1 Game-Theoretical Problem Formulation

The coupled interference among the *D2D* and cellular links brings interactions between the *D2D* users and *CU*s that look to maximize their EE while satisfying their own QoS constraints (4.7). Such scenario can be analyzed using the non-cooperative game theory. In particular, the

maximization problems in (4.6) can be formulated as the non-cooperative game in normal form:

$$\mathcal{G} \triangleq \{\mathcal{K}, \{\mathcal{A}_k\}_{k\in\mathcal{K}}, \{EE_k(p_k, \mathbf{p}_{-k})\}_{k\in\mathcal{K}}\} \tag{4.8}$$

where:

- $\mathcal{K} = \{c, d_1, d_2\}$ is the set of players. Here, the elements of $\mathcal{K}$ are respectively indicating the CU, D_1, and D_2.
- $\mathcal{A}_k$ is the strategy set of player k.
- $EE_k(p_k, \mathbf{p}_{-k})$ given in 4.5 is player k's utility function.

Moreover, the optimization problems in (4.6) are known as the best-response dynamics (BRD) of the game $\mathcal{G}$, and the solution of the k-th optimization problem in (4.6) defines the best-response (BR) of the k-th player to the remaining players' actions $\mathbf{p}_{-k}$. Hence, we define the kth player's BR $\mathcal{B}_k(\mathbf{p}_{-k})$ as

$$\mathcal{B}_k(\mathbf{p}_{-k}) \triangleq arg \max_{p_k\in\mathcal{A}_{-k}} EE_k(p_k, \mathbf{p}_{-k}). \tag{4.9}$$

Any steady point of the BRD represents a solution of $\mathcal{G}$ and it is called a Nash equilibrium (NE) point. Generally speaking, a non-cooperative game may have zero, one, or multiple NE points. Further, in the case of the existence of an equilibrium point, the convergence of the BRD is not guaranteed. Accordingly, the main concerns when analyzing a non-cooperative game are to prove the existence and uniqueness of an NE and to show the convergence of BRD towards this unique NE. Unlike the regular non-cooperative game, both the utility function EE_k and the action set $\mathcal{A}_k$ of the k-th player are depending on the other players' actions $\mathbf{p}_{-k}$, which which makes answering the previous questions a challenging task. Such game is usually called a *generalized non-cooperative game* and it requires more tight conditions for a unique generalized Nash equilibrium point to exist and for the BRD to converge. The following sections explore these restrictive conditions and prove that our PA game $\mathcal{G}$ has an achievable unique NE point.

4.2.2 Existence of an equilibrium

The aim of this sub-section is to prove the existence of an NE solution for the power allocation game $\mathcal{G}$. To that end, first, we present the following two Lemmas:

Lemma 4.1. *The energy efficiency function EE_k is strictly quasi-concave for $p_k \in \mathbb{R}_+$, and the rate function R_k is strictly concave for $p_k \in \mathbb{R}_+$.*

Proof: First, let us show the convexity feature of $R_k(\Gamma_{k,\mathrm{rx}}(p_k))$. Applying the chain rule, the second-order derivative of R_k can be expressed as

$$\frac{\partial^2 R_k}{\partial^2 p_k} = \underbrace{\frac{\partial R_k}{\partial \Gamma_{k,\mathrm{rx}}} \frac{\partial^2 \Gamma_{k,\mathrm{rx}}}{\partial p_k^2}}_{A} + \underbrace{\frac{\partial^2 R_k}{\partial \Gamma_{k,\mathrm{rx}}^2}}_{B} \underbrace{\left(\frac{\partial \Gamma_{k,\mathrm{rx}}}{\partial p_k}\right)^2}_{C} \tag{4.10}$$

Now, to prove the concavity of R_k we must show that (4.10) is always negative. It is easily found that $\frac{\partial^2 \Gamma_{k,\mathrm{rx}}}{\partial p_k^2} = 0$, thus A is equal to zero. Moreover, we observe that C is always greater than zero. Hence, the convexity of EE_k only depends on B. Computing B shows that it is always negative and it is equal to $\frac{-1}{(1+\Gamma_{k,\mathrm{rx}})^2 \ln(2)}$. Hence, the concavity of R_k is proved. Then, EE_k is given by the ratio between a strictly concave function (R_k) and a linear function, which results in a strictly pseudo-concave function [133]. Moreover, any strictly pseudo-concave function is also quasi-concave [133], thus Lemma 4.1 is proved. ■

Lemma 4.2. *If*

$$\begin{cases} P_{\max} \geq \dfrac{\gamma_{\min}^{c}}{g_{c,bs}} \left(p_{d_1} h_{d1,bs} + p_{d_2} h_{d2,bs} + \sigma_N^2\right) \triangleq P_{\min}^{c}(\boldsymbol{p}_{-c}), & (4.11) \\ P_{\max} \geq \dfrac{\gamma_{\min}^{d1}}{g_d} \left(P_c g_{c,d1} + \eta P_{d1} + \sigma_N^2\right) \triangleq P_{\min}^{d2}(\boldsymbol{p}_{-d2}), & (4.11a) \\ P_{\max} \geq \dfrac{\gamma_{\min}^{d2}}{g_d} \left(P_c\, g_{c,d2} + \eta P_{d2} + \sigma_N^2\right) \triangleq P_{\min}^{d1}(\boldsymbol{p}_{-d1}), & (4.11b) \end{cases}$$

where $P_{\max} = P_{\max}^{c} = P_{\max}^{d1} = P_{\max}^{d2}$, *then the BR of the players are:*

$$\mathcal{B}_k(\boldsymbol{p}_{-k}) = \min\left\{P_{\max}^{k}, \max\left\{p_k^{\star}, P_{\min}^{k}\right\}\right\} \forall k \in \mathcal{K}. \tag{4.12}$$

wherein

$$p_k^{\star} = arg\max_{p_k} EE_k(p_k, \boldsymbol{p}_{-k}) \;\; s.t \; p_k \in \mathbb{R}_+. \tag{4.13}$$

Proof: The first part of Lemma 4.2 can be obtained by using the fact that $p_k \leq P_{\max}^{k}$ for all $k \in \mathcal{K}$ and reformulating the QoS requirements $\gamma_k \geq \gamma_{\min}^{k} \forall k \in \mathcal{K}$ as

$$p_c \geq \frac{\gamma_{\min}^{c}(I_{-c}+\sigma_N^2)}{g_{c,bs}}, \quad p_{d_2} \geq \frac{\gamma_{\min}^{d1}(I_{-d_2}+\sigma_N^2)}{g_d}, \quad p_{d_1} \geq \frac{\gamma_{\min}^{d2}(I_{-d_1}+\sigma_N^2)}{g_d}. \tag{4.14}$$

Hence if (4.11)-(4.11b) hold, there is always a power $p_k \in [0, P_{\max}^{k}]$ such that the QoS constraint $\Gamma_{k,\mathrm{rx}} \geq \gamma_{\min}^{k}$ is satisfied for all $k \in \mathcal{K}$.

To prove the second part of Lemma 4.2, first, we note that EE_k is a quasi-concave function with p_k (See Lemma 4.1). Thus, it has a unique optimal point $p_k^{\star} \in \mathbb{R}_+$. Hence, EE_k is increasing for $p_k \leq p_k^{\star}$ and decreasing for $p_k \geq p_k^{\star}$. This means that if $p_k^{\star} > P_{\max}^{k}$, then $P_{\max}^{k}$ is

the maximizer of EE_k. Next, by considering the QoS and maximum power constraints, and applying (4.11)-(4.11b), we obtain (4.12). ■

Now, we show that in our context the game $\mathcal{G}$ always admits an NE assuming that (4.11)-(4.11a) are satisfied. The author of [140] showed that the existence of an NE is guaranteed under the following assumptions:

1. The feasible action sets $\mathcal{A}_k$ of the players are nonempty, closed, convex, and contained in some compact set $\mathcal{C}_k$ for all $\mathbf{p}_{-k} \in \mathcal{A}_{-k} \equiv \prod_{l \neq k} \mathcal{A}_l$.

2. The sets $\mathcal{A}_k$ vary continuously with $\mathbf{p}_{-k}$ (in the sense that the graph of the set-valued correspondence $\mathbf{p}_{-k} \mapsto \mathcal{A}_k$ is closed).

3. The utility function $EE_k(p_k, \mathbf{p}_{-k})$ of each user is quasi concave in p_k for all $\mathbf{p}_{-k} \in \mathcal{A}_{-k}$.

In our framework, when (4.11)-(4.11b) hold true, then the feasible sets $\mathcal{A}_k$ are non-empty, convex (since based on Lemma 4.1 $R_k = \log_2(1+\Gamma_{k,\mathrm{rx}})$ is convex in p_k), closed and bounded for every $\mathbf{p}_{-k}$. Moreover, all the sets $\mathcal{A}_k$ vary continuously with $\mathbf{p}_{-k}$ because the QoS requirements $\Gamma_k \geq \gamma^k_{\min}$ is continuous in $\mathbf{p}_{-k}$ for all $k \in \{c, d1, d2\}$. Besides, and based on Lemma 4.1, the utility function EE_k is quasi-concave function. Thus, in our scenario, all the above three conditions are satisfied and the power allocation game $\mathcal{G}$ admits at least one NE point. The following section shows that $\mathcal{G}$ has a unique NE point, and that BRD always converges to such point.

4.2.3 Analysis of the equilibria

According to [141] a non-cooperative game has a unique NE which can be acieved by iteratively solving the BR of the players if: 1) the game has a non-empty set of NE points and 2) the BR function is a standard function. In the previous section we have already shown that $\mathcal{G}$ has at least one NE point. Thus, it only remains to prove that the BR of the players defined in (4.12) are standard functions[1]. In [133] it is proved that $p^\star_k$ is a standard function. On the other hand, since σ^2_N is always positive, $P^k_{\min} \forall k \in \mathcal{K}$ in (4.11)-(4.11a) is non-negative function. Moreover, it is also monotonic function because it is increasing in all $\{p_j\}_{j \neq k}$. Now, to prove the scalability feature of $P^k_{\min}$, take any scaling factor $\beta > 1$, then we will have

$$P^c_{\min}(\beta \mathbf{p}_{-c}) = \beta \gamma^c_{\min} \frac{I_{-c} + \frac{\sigma^2_N}{\beta}}{g_{c,bs}} < \beta \frac{I_{-c} + \sigma^2_N}{g_{c,bs}} = \beta P^c_{\min}(\mathbf{p}_{-c}), \tag{4.15}$$

$$P^{d2}_{\min}(\beta \mathbf{p}_{-d2}) = \beta \gamma^{d2}_{\min} \frac{I_{-d2} + \frac{\sigma^2_N}{\beta}}{g_{d}} < \beta \frac{I_{-d2} + \sigma^2_N}{g_{d}} = \beta P^{d2}_{\min}(\mathbf{p}_{-d2}),$$

[1] A function $f(\mathbf{x})$ is standard if it fulfills the properties of *i*) Positivity: $f(\mathbf{x}) \geq 0$ for all $\mathbf{x} \geq 0$; *ii*) Monotonicity: $f(\mathbf{x}_1) \geq f(\mathbf{x}_2) \forall \mathbf{x}_1 \succeq \mathbf{x}_2$; *iii*) Scalability: $f(\beta \mathbf{x}) < \beta f(\mathbf{x})$ for all $\mathbf{x} \geq 0$, $\beta > 1$.

$$P_{\min}^{d1}(\beta \mathbf{p}_{-d1}) = \beta \gamma_{\min}^{d2} \frac{I_{-d1} + \frac{\sigma_N^2}{\beta}}{g_d} < \beta \frac{I_{-d1} + \sigma_N^2}{g_d} = \beta P_{\min}^{d1}(\mathbf{p}_{-d1}).$$

At this stage, we have shown that both $P_{\min}^{k}$ and $p_k^\star$ are standard functions. Now, observe that $P_{\max}^{k}$ does not depend on $\mathbf{p}_k$ for all $k \in \mathcal{K}$, it follows that the best responses defined in (4.12) are standard functions because both max(.) and min(.) are increasing functions. As a result, the power allocation game $\mathcal{G}$ admits a unique solution and its BRC converges to this unique point. The next section provides a distributed algorithm that can solve $\mathcal{G}$.

4.3 Distributed power allocation algorithm

In this section, we aim at providing a distributed power allocation algorithm that converges to the unique NE point of the game $\mathcal{G}$. To do so, we need to derive the point $p_k^\star$ defined in (4.13). For ease of notation, we denote by $\Delta_k \triangleq I_{-k} + \sigma_N^2$ the equivalent interference-plus-noise gain on the k-th link, and call $\gamma_{\max}^{c} \triangleq g_{c,bs}$, $\gamma_{\max}^{d1} \triangleq g_d$, $\gamma_{\max}^{d2} \triangleq g_d$ the maximum SINRs values that can be obtained at the cellular link and the D2D links respectively when these nodes do not receive interference and the thermal noise is negligible. Using these definitions the SINRs defined in (4.1)-(4.3) can be rewritten as

$$\Gamma_{k,\mathrm{rx}} = \frac{\gamma_{\max}^{k}}{\Delta_k} p_k \forall k \in \mathcal{K}. \tag{4.16}$$

Now, the solution of (4.13), $p_k^\star$, is given in the following Lemma.

Lemma 4.3. *For any given $\boldsymbol{p}_{-k}$, $p_k^\star$ is given by*

$$p_k^\star = \Phi_k(\lambda_k^\star) = \left[\frac{1}{\lambda_k^\star} - \frac{\Delta_k}{\gamma_{\max}^{k}} \right]^+ \tag{4.17}$$

with $\lambda^\star$ being the root of the following function:

$$F(\lambda_k) = \max_{p_k \in \mathbb{R}_+} \log_2(1 + \frac{\gamma_{\max}^{k}}{\Delta_k} p_k) - \lambda_k (p_k + P_{cir}). \tag{4.18}$$

Proof: Observe that EE_k is a ratio of two functions. Hence, it belongs to the class of fractional programming theory. Consequently, the solution of (4.13) can be found by means of Dinkelbach's algorithm [132]. By means of the latter, solving the *EE* maximization problem in (4.13) is equivalent to finding the solution $\lambda_k^\star$ of (4.18). Now, taking the derivative of (4.18) w.r.t p_k and setting it to zero results in:

$$\frac{1}{1 + \Gamma_{k,\mathrm{rx}}} \frac{\partial \Gamma_{k,\mathrm{rx}}}{\partial p_k} - \lambda_k = 0. \tag{4.19}$$

Using (4.16), $\frac{\partial \Gamma_{k,\mathrm{rx}}}{\partial p_k} = \frac{\gamma^k_{\max}}{\Delta_k}$ and taking into account that $p^\star_k \geq 0$ eventually yield to (4.17). ■

Now let $p_k[i]$ be the k-th player's transmit power at the i-th iteration step. Based on the results of Section 4.2 and Lemma 4.3, there is an algorithm that converges to the unique NE of $\mathcal{G}$ and it operates by iteratively updating the players' BR

$$p_k[i+1] = \min\{P^k_{\max}, \max\{p^\star_k[i], P^k_{\min}[i]\}\} \tag{4.20}$$

where $P^k_{\min}[i]$ is calculated using (4.16) as follows

$$P^k_{\min}[i] = \frac{\gamma^k_{\min}}{\gamma^k_{\max}} \Delta_k[i]. \tag{4.21}$$

Algorithm 5 presents the pseudo-code of this iterative process. From (4.17) and (4.18) it is clear that the calculation of $p_k[i+1]$ in (4.20) needs only information about $\Delta_k[i]$ because $\gamma^k_{\max}$, $\gamma^k_{\in}$, and $P\mathrm{max}^k$ are locally available at each receiver. Now, to earn this info we reformulate $\Delta_k[i]$ using (4.16) as

$$\Delta_k[i] = \frac{\gamma^k_{\max}}{\Gamma_{k,\mathrm{rx}}[i]} p_k[i] \tag{4.22}$$

where $\Gamma_{k,\mathrm{rx}}[i]$ is the SINR of the k-th node's intended receiver at the i-th iteration, and $p_k[i]$ is the transmit power of the k-th receiver's intended transmitter at the i-th iteration. Inspecting (4.22) shows that $\Delta_k[i]$ can be easily obtained when each transmitter knows the SINR value at its intended receiver $\Gamma_{k,\mathrm{rx}}[i]$. This is because each node knows the value of its transmit power $p_k[i]$ and its maximum achievable SINR value $\gamma^k_{\max}$. Note that, the intended receiver of a transmitter k can easily estimate its SINR and return it to the k-th transmitter using a feedback downlink channel. Thus, the PA algorithm reported in Algorithm 5 can be executed in a fully distributed manner.

4.4 Simulation results

In this section, numerical simulations under different operating conditions are used to analyze the performance of the proposed distributed PA (Algorithm 5). Moreover, since none of the previous works address the distributed implementation of PA in the context of FD-D2D network, we compare Algorithm 5 with two PA strategies: i) the centralized PA algorithm in [139] which aims to maximize the global energy efficiency (GEE) of the FD-D2D network defined as $GEE = \frac{\sum_{k\in\mathcal{K}} R_k}{\sum_{k\in\mathcal{K}} p_k + 3P_{cir}}$, ii) the fixed power allocation strategy in which each user transmits at its maximum allowed transmission power P^k_{max}.

Besides, three metrics are used to assess the performance:

Algorithm 5 The proposed distributed PA algorithm

Set $i = 0$, and for all $k \in \mathcal{K}$ set $p_k[0]$ to an arbitrary feasible value.
repeat
for all $k \in \mathcal{K}$ **do**
    receive $\Gamma_{k,\mathrm{rx}}[i]$ from the intended receiver, then
    compute $\Delta_k[i]$ using (4.22).
    Update $P^k_{\min}[i]$ in (4.21) using $\Delta_k[i]$.
    Compute $p^\star_k[i]$ using $\Delta_k[i]$ and Dinkelbach's algorithm
    as shown in (4.17) and (4.18).
    adjust the k-th user's transmit power as:

$$p_k[i+1] = \min\{P^k_{\max}, \max\{(p^\star_k[i]), P^k_{\min}[i]\}\}$$

end for
update $i = i + 1$
until convergence

(i) the D2D rate gain brought by the accessed FD-D2D pairs defined as $R_{gain} \triangleq \frac{\sum_{k\in\mathcal{K}} R_k - R_c^{\max}}{R_c^{\max}} \times 100$, with $R_c^{\max} = \log_2(1 + \frac{g_{c,bs}}{\sigma_N^2} P^c_{\max})$ being the maximum achievable cellular link throughput when the FD-D2D pairs do not exist,

(ii) the rate of the FD-D2D pair R_{d2d} defined as $R_{d2d} = R_{d1} + R_{d2}$,

(iii) and the *GEE* of the accessed couples (*D2D*, CU).

4.4.1 Simulation setup

We consider a single cell network with radius $R = 500m$ in which M FD-D2D pairs coexist with M *CUs*. The *CUs* are equally sharing the uplink bandwidth and they are uniformly distributed in the cell. Moreover, each $D2D_j$ is sharing the same resource of CU_j and it is uniformly distributed within a randomly located cluster with radius r. Throughout our simulation, we consider 500 realizations each with $M = 15$ *CUs* and $M = 15$ *D2D* pairs and the results are averaged over the M couples $(D2D_j, CU_j)$ and the 500 realizations. Besides, in our simulation, we declare the convergence of Algorithm 5 when the relative squared error between the obtained power vector $\mathbf{p} = [p_c, p_{d1}, p_{d2}]$ of two successive iterations is not larger than 10^{-6}. All the simulation parameters are summarized in Table 4.1.

4.4.2 Numerical assessment

Considering the above simulation setup, we show in Fig.4.2 the behavior of FD-D2D rate gain with respect to (w.r.t.) the self-interference cancellation factor η and the D2D cluster radius r. As it can be seen, R_{gain} increases as η decreases. This is because at low η the self-interference

Table 4.1 – Simulation parameters

Cell radius (R)	500m
D2D cluster radius(r)	10, 20, 40, 80 (m)
Number of *CUs* and D2D pairs (M)	15
Noise power (σ_N^2)	-114 dBm
Path-loss exponent (α)	4
Maximum power of *CUs* and D2D users	24 dBm
The wasted circuit power during transmission (P_{cir})	10 dBm
SINR requirements for *CUs* and D2D users ($\gamma_{\min}^k$)	uniform distributed in [0,25] dB
SI cancellation factor (η)	-100,-90,...,-50 dB
Multiple-path fading	Exponential distribution with l_{ij} mean
Convergence criterion of Algorithm 5	$\frac{\|\|\mathbf{p}[i]-\mathbf{p}[i-1]\|\|^2}{\|\|\mathbf{p}[i]\|\|^2} \leq 10^{-6}$

decreases which reflects in lower interference and higher rate. Moreover, the FD-D2D rate gain decreases as r increases because when r increases more power is needed to meet the QoS which results in higher interference and lower rate. Thus, to achieve the highest possible rate gain of an FD-D2D network, the D2D users must be in low proximity distance and they need to have a good SI cancellation technique.

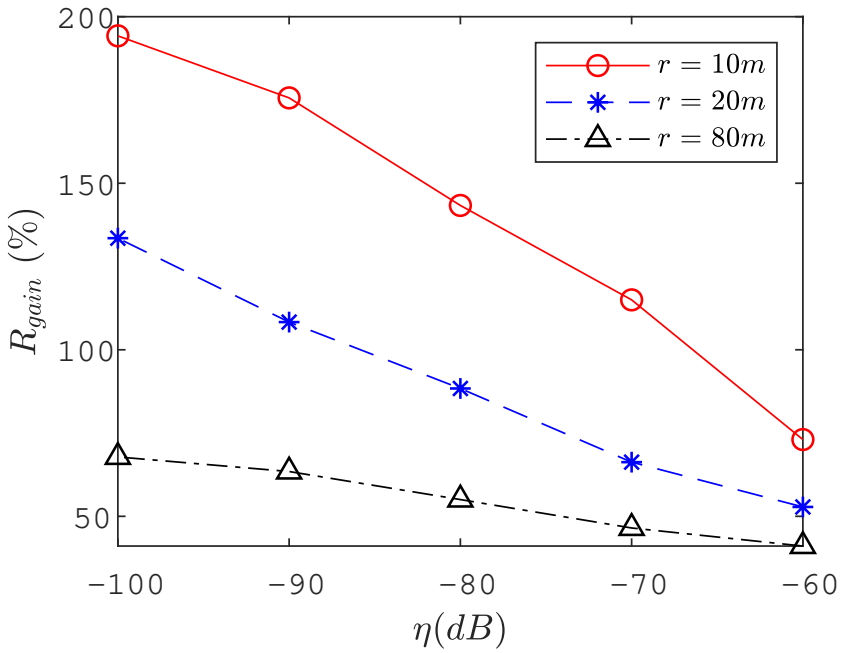

Figure 4.2 – The rate gain behavior of the proposed distributed PA w.r.t. the self-interference cancellation factor η and D2D proximity distance r.

Focusing on the case of small *D2D* distance ($r = 10m$), Fig. 4.3 compares the *GEE* of the links for the three power allocation strategies. As expected the centralized PA algorithm proposed in [139] outperforms our proposed distributed algorithm, as well as the full-power transmission algorithm, in terms of global energy efficiency. This is because the centralized algorithm in [139] originally created to optimized the *GEE* of an FD-D2D network, while our proposed distributed algorithm aims to find an equilibrium point when each user seeks to selfishly maximize its own *EE*. Yet, the proposed distributed algorithm reaches 84% of the optimal *GEE* point achieved by the centralized solution at $\eta = -100dB$. Notice that the proposed distributed power allocation requires much less feedback overhead comparing to the centralized approach which makes it more attractive for real implementation.

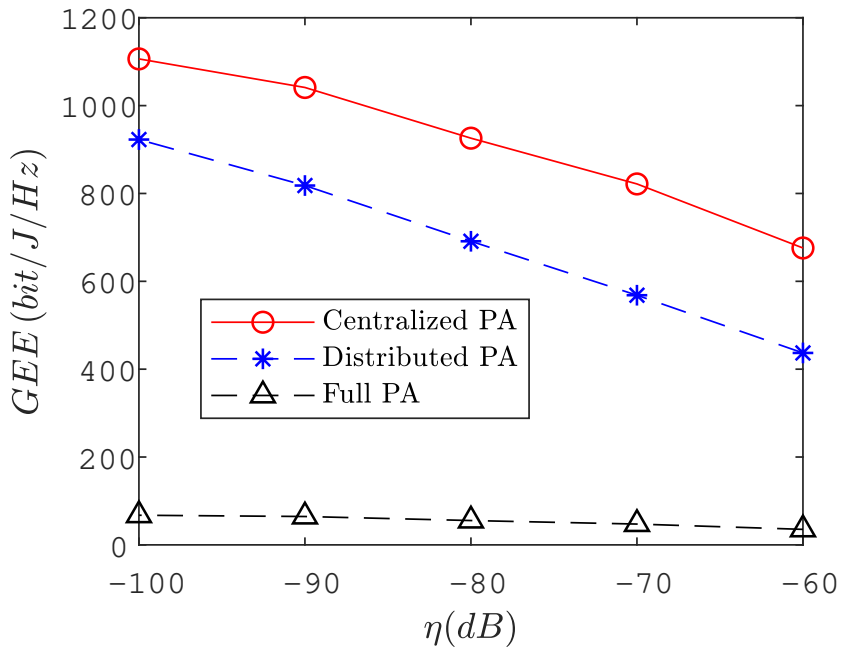

Figure 4.3 – The *GEE* behavior w.r.t. the self-interference cancellation factor η when allocating power according to: 1) the centralized PA algorithm proposed in [139], 2) the proposed distributed PA algorithm, and 3) the full-power transmission strategy.

Now, to have a complete picture about the performance of our proposed algorithm, we set $r = 10m$ and we show in Fig.4.4 the achieved *D2D* rate by the three PA strategies. As it can be seen, our proposed algorithm achieves higher *D2D* rate comparing to both the centralized solution and the full power transmission algorithm. This is because our proposed algorithm consumes more energy comparing to the centralized solution (See Fig. 4.3). Since the aim of an FD-D2D network is to offload as much data as possible from the cellular network, the proposed distributed algorithm seems to be much more attractive for the FD-D2D network designers. Moreover, from both Fig. 4.3 and Fig. 4.4, we can see that the full-power transmission algorithm is the worst strategy in terms of both *EE* and rate. This is because, transmission at

the maximum power when users are in low proximity distances yields to high interference and low rate.

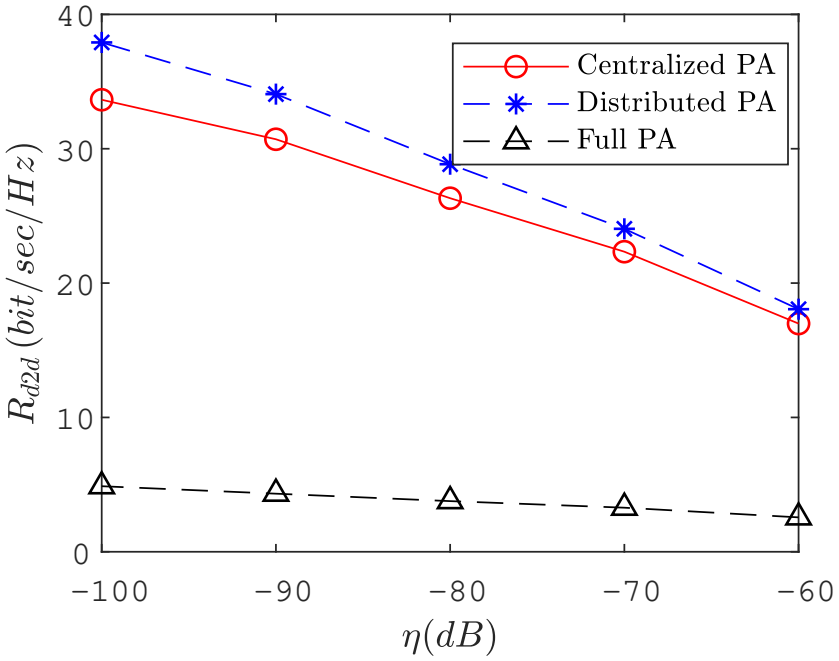

Figure 4.4 – The achieved D2D rate when allocating power according to: 1) the centralized PA algorithm proposed in [120], 2) the proposed distributed PA algorithm, and 3) the full-power transmission strategy.

Finally, to show the superiority of our proposed algorithm in terms of complexity, we present in Table.4.2 the average number of iterations and execution time of the proposed distributed algorithm and the centralized algorithm. As it can be seen, the distributed algorithm required slightly greater number of iterations but with much more less time to achieve the equilibrium. This is because the centralized approach needs to solve a convex problem at each iteration using the well known interior point method.

Table 4.2 – The average number of iterations and execution time of the proposed distributed algorithm and the centralized algorithm.

	Number of iterations				Execution time (ms)			
$\eta(dB)$	$r = 10(m)$		$r = 20(m)$		$r = 10(m)$		$r = 20(m)$	
	Centralized	Distributed	Centralized	Distributed	Centralized	Distributed	Centralized	Distributed
−60	4.3	6.9	4.3	8.8	1429.1	0.013	1139.2	0.09
−70	4.1	5.6	4.3	8.6	1228.1	0.01	1323.8	0.01
−80	4.0	4.7	4.1	5.9	943.1	0.01	940.5	0.01
−90	4.0	4.7	4.0	5.5	656.4	0.01	747.5	0.01
−100	4.0	4.5	4.0	4.9	442	0.01	513.2	0.01

4.5 Conclusions

In Chapter 4 we address the PA problem of an FD-D2D underlaying cellular network. In particular, we propose a distributed PA algorithm for such kind of network by using Game theory analysis. First, we model the interactions between the *CU*s and the *D2D* users as a non-cooperative game $\mathcal{G}$. Next, we show that $\mathcal{G}$ admits a unique Nash equilibrium point which can be achieved through an iterative algorithm. After that we show that this iterative algorithm can be implemented in a fully distributed manner. Provided simulation results verify the effectiveness of our proposed distributed power allocation algorithm and show that the self-interference cancellation capability and the proximity distance of the *D2D* devices highly affect the performance of the FD-D2D network. However, this chapter did not consider the CA issue for the FD-D2D network which is left for future work as we will describe in the next chapter. Chapter 5 also provides a quick summary of this thesis and lists the potential research direction to be addressed in the future.

Chapter 5

Conclusions and Perspectives

The work presented in this dissertation fits into a wide body of research that has been looking for novel wireless technologies to deal with the ever-increasing demand on the limited wireless cellular spectrum. In particular, this thesis studies the possibility of integrating the promising *D2D* communication network with the Full-duplex technology to further enhance the SE, data rate of the network. However, as stated in Chapter 1, this integration creates a harsh co-channel interference environment which must be carefully coordinated to achieve the integration advantages. Here, we recognized the importance of designing appropriate radio resource management schemes to mitigate such interference ambiance. Our main contributions have been in the context of PA and CA as explained in the follows.

5.1 Main results and finding of the thesis

Analysis of the ergodic rate behavior

With the aim of understanding the general performance of the FD-D2D network and recognizing the parameters that may impact its gains, we first derived in Chapter 1 the closed-form expression of the ergodic D2D rate. Then, we thoroughly analyzed this expression and we found that the *D2D* proximity distance, the FD device SIC capability, the CUs distance from the *D2D* pair play a pivot role in determining the network performance. Therefore, in all the simulation experiment we validate our proposed algorithms with various D2D proximity distance and several SIC factors.

Developing an efficient optimal PA scheme

In general, power control is considered as one of the most essential parts to control the interference of any wireless network. This is because the interference power is directly related

to the users' transmit power. Therefore, finding the optimal power profile has always been the target of the network operators. In this thesis also, we aim at finding the best PA scheme of the FD-D2D network, but, unfortunately, the PA problem is shown to be non-concave. To deal with this issue, most of the related works relied on the SCO tool to provide an efficient PA solution. Chapter 2 filled this blank and provides the GALEN framework which finds the optimal PA by taking advantage of the feasible set's geometry. In particular, Chapter 2 explored the structure of the feasible set and restricted the optimal point inside a set of vertices with known coordinates.

Finding the ultimate gain of an FD-D2D network

Besides the PA, when multiple *D2D* pairs coexist with cellular users, the CA becomes a crucial point in determining the performance of the network. Normally, the joint CA and PA problem belongs to the class of mixed-integer non-linear programming (MINLP) which make it very hard to solve. That is why most of the related work in the context of FD-D2D network only provided a sub-optimal RA scheme. To seal this gap, Chapter 3 proposes a MO-based RA framework which can achieve the optimal solution. Specifically, Chapter 3 first decomposes the RA problem into PA and CA sub-problems. After that, it develops a polyblock-based algorithm denoted as MARIO to globally solve the PA sub-problem. Then, it uses the Hungarian algorithm to assign the users' channel. Moreover, Chapter 3 presents a novel sub-optimal solution called CATPA which competes the existing work in terms of complexity and accuracy.

Proposing a distributed PA algorithm

Although the optimal PA and RA schemes were found in Chapter 2 and Chapter 3 respectively, the proposed solutions therein are centralized in the sense that the CSI of all users are assumed to be known at the central BS unit. The same assumption was made by all the related work. However, this assumption is not realistic and cannot be implemented in a real network scenario. To overcome this issue, Chapter 4 leverages the powerful GT framework to solve the PA problem in a distributed manner. Particularly, Chapter 4 models the PA as a non-cooperative game in which each user decides how much power to transmit over its allocated channel to maximize its own utility. The existence and the uniqueness of the game's solution are also discussed in this chapter.

The overall results achieved in this thesis show that the promises of FD-D2D are highly related to the employed interference mitigation technique in the network. Therefore, to achieve all the possible gains of the FD-D2D network more in depth study is required. The following section provides several possible extensions of this thesis.

5.2 Perspectives for future works

This thesis mainly tackled the PA and RA problems of an FD-D2D network. The assumptions we have made and the results we have obtained open the door for potential perspectives for future works that we list in the following:

Resource allocation management with statistical CSI scenario

The proposed PA and CA algorithms in Chapter 2 and Chapter 3 require perfect CSI for all the users. In practice, the channel status between the CUs/*D2D* users and the BS can be obtained from the pilot signals. However, the channel status between any two users cannot be obtained directly unless one of these users, i.e., either the CU or the *D2D* users, measure it and sent it back to the BS. This process increases the signaling overhead and the computational complexity, thus it is worthy to propose a RA scheme assuming a statistical CSI scenario. The work in [119] propose a RA framework with statistical CSI to maximize the ergodic rate of the network. With the focus on the green signaling in today's networks, it would be interesting to extend this work to maximize the EE of the network assuming a statistical CSI scenario.

Resource allocation management with restrictions-less on the channel sharing

Due to the harmful interference in a FD-D2D network, in this thesis we assume that an FD-D2D pair can reuse the UL resources of at most one CU, and the CU may share its resources with at most one *D2D* pairs. Although this technique may help in moderating the network's interference, it may miss the opportunity of further enhancing the SE especially when the CUs are expressing good channel situations. Thus, a possible extension of this work is to analyze the PA and RA problems assuming multiple FD-D2D pairs can share the same UL resources, or one FD-D2D pair can reuse multiple CUs resources, or multiple CUs are sharing their bandwidths with multiple FD-D2D pairs.

Multi-cell analysis

The studies done in this dissertation only considers a single cell scenario, neglecting the impact of the interference introduced by the neighboring CUs who are transmitting on the same UL channel. Therefore, a good work continuation would be studding the resource allocation management (RRM) of an FD-D2D network under a multi-cell setup. The works in [6] and [95] evaluated such scenario using the stochastic geometry tools . However in their work a simple on-off PA strategy was proposed. To have better power control mechanism, we suggest to address the PA problem for an FD-D2D network in a two-cell scenario and then generalize it

for a multi-cell network. Giving the distance between the cell, the co-cell interference between the cells with no direct borders is very low, and thus validate the generalization technique.

Interference coordination for FD-D2D underlaying heterogeneous network in multi-cell environment

The current work proposes several PA and RA schemes to mitigate the network's interference only taking into account the coexisting between FD-D2D pairs and macro CUs. Thus, the situation will be much more complicated when FD-D2D communication takes place in heterogeneous network, especially the coexisting with the envisioned hyper small cells in 5G. In such case, novel interference coordination techniques must be proposed. This challenge was reported in [142] and partially studied in [143]. Specifically, the authors in [143] proposed a stochastic geometry-based model to assess the performance of FD-D2D network in multi-tier single cell network assuming a simple distance based PC was applied. However, different aspects still need further analysis such as the mode selection and the cell association. Moreover, in their work only a single Macro-cell was considered. So, a good extension would be analyzing the network performance assuming a multi-macro cells scenario where each one contains a multi-tier small cells.

Distributed joint CA and PA algorithm

Chapter 4 proposes a non-cooperative game to solve the PA problem of an FD-D2D network in a decentralized way. Thus, a natural extension of this work would be solving the joint CA and PA problem in a distributed fashion. Such a problem can be well analyzed by the Stackelberg-type game due to its hierarchical structure. In literature, this type of game has been used to coordinate the HD-D2D network's interference environment by modeling the BS as the Stackelberg-leader who aims to protect the CUs by setting a price of each *D2D* channel usage as in [144, 145].

Dynamic FD-D2D network

Similar to the existing FD-D2D works, this thesis assumes a static FD-D2D scenario. As a future work, we suggest to investigate the resource allocation issue of a dynamic FD-D2D network in which the *D2D* users are in motion. This will impose new RRM challenges. For instance, if a moving *D2D* pair enters a new cell, it may affect the cellular link taking places on the same resources. Thus, the BS must always observes the interference level of such a link. Here we did not find any direct research on this aspect, which makes this subject attractive for researchers to add contributions to it.

Appendix A

Approximation for the expectation of a ratio of random variables

In this appendix, we prove how we derived the first order Taylor expansion of $\mathbb{E}[\Gamma_{bs}]$ in (2.28). To generalize the proof, we consider two random variables X and Y where Y has support $[0, \infty)$, and we assumed $R = f(X, Y) = \frac{X}{Y}$.

The first order Taylor expansion of a two-variables function $f(x, y)$ at the point $\theta = (\theta_x, \theta_y)$ is

$$f(x, y) = f(\theta) + f'_x(\theta)(x - \theta_x) + f'_y(\theta)(y - \theta_y) \tag{A.1}$$

where f'_x and f'_y are the first derivative of the function $f(x, y)$ w.r.t x and y respectively. To apply the same concept on the ratio random variable $R = f(X, Y)$, we assume that both X and Y have finite means defined as $\mathbb{E}[X] = \mu_x$ and $\mathbb{E}[Y] = \mu_y$ respectively. Then, we expand R over the point $\theta = (\mu_x.\mu_y)$ as follows:

$$f(X, Y) = f(\theta) + f'_x(\theta)(X - \mu_x) + f'_y(\theta)(Y - \mu_y). \tag{A.2}$$

The first-order approximation of $\mathbb{E}[f(X, Y)]$ is then given by:

$$\begin{aligned}
\mathbb{E}[f(X,Y)] &= \mathbb{E}\left[f(\theta) + f'_x(\theta)(X - \mu_x) + f'_y(\theta)(Y - \mu_y)\right] \\
&= \mathbb{E}[f(\theta)] + \mathbb{E}[f'_x(\theta)(X - \mu_x)] + \mathbb{E}[f'_y(\theta)(Y - \mu_y)] \\
&= \mathbb{E}[f(\theta)] + f'_x(\theta)\mathbb{E}[X - \mu_x] + f'_y(\theta)\mathbb{E}[Y - \mu_y] \\
&= \mathbb{E}[f(\theta)] \\
&= f(\mu_x, \mu_y)
\end{aligned} \tag{A.3}$$

Therefore, $\mathbb{E}[\frac{X}{Y}] = \frac{\mu_x}{\mu_y}$.

Appendix B

Appendix for Chapter 2 Section 2.2.1

We begin our proof by providing the following conjecture.

Conjecture B.1. *In wireless communication the receiver decodes correctly the signals when the following inequality holds:*

$$\mathbb{E}[P] \geq \mathbb{E}[I]$$

where $\mathbb{E}[P]$ *is the average power of the useful signal and* $\mathbb{E}[I]$ *is the average interference power.*

Now by applying Conjecture B.1 on (2.3) and (2.4) and neglecting the effect of the noise we can see that the FD communication can be useful only when the SIC factor, η, is less than a certain value as follows:

$$\eta < \min\left(\frac{yl_d - l_{c,d_1}}{x}, \frac{xl_d - l_{c,d_2}}{y}\right) \tag{B.1}$$

Since η is positive, the following inequalities must be satisfied:

$$x > \frac{l_{c,d_2}}{l_d} \text{ and } y > \frac{l_{c,d_1}}{l_d} \tag{B.2}$$

Note that, (B.2) is the same as $\mathcal{R}_4$. Moreover, if (B.2) does not hold the SIC factor will be negative which means that the FD transmission is unsuitable in such situation. Thus, the *D2D* users must switch to the HD mode. Now in order to investigate the rates in the remaining regions we derived the limits of $R_{D1}, R_{D2}, R_{D1}^{HD}$, and R_{D2}^{HD}, which are respectively defined in (2.17) and (2.9), as follows:

$$\lim_{y \to \frac{l_{c,d_1}}{l_d}} R_{D1} = 1 - \frac{\eta x}{l_{c,d_1}} E_1\left(\frac{\eta x}{l_{c,d_1}}\right) e^{\frac{\eta x}{l_{c,d_1}}}$$

$$\lim_{x\to\frac{l_{c,d_2}}{l_d}} R_{D2} = 1 - \frac{\eta y}{l_{c,d_2}} E_1\left(\frac{\eta y}{l_{c,d_2}}\right) e^{\frac{\eta y}{l_{c,d_2}}} \tag{B.3}$$

$$\lim_{y\to\frac{l_{c,d_1}}{l_d}} R_{D1}^{HD} = 1, \qquad \lim_{x\to\frac{l_{c,d_2}}{l_d}} R_{D2}^{HD} = 1$$

Based on (B.3) and the monotonic increasing property of the *D2D* users rate, the maximum rate of $D1$ and $D2$ when $y < \frac{l_{c,d_1}}{l_d}$ and $x < \frac{l_{c,d_2}}{l_d}$ will be $1bit/s/Hz$ respectively. Hence, the FD transmission can show its efficiency only in $\mathcal{R}_4$.

Appendix C

The Hungarian algorithm

The Hungarian algorithms aims at solving an assignment problem in polynomial time and it is based on the works of two Hungarian mathematicians Dénes Kőnig and Jenő Egerváry. This Appendix informally presents the Hungarian algorithm through an example, and for more formal presentation the reader may refer to [128].

Assume a network operator which has four base stations that need to be deployed to enhance network coverage for a certain town. Additionally, the operator has four teams in the area for deploying the BSs and each team has a specific travelling cost as showing the cost matrix given in Table C.1. The operator aims at finding the best assignment that minimizes the total traveling cost such that each team can deploy at most one BS and each BS can be assigned to at most one team.

Table C.1 – Traveling cost (Euros)

	BS1	BS2	BS3	BS4
Team 1	400	200	250	230
Team 2	200	350	100	125
Team 3	150	50	100	150
Team 4	175	100	125	150

In a non-negative matrix, if there exist an assignment solution with zero cost, then this solution will obviously be the optimal assignment. Based on this, the Hungarian algorithm finds the optimal assignment by performing several matrix transformation steps as indicating below.

Step 1: ***Row reduction***

In this step the algorithm finds the minimum element of each row and subtracts it from every value in its row, leading to at least one zero in each row as illustrated sin the following matrix.

$$\begin{pmatrix} 200 & 0 & 50 & 30 \\ 100 & 250 & 0 & 25 \\ 100 & 0 & 50 & 100 \\ 75 & 0 & 25 & 50 \end{pmatrix}$$

Step 2: ***Column reduction***

In this step the algorithm finds the minimum element of each column and subtracts it from every value in its column, leading to at least one zero in each column as illustrated in the below matrix.

$$\begin{pmatrix} 125 & 0 & 50 & 5 \\ 25 & 250 & 0 & 0 \\ 25 & 0 & 50 & 75 \\ 0 & 0 & 25 & 25 \end{pmatrix}$$

Step 3: ***Test for an optimal assignment***

This step first draws the minimum number of straight lines that cover all the zeros. If the number of lines is equal to the number of rows and columns then an optimal assignment can be made and the algorithm jumps to step 5, else a shifting zero process must be done as indicated in step 4.

The below matrix indicates in red lines the required minimum number lines to cover all the zeros in our example. It is clear that the number of red lines is less than the number of rows and columns and thus the algorithm must go to step 4.

$$\begin{pmatrix} 125 & 0 & 50 & 5 \\ 25 & 250 & 0 & 0 \\ 25 & 0 & 50 & 75 \\ 0 & 0 & 25 & 25 \end{pmatrix}$$

Step 4: ***Shift zeros***

To increase the minimum number of lines required to cover all of the zeros, this step needs to shift at least one zero to an uncovered position. To that end, the algorithm in this step first finds the smallest uncovered value which is 5 in our example. This value is then subtracted from all the uncovered elements and added to each element at the intersection of two lines. The lines are then removed, and the algorithm jumps back to step 3 to test if there is an optimal assignment. The below matrices show this process and show that the minimum number of lines

required to cover all of the zeros is now equal to the number of rows and columns and thus the algorithm jumps to step 5.

$$\begin{pmatrix} 120 & 0 & 45 & 0 \\ 25 & 255 & 0 & 0 \\ 25 & 0 & 45 & 70 \\ 0 & 5 & 25 & 25 \end{pmatrix} \longrightarrow \begin{pmatrix} \cancel{120} & \cancel{0} & \cancel{45} & \cancel{0} \\ \cancel{25} & \cancel{255} & \cancel{0} & \cancel{0} \\ \cancel{25} & \cancel{0} & \cancel{45} & \cancel{70} \\ \cancel{0} & \cancel{5} & \cancel{25} & \cancel{25} \end{pmatrix}$$

Step 5: ***Making the final assignment***

This step assigns the BS that must be deployed for each team based on the locations of the zeros. The final assignment of our example is given below in blue texts. This assignment has a total cost equal to 555 euros.

$$\begin{pmatrix} 120 & 0 & 45 & 0 \\ 25 & 255 & 0 & 0 \\ 25 & 0 & 45 & 70 \\ 0 & 5 & 25 & 25 \end{pmatrix} \longrightarrow$$

	BS1	BS2	BS3	BS4
Team 1	400	200	250	230
Team 2	200	350	100	125
Team 3	150	50	100	150
Team 4	175	100	125	150

Before terminating this appendix, it is worthy to highlight the following point. Imagine the case where the values of Table C.1 are the estimated network's profit after assigning each BS to a team, and the operator aims at maximizing its profit. In this case, the problem can be altered to fit the setting by subtracting the maximum profit value from the profit matrix and then performing the same steps as before.

Appendix D List of Publications

Publication related to the thesis

The contributions related to the works presented in this manuscript are listed as follows:

Journal articles

[J1] H. Chour, E. Jorswieck, F. Bader, Y. Nasser, and O. Bazzi, "Global Optimal Resource Allocation for Efficient FD-D2D Enabled Cellular Network," IEEE Access, Vol. 7, pp. 59690-59707, May 2019.

International conferences

[C1] H. Chour, Y. Nasser, O. Bazzi, and F. Bader, "Full-duplex or half-duplex D2D Mode Closed Form Expression of the Optimal Power Allocation," in Proc. 25th Int. Conf. Telecommunications (ICT), Jun.2018.

[C2] H. Chour, O. Bazzi, F. Bader, and Y. Nasser, "Analytical Framework for Joint Mode Selection and Power Allocation for Full-Duplex D2D Network," in Proc. IEEE Wireless Communications and Networking Conf. (WCNC2019), Apr. 2019.

[C3] H. Chour, F. Bader, Y. Nasser, and O. Bazzi, "Galen: A Geometric Framework for Global Optimal Power Allocation in a Full-Duplex D2D Network," in Proc. IEEE Wireless Communications and Networking Conf (WCNC2019), Apr. 2019.

[C4] H. Chour, Y. Nasser, F.Bader, and O.Bazzi, "Game-Theoretic Based Power Allocation for a Full-Duplex D2D Network" in Proc. IEEE International Workshop on Computer Aided Modeling and Design of Communication Links and Networks (CAMAD2019), Sept. 2019.

Poster

[P1] H. CHour, "Closed-Form expression of the Optimal Power allocation for Full Duplex D2D communication", IETR PhD student Day, Rennes, France, Jul. 2017.

Technical deliverable

[TR1] French ANR-funded project ACCENT5, D1.3 : "Resource allocation for D2D communications: gain of advanced FBMC", technical contribution, Mar. 2018.

Talks without proceedings

[T1] H. Chour, "Full-Duplex D2D Communications Underlaying Cellular Networks", Seminar, Communication Theory Lab-TUD, Dresden, Germany, Apr. 2018.

[T2] H. Chour, "Global Optimal Resource Allocation in a Full-Duplex D2D Based Cellular Network", seminar, SCEE research team, Rennes, France, Nov. 2018.

Publications indirectly related to this thesis

During my PhD, I have had the opportunity to work on broader research aspects indirectly related to this dissertation, in the fields of Vehicular Ad-hoc Network (VANET) and *D2D* communication. The relevant published works are listed here.

Journal articles

[J2] A. Kachouh, H. Chour, Y. Nasser, and H. Artail, “Ergodic capacity analysis and transmission power optimization in D2D underlaying cellular communication,” Physical Communication, Elsevier Journal, vol. 34, pp.144-156, June 2019.

[J3] H. Chour, Y. Nasser, H. Artail, A. Kachouh, and A. Al-Dubai, "VANET Aided D2D Discovery: Delay Analysis and Performance", IEEE Transactions on Vehicular Technology, vol. 66, pp. 8059 - 8071, Sep. 2017.

International conferences

[C5] H. Chour, Y. Nasser, H. Artail, and A. Kachouh, “Freddy: A framework for VANET Aided D2D Discovery,” in Proc. IEEE Wireless Communications and Networking Conf. (WCNC2016), Apr. 2016.

Involvement in R&D Projects

ACCENT5

ACCENT5 was a French project funded by the ANR under Grant agreement ANR-14-CE28-0026. Its goal is to study the coexistence of *D2D* and cellular communications in future 5G networks. My role in this project has been to study the impact of integrating the full-duplex operation with *D2D* communication to further increase the spectrum efficiency of the network. Publication [C1] directly contribute to this project. Furthermore, I participated in the project by taking part in some technical meetings and contributing to the deliverable [TR1].

Others

- Working in the local organizing committee of the International Conference on Telecommunication (ICT) that held at France Saint-Malo in June 2018.
- Earning two mobility grants for research collaboration between IETR-CentralSupélec and Information Theory Lab-TUD from European Cooperation in Science & Technology (eCOST) action CA15104 entitled: "The Inclusive Radio Communication Networks for 5G and Beyond (IRACON)," and the French National Center for Scientific Research (CNRS) jointly with GdR-ISIS organization in 2018.

Bibliography

[1] V. Cisco Mobile, "Cisco visual networking index: Global mobile data traffic forecast update, 2016–2021 white paper," 2017.

[2] M. N. Tehrani, M. Uysal, and H. Yanikomeroglu, "Device-to-device communication in 5G cellular networks: challenges, solutions, and future directions," *IEEE Communications Magazine*, vol. 52, pp. 86–92, May 2014.

[3] X. Zhang, W. Cheng, and H. Zhang, "Full-duplex transmission in PHY and MAC layers for 5G mobile wireless networks," *IEEE Wireless Communications*, vol. 22, pp. 112–121, Oct. 2015.

[4] S. Mumtaz and J. Rodriguez, *Smart device to smart device communication*. Springer-Verlag, 2014.

[5] V. Tapio, "System scenarios and technical requirements for full-duplex concept," tech. rep., CORDIS, 2013.

[6] K. S. Ali, H. ElSawy, and M. Alouini, "Modeling cellular networks with full-duplex D2D communication: A stochastic geometry approach," *IEEE Transactions on Communications*, vol. 64, pp. 4409–4424, Oct. 2016.

[7] A. Asadi, Q. Wang, and V. Mancuso, "A survey on device-to-device communication in cellular networks," *IEEE Communications Surveys Tutorials*, vol. 16, pp. 1801–1819, Fourthquarter 2014.

[8] S. Research, "Prose (proximity services) for lte & 5g networks: 2017 - 2030 opportunities, challenges, strategies & forecasts," tech. rep., Social networking service (SNC) Telecom & IT, Jan. 2017.

[9] K. Doppler, C. B. Ribeiro, and J. Kneckt, "Advances in d2d communications: Energy efficient service and device discovery radio," in *Proc. Information Theory and Aerospace Electronic Systems Technology (Wireless VITAE) 2011 2nd Int. Conf. Wireless Communication, Vehicular Technology*, pp. 1–6, Feb. 2011.

[10] X. Wu, S. Tavildar, S. Shakkottai, T. Richardson, J. Li, R. Laroia, and A. Jovicic, "Flashlinq: A synchronous distributed scheduler for peer-to-peer ad hoc networks," *IEEE/ACM Transactions on Networking*, vol. 21, pp. 1215–1228, Aug. 2013.

[11] 3GPP, "Study on architecture enhancements to support proximity services (prose)," Tech. Rep. 23.703, 3GPP, Dec. 2013.

[12] S. Doumiati and H. Artail, "Analytical study of a service discovery system based on an lte-a d2d implementation," *Physical Communication*, vol. 19, pp. 145 – 162, 2016.

[13] L. Lei, Z. Zhong, C. Lin, and X. Shen, "Operator controlled device-to-device communications in LTE-advanced networks," *IEEE Wireless Communications*, vol. 19, pp. 96–104, June 2012.

[14] P. Mach, Z. Becvar, and T. Vanek, "In-band device-to-device communication in OFDMA cellular networks: A survey and challenges," *IEEE Communications Surveys Tutorials*, vol. 17, pp. 1885–1922, Fourthquarter 2015.

[15] K. Doppler, M. Rinne, C. Wijting, C. B. Ribeiro, and K. Hugl, "Device-to-device communication as an underlay to LTE-advanced networks," *IEEE Communications Magazine*, vol. 47, no. 12, 2009.

[16] D. Feng, L. Lu, Y. Yuan-Wu, G. Y. Li, G. Feng, and S. Li, "Device-to-device communications underlaying cellular networks," *IEEE Transactions on Communications*, vol. 61, pp. 3541–3551, Aug. 2013.

[17] Z. Zhang, K. Long, A. V. Vasilakos, and L. Hanzo, "Full-duplex wireless communications: challenges, solutions, and future research directions," *Proceedings of the IEEE*, vol. 104, no. 7, pp. 1369–1409, 2016.

[18] R. Yin, C. Zhong, G. Yu, Z. Zhang, K. K. Wong, and X. Chen, "Joint spectrum and power allocation for D2D communications underlaying cellular networks," *IEEE Transactions on Vehicular Technology*, vol. 65, pp. 2182–2195, Apr. 2016.

[19] J. G. Andrews, S. Buzzi, W. Choi, S. V. Hanly, A. Lozano, A. C. K. Soong, and J. C. Zhang, "What will 5g be?," *IEEE Journal on Selected Areas in Communications*, vol. 32, pp. 1065–1082, June 2014.

[20] A. J. PAULRAJ, D. A. GORE, R. U. NABAR, and H. BOLCSKEI, "An overview of MIMO communications - a key to gigabit wireless," *Proceedings of the IEEE*, vol. 92, pp. 198–218, Feb. 2004.

[21] Z. Zhang, X. Wang, K. Long, A. V. Vasilakos, and L. Hanzo, "Large-scale MIMO-based wireless backhaul in 5g networks," *IEEE Wireless Communications*, vol. 22, pp. 58–66, Oct. 2015.

[22] S. M. R. Islam, N. Avazov, O. A. Dobre, and K. Kwak, "Power-domain non-orthogonal multiple access (noma) in 5g systems: Potentials and challenges," *IEEE Communications Surveys Tutorials*, vol. 19, pp. 721–742, Secondquarter 2017.

[23] S. M. A. Kazmi, N. H. Tran, T. M. Ho, A. Manzoor, D. Niyato, and C. S. Hong, "Coordinated device-to-device communication with non-orthogonal multiple access in future wireless cellular networks," *IEEE Access*, vol. 6, pp. 39860–39875, 2018.

[24] Z. Zhang, K. Long, and J. Wang, "Self-organization paradigms and optimization approaches for cognitive radio technologies: a survey," *IEEE Wireless Communications*, vol. 20, pp. 36–42, Apr. 2013.

[25] T. Riihonen, S. Werner, and R. Wichman, "Hybrid full-duplex/half-duplex relaying with transmit power adaptation," *IEEE Transactions on Wireless Communications*, vol. 10, pp. 3074–3085, Sept. 2011.

[26] 3GPP, "Full duplex configuration of un and uu subframes for type i relay," techreport, 3GPP TSG RAN WG1 R1-100139, Jan. 2010.

[27] 3GPP, "Text proposal on inband full duplex relay for tr 36.81," techreport, 3GPP TSG RAN WG1 R1-101659, Feb. 2010.

[28] A. Sabharwal, P. Schniter, D. Guo, D. W. Bliss, S. Rangarajan, and R. Wichman, "In-band full-duplex wireless: Challenges and opportunities," *IEEE Journal on Selected Areas in Communications*, vol. 32, pp. 1637–1652, Sept. 2014.

[29] D. Bharadia, E. McMilin, and S. Katti, "Full duplex radios," *ACM SIGCOMM Computer Communication Review*, vol. 43, no. 4, pp. 375–386, 2013.

[30] M. Duarte and A. Sabharwal, "Full-duplex wireless communications using off-the-shelf radios: Feasibility and first results," in *Proc. Systems and Computers 2010 Conf. Record of the Forty Fourth Asilomar Conf. Signals*, pp. 1558–1562, Nov. 2010.

[31] M. Duarte, C. Dick, and A. Sabharwal, "Experiment-driven characterization of full-duplex wireless systems," *IEEE Transactions on Wireless Communications*, vol. 11, pp. 4296–4307, Dec. 2012.

[32] M. Jain, J. I. Choi, T. Kim, D. Bharadia, S. Seth, K. Srinivasan, P. Levis, S. Katti, and P. Sinha, "Practical, real-time, full duplex wireless," in *Proceedings of the 17th Annual International Conference on Mobile Computing and Networking*, MobiCom '11, pp. 301–312, ACM, 2011.

[33] A. Sahai, G. Patel, and A. Sabharwal, "Pushing the limits of full-duplex: Design and real-time implementation," *CoRR*, vol. abs/1107.0607, 2011.

[34] M. Duarte, A. Sabharwal, V. Aggarwal, R. Jana, K. K. Ramakrishnan, C. W. Rice, and N. K. Shankaranarayanan, "Design and characterization of a full-duplex multiantenna system for wifi networks," *IEEE Transactions on Vehicular Technology*, vol. 63, pp. 1160–1177, Mar. 2014.

[35] M. Chung, M. S. Sim, J. Kim, D. K. Kim, and C. Chae, "Prototyping real-time full duplex radios," *IEEE Communications Magazine*, vol. 53, pp. 56–63, Sept. 2015.

[36] K. E. Kolodziej, J. G. McMichael, and B. T. Perry, "Multitap RF canceller for in-band full-duplex wireless communications," *IEEE Transactions on Wireless Communications*, vol. 15, pp. 4321–4334, June 2016.

[37] D. Korpi, J. Tamminen, M. Turunen, T. Huusari, Y. Choi, L. Anttila, S. Talwar, and M. Valkama, "Full-duplex mobile device: pushing the limits," *IEEE Communications Magazine*, vol. 54, pp. 80–87, Sept. 2016.

[38] D. Korpi, M. Heino, C. Icheln, K. Haneda, and M. Valkama, "Compact inband full-duplex relays with beyond 100 dB self-interference suppression: Enabling techniques and field measurements," *IEEE Transactions on Antennas and Propagation*, vol. 65, pp. 960–965, Feb. 2017.

[39] L. Laughlin, C. Zhang, M. A. Beach, K. A. Morris, and J. Haine, "A widely tunable full duplex transceiver combining electrical balance isolation and active analog cancellation," in *Proc. IEEE 81st Vehicular Technology Conf. (VTC Spring)*, pp. 1–5, May 2015.

[40] R. Askar, B. Schubert, W. Keusgen, and T. Haustein, "Full-duplex wireless transceiver in presence of I/Q mismatches: Experimentation and estimation algorithm," in *Proc. IEEE Globecom Workshops (GC Wkshps)*, pp. 1–7, Dec. 2015.

[41] D. Kim, H. Lee, and D. Hong, "A survey of in-band full-duplex transmission: From the perspective of PHY and MAC layers," *IEEE Communications Surveys Tutorials*, vol. 17, pp. 2017–2046, Fourthquarter 2015.

[42] Z. Zhang, K. Long, A. V. Vasilakos, and L. Hanzo, "Full-duplex wireless communications: Challenges, solutions, and future research directions," *Proceedings of the IEEE*, vol. 104, pp. 1369–1409, July 2016.

[43] J. I. Choi, M. Jain, K. Srinivasan, P. Levis, and S. Katti, "Achieving single channel, full duplex wireless communication," in *Proceedings of the Sixteenth Annual International Conference on Mobile Computing and Networking*, MobiCom '10, pp. 1–12, ACM, 2010.

[44] M. A. Khojastepour, K. Sundaresan, S. Rangarajan, X. Zhang, and S. Barghi, "The case for antenna cancellation for scalable full-duplex wireless communications," in *Proceedings*

of the 10th ACM Workshop on Hot Topics in Networks, HotNets-X, pp. 17:1–17:6, ACM, 2011.

[45] C. R. Anderson, S. Krishnamoorthy, C. G. Ranson, T. J. Lemon, W. G. Newhall, T. Kummetz, and J. H. Reed, "Antenna isolation, wideband multipath propagation measurements, and interference mitigation for on-frequency repeaters," in *Proc. IEEE SoutheastCon*, pp. 110–114, Mar. 2004.

[46] E. Everett, A. Sahai, and A. Sabharwal, "Passive self-interference suppression for full-duplex infrastructure nodes," *IEEE Transactions on Wireless Communications*, vol. 13, pp. 680–694, Feb. 2014.

[47] E. Aryafar, M. A. Khojastepour, K. Sundaresan, S. Rangarajan, and M. Chiang, "Midu: Enabling mimo full duplex," in *Proceedings of the 18th Annual International Conference on Mobile Computing and Networking*, Mobicom '12, pp. 257–268, ACM, 2012.

[48] E. Everett, *Full-duplex infrastructure nodes: Achieving long range with half-duplex Mobiles*. PhD thesis, Rice University, 2011.

[49] E. Everett, M. Duarte, C. Dick, and A. Sabharwal, "Empowering full-duplex wireless communication by exploiting directional diversity," in *Proc. Systems and Computers (ASILOMAR) 2011 Conf. Record of the Forty Fifth Asilomar Conf. Signals*, pp. 2002–2006, Nov. 2011.

[50] L. Laughlin, M. A. Beach, K. A. Morris, and J. L. Haine, "Optimum single antenna full duplex using hybrid junctions," *IEEE Journal on Selected Areas in Communications*, vol. 32, pp. 1653–1661, Sept. 2014.

[51] J. Zhou, N. Reiskarimian, J. Diakonikolas, T. Dinc, T. Chen, G. Zussman, and H. Krishnaswamy, "Integrated full duplex radios," *IEEE Communications Magazine*, vol. 55, pp. 142–151, Apr. 2017.

[52] J. Zhou, N. Reiskarimian, and H. Krishnaswamy, "Receiver with integrated magnetic-free n-path-filter-based non-reciprocal circulator and baseband self-interference cancellation for full-duplex wireless," in *Proc. IEEE Int. Solid-State Circuits Conf. (ISSCC)*, pp. 178–180, Jan. 2016.

[53] D. Korpi, T. Riihonen, V. Syrjälä, L. Anttila, M. Valkama, and R. Wichman, "Full-duplex transceiver system calculations: Analysis of ADC and linearity challenges," *IEEE Transactions on Wireless Communications*, vol. 13, pp. 3821–3836, July 2014.

[54] M. E. Knox, "Single antenna full duplex communications using a common carrier," in *Proc. WAMICON 2012 IEEE Wireless Microwave Technology Conf*, pp. 1–6, Apr. 2012.

[55] N. Phungamngern, P. Uthansakul, and M. Uthansakul, "Digital and RF interference cancellation for single-channel full-duplex transceiver using a single antenna," in *Proc. Telecommunications and Information Technology 2013 10th Int. Conf. Electrical Engineering/Electronics, Computer*, pp. 1–5, May 2013.

[56] A. Balatsoukas-Stimming, A. C. Austin, P. Belanovic, and A. Burg, "Baseband and rf hardware impairments in full-duplex wireless systems: experimental characterisation and suppression," *EURASIP Journal on Wireless Communications and Networking*, vol. 2015, no. 1, p. 142, 2015.

[57] D. Korpi, L. Anttila, V. Syrjälä, and M. Valkama, "Widely linear digital self-interference cancellation in direct-conversion full-duplex transceiver," *IEEE Journal on Selected Areas in Communications*, vol. 32, pp. 1674–1687, Sept. 2014.

[58] E. Ahmed, A. M. Eltawil, and A. Sabharwal, "Self-interference cancellation with nonlinear distortion suppression for full-duplex systems," in *2013 Asilomar Conference on Signals, Systems and Computers*, pp. 1199–1203, IEEE, 2013.

[59] D. Korpi, T. Huusari, Y.-S. Choi, L. Anttila, S. Talwar, and M. Valkama, "Digital self-interference cancellation under nonideal rf components: Advanced algorithms and measured performance," in *2015 IEEE 16th international workshop on signal processing advances in wireless communications (SPAWC)*, pp. 286–290, IEEE, 2015.

[60] D. Korpi, L. Anttila, and M. Valkama, "Nonlinear self-interference cancellation in mimo full-duplex transceivers under crosstalk," *EURASIP journal on wireless Communications and Networking*, vol. 2017, no. 1, p. 24, 2017.

[61] E. Ahmed and A. M. Eltawil, "All-digital self-interference cancellation technique for full-duplex systems," *IEEE Transactions on Wireless Communications*, vol. 14, pp. 3519–3532, July 2015.

[62] D. Korpi, L. Anttila, and M. Valkama, "Reference receiver based digital self-interference cancellation in MIMO full-duplex transceivers," in *Proc. IEEE Globecom Workshops (GC Wkshps)*, pp. 1001–1007, Dec. 2014.

[63] P. Ferrand and M. Duarte, "Multi-tap digital canceller for full-duplex applications," in *2017 IEEE 18th International Workshop on Signal Processing Advances in Wireless Communications (SPAWC)*, pp. 1–5, IEEE, 2017.

[64] V. R. Cadambe and S. A. Jafar, "Can feedback, cooperation, relays and full duplex operation increase the degrees of freedom of wireless networks?," in *Proc. IEEE Int. Symp. Information Theory*, pp. 1263–1267, July 2008.

[65] V. R. Cadambe and S. A. Jafar, "Degrees of freedom of wireless networks with relays, feedback, cooperation, and full duplex operation," *IEEE Transactions on Information Theory*, vol. 55, pp. 2334–2344, May 2009.

[66] A. Sahai, S. Diggavi, and A. Sabharwal, "On degrees-of-freedom of full-duplex uplink/downlink channel," in *Proc. IEEE Information Theory Workshop (ITW)*, pp. 1–5, Sept. 2013.

[67] N. V. Shende, Ö. Gürbüz, and E. Erkip, "Half-duplex or full-duplex communications: Degrees of freedom analysis under self-interference," *IEEE Transactions on Wireless Communications*, vol. 17, pp. 1081–1093, Feb. 2018.

[68] I. Atzeni and M. Kountouris, "Full-duplex MIMO small-cell networks with interference cancellation," *IEEE Transactions on Wireless Communications*, vol. 16, pp. 8362–8376, Dec. 2017.

[69] I. Atzeni and M. Kountouris, "Full-duplex MIMO small-cell networks: Performance analysis," in *Proc. IEEE Global Communications Conf. (GLOBECOM)*, pp. 1–6, Dec. 2015.

[70] S. Goyal, C. Galiotto, N. Marchetti, and S. Panwar, "Throughput and coverage for a mixed full and half duplex small cell network," in *Proc. IEEE Int. Conf. Communications (ICC)*, pp. 1–7, May 2016.

[71] Z. Tong and M. Haenggi, "Throughput analysis for full-duplex wireless networks with imperfect self-interference cancellation," *IEEE Transactions on Communications*, vol. 63, pp. 4490–4500, Nov. 2015.

[72] X. Xie and X. Zhang, "Does full-duplex double the capacity of wireless networks?," in *Proc. IEEE INFOCOM 2014 - IEEE Conf. Computer Communications*, pp. 253–261, Apr. 2014.

[73] P. Gupta and P. R. Kumar, "The capacity of wireless networks," *IEEE Transactions on Information Theory*, vol. 46, pp. 388–404, Mar. 2000.

[74] M. Fukumoto and M. Bandai, "MIMO full-duplex wireless: Node architecture and medium access control protocol," in *Proc. Seventh Int. Conf. Mobile Computing and Ubiquitous Networking (ICMU)*, pp. 76–77, Jan. 2014.

[75] W. Choi, J. Park, Y. Kim, A. Sabharwal, and H. Lim, "Design and implementation of a full-duplex pipelined MAC protocol for multihop wireless networks," *IEEE Access*, vol. 5, pp. 14930–14942, 2017.

[76] W. Cheng, X. Zhang, and H. Zhang, "Full-duplex spectrum-sensing and MAC-protocol for multichannel nontime-slotted cognitive radio networks," *IEEE Journal on Selected Areas in Communications*, vol. 33, pp. 820–831, May 2015.

[77] Z. Wang, Y. Liu, Y. Lin, and S. Huang, "Full-duplex MAC protocol based on adaptive contention window for visible light communication," *IEEE/OSA Journal of Optical Communications and Networking*, vol. 7, pp. 164–171, Mar. 2015.

[78] S. Liu, B. Han, and W. Peng, "A polling-based traffic-aware MAC protocol for centralized full-duplex wireless networks," *IEEE Access*, vol. 6, pp. 28225–28238, 2018.

[79] T. Yang, R. Zhang, X. Cheng, and L. Yang, "Resource sharing for device-to-device communications underlaying full-duplex cellular networks," in *Proc. IEEE Int. Conf. Communication Systems*, pp. 16–20, Nov. 2014.

[80] L. Ren, M. Zhao, X. Gu, and L. Zhang, "A two-step resource allocation algorithm for d2d communication in full duplex cellular network," in *Proc. and Mobile Radio Communications (PIMRC) 2016 IEEE 27th Annual Int. Symp. Personal, Indoor*, pp. 1–7, Sept. 2016.

[81] and Jing-Wei Kao, Yuan-Yao Shih, Ai-Chun Pang, and Yung-Chun Lin, "Radio resource allocation for d2d-assisted full-duplex cellular networks," in *Proc. Seventh Int. Conf. Ubiquitous and Future Networks*, pp. 721–726, July 2015.

[82] L. Liu, Z. Zhang, and Y. Xu, "Joint subcarrier assignment and power allocation for d2d communication underlaying full-duplex cellular networks," in *Proc. and Mobile Radio Communications (PIMRC) 2016 IEEE 27th Annual Int. Symp. Personal, Indoor*, pp. 1–6, Sept. 2016.

[83] S. Han, P. Chen, and C. Yang, "Full duplex assisted interference suppression for underlay device-to-device communications," in *Proc. IEEE Globecom Workshops (GC Wkshps)*, pp. 851–856, Dec. 2014.

[84] B. Ma, H. Shah-Mansouri, and V. W. S. Wong, "A matching approach for power efficient relay selection in full duplex d2d networks," in *Proc. IEEE Int. Conf. Communications (ICC)*, pp. 1–6, May 2016.

[85] and Bin Zhong, Jiajia Zhang, Qian Zeng, and Xiaoming Dai, "Coverage probability analysis for full-duplex relay aided device-to-device communications networks," *China Communications*, vol. 13, pp. 60–67, Nov. 2016.

[86] G. Zhang, K. Yang, and H. Chen, "Socially aware cluster formation and radio resource allocation in d2d networks," *IEEE Wireless Communications*, vol. 23, pp. 68–73, Aug. 2016.

[87] S. Dang, G. Chen, and J. P. Coon, "Outage performance analysis of full-duplex relay-assisted device-to-device systems in uplink cellular networks," *IEEE Transactions on Vehicular Technology*, vol. 66, pp. 4506–4510, May 2017.

[88] S. Dang, J. P. Coon, and G. Chen, "Resource allocation for full-duplex relay-assisted device-to-device multicarrier systems," *IEEE Wireless Communications Letters*, vol. 6, pp. 166–169, Apr. 2017.

[89] S. Kim and W. Stark, "Full duplex device to device communication in cellular networks," in *Proc. Networking and Communications (ICNC) 2014 Int. Conf. Computing*, pp. 721–725, Feb. 2014.

[90] W. Cheng, X. Zhang, and H. Zhang, "Optimal power allocation for full-duplex D2D communications over wireless cellular networks," in *2014 IEEE Global Communications Conference*, pp. 4764–4769, Dec. 2014.

[91] W. Cheng, X. Zhang, and H. Zhang, "Heterogeneous statistical QoS provisioning for full-duplex d2d communications over 5g wireless networks," in *Proc. IEEE Global Communications Conf. (GLOBECOM)*, pp. 1–7, Dec. 2015.

[92] S. Ali, N. Rajatheva, and M. Latva-aho, "Full duplex device-to-device communication in cellular networks," in *Proc. European Conf. Networks and Communications (EuCNC)*, pp. 1–5, June 2014.

[93] S. Ali, A. Ghazanfari, N. Rajatheva, and M. Latva-aho, "Effect of residual of self-interference in performance of full-duplex D2D communication," in *Proc. 1st Int. Conf. 5G for Ubiquitous Connectivity*, pp. 46–51, Nov. 2014.

[94] S. Ali, N. Rajatheva, and M. Latva-aho, "Effect of interference of full-duplex transmissions in underlay device-to-device communication," in *Proc. IEEE 14th Canadian Workshop Information Theory (CWIT)*, pp. 54–57, July 2015.

[95] H. V. Vu, N. H. Tran, and T. Le-Ngoc, "On coverage probabilities and sum-rate of full-duplex device-to-device cellular networks," in *Proc. IEEE Int. Conf. Communications (ICC)*, pp. 1–6, May 2018.

[96] N. Giatsoglou, K. Ntontin, E. Kartsakli, A. Antonopoulos, and C. Verikoukis, "D2d-aware device caching in mmwave-cellular networks," *IEEE Journal on Selected Areas in Communications*, vol. 35, pp. 2025–2037, Sep. 2017.

[97] M. Naslcheraghi, M. Afshang, and H. S. Dhillon, "Modeling and performance analysis of full-duplex communications in cache-enabled d2d networks," in *2018 IEEE International Conference on Communications (ICC)*, pp. 1–6, May 2018.

[98] K. T. Hemachandra, O. Ochia, and A. O. Fapojuwo, "Performance study on cache enabled full-duplex device-to-device networks," in *2018 IEEE Wireless Communications and Networking Conference (WCNC)*, pp. 1–6, April 2018.

[99] Y. Chen, L. Wang, R. Ma, B. Jiao, and L. Hanzo, "Cooperative full duplex content sensing and delivery improves the offloading probability of d2d caching," *IEEE Access*, vol. 7, pp. 29076–29084, 2019.

[100] M. Naslcheraghi, S. A. Ghorashi, and M. Shikh-Bahaei, "Fd device-to-device communication for wireless video distribution," *IET Communications*, vol. 11, pp. 1074–1081(7), May 2017.

[101] M. Naslcheraghi, S. A. Ghorashi, and M. Shikh-Bahaei, "Full-duplex device-to-device collaboration for low-latency wireless video distribution," in *2017 24th International Conference on Telecommunications (ICT)*, pp. 1–5, May 2017.

[102] M. Naslcheraghi, S. A. Ghorashi, and M. Shikh-Bahaei, "Performance analysis of inband fd-d2d communications with imperfect si cancellation for wireless video distribution," in *2017 8th International Conference on the Network of the Future (NOF)*, pp. 176–181, Nov 2017.

[103] H. Bagheri, F. A. Miranda Bonomi, and M. Katz, "Spectral efficiency and throughput enhancement by full-duplex d2d communication in mobile clouds," in *Proc. European Wireless 2015; 21th European Wireless Conf*, pp. 1–6, May 2015.

[104] C. Liu, T. Lv, W. Tang, H. Gao, and Y. Lu, "On the performance of mode selection for hybrid-duplex d2d communications," in *Proc. MILCOM 2017 - 2017 IEEE Military Communications Conf. (MILCOM)*, pp. 852–857, Oct. 2017.

[105] K. T. Hemachandra and A. O. Fapojuwo, "Duplex mode selection for throughput maximization in device-to-device underlaid cellular networks," in *2018 IEEE Wireless Communications and Networking Conference (WCNC)*, pp. 1–6, April 2018.

[106] A. N. Kadhim, F. Hajiaghajani, and M. Rasti, "On selecting duplex-mode and resource allocation strategy in full duplex d2d communication," in *Proc. Iranian Conf. Electrical Engineering (ICEE)*, pp. 1640–1645, May 2017.

[107] L. Han, W. Zou, and G. Zhao, "Duplex mode selection for device-to-device communications underlaying the cellular uplink," in *Proc. IEEE Conf. Computer Communications Workshops (INFOCOM WKSHPS)*, pp. 157–162, May 2017.

[108] N. Giatsoglou, A. Antonopoulos, E. Kartsakli, J. Vardakas, and C. Verikoukis, "Transmission policies for interference management in full-duplex d2d communication," in *2016 IEEE Global Communications Conference (GLOBECOM)*, pp. 1–6, Dec 2016.

[109] X. Chai, T. Liu, C. Xing, H. Xiao, and Z. Zhang, "Throughput improvement in cellular networks via full-duplex based device-to-device communications," *IEEE Access*, vol. 4, pp. 7645–7657, 2016.

[110] X. Hou, F. Liu, and Y. Liu, "Capacity gain analysis for underlaying full-duplex d2d communications with a novel interference management scheme," in *2017 IEEE 28th Annual International Symposium on Personal, Indoor, and Mobile Radio Communications (PIMRC)*, pp. 1–5, Oct 2017.

[111] F. Liu, X. Hou, and Y. Liu, "Capacity improvement for full duplex device-to-device communications underlaying cellular networks," *IEEE Access*, vol. 6, pp. 68373–68383, 2018.

[112] B. Zuo, L. Jiang, C. He, and Z. Lian, "Power allocation optimization for full-duplex D2D communications underlaying cellular networks," in *2016 International Conference on Networking and Network Applications (NaNA)*, pp. 103–108, IEEE, 2016.

[113] K. T. Hemachandra and A. O. Fapojuwo, "Power control schemes for full-duplex device-to-device networks underlaying a primary full-duplex network," in *2017 IEEE 30th Canadian Conference on Electrical and Computer Engineering (CCECE)*, pp. 1–4, April 2017.

[114] J. Ding, L. Jiang, and C. He, "Energy-efficient power control for underlaying full-duplex device-to-device communications," in *Proc. Asia Modelling Symp. (AMS)*, pp. 155–160, Dec. 2017.

[115] Z. ZHANG, H. QU, J. ZHAO, and Z. LUAN, "Fairness based power allocation optimization in dense full duplex d2d networks," in *2019 21st International Conference on Advanced Communication Technology (ICACT)*, pp. 206–211, Feb 2019.

[116] H. V. Vu, N. H. Tran, and T. Le-Ngoc, "Full-duplex device-to-device cellular networks: Power control and performance analysis," *IEEE Transactions on Vehicular Technology*, vol. 68, pp. 3952–3966, April 2019.

[117] and Gaojie Chen, Dandan Liang, M. Ghoraishi, Pei Xiao, and R. Tafazolli, "Optimum user selection for hybrid-duplex device-to-device in cellular networks," in *Proc. Int. Symp. Wireless Communication Systems (ISWCS)*, pp. 16–20, Aug. 2015.

[118] G. Lee, W. Saad, M. Bennis, A. Mehbodniya, and F. Adachi, "Online channel allocation for full-duplex device-to-device communications," in *2016 IEEE Globecom Workshops (GC Wkshps)*, pp. 1–6, IEEE, 2016.

[119] S. Li, Q. Ni, Y. Sun, and G. Min, "Resource allocation for weighted sum-rate maximization in multi-user full-duplex device-to-device communications: Approaches for perfect and statistical csis," *IEEE Access*, vol. 5, pp. 27229–27241, 2017.

[120] R. Tang, J. Zhao, H. Qu, and Z. Zhang, "Energy-efficient resource allocation for 5G full-duplex enabled device-to-device communication," in *Proc. IEEE Globecom Workshops*, pp. 1–7, Dec. 2016.

[121] K. T. Hemachandra, N. Rajatheva, and M. Latva-aho, "Sum-rate analysis for full-duplex underlay device-to-device networks," in *2014 IEEE Wireless Communications and Networking Conference (WCNC)*, pp. 514–519, Apr. 2014.

[122] V. Raghavan, S. V. Hanly, and V. V. Veeravalli, "Statistical beamforming on the grassmann manifold for the two-user broadcast channel," *IEEE Transactions on Information Theory*, vol. 59, no. 10, pp. 6464–6489, 2013.

[123] M. Abramowitz and I. A. Stegun, *Handbook of Mathematical Functions with Formulas, Graphs and Mathematical Tables*. Gaithersburg, MD, USA: National Bureau of Standards, 10th edt ed., 1972.

[124] S. Boyd and L. Vandenberghe, *Convex optimization*. Cambridge university press, 2004.

[125] M. Chiang, C. W. Tan, D. P. Palomar, D. O'neill, and D. Julian, "Power control by geometric programming," *IEEE Transactions on Wireless Communications*, vol. 6, pp. 2640–2651, July 2007.

[126] M. Grant, S. Boyd, and Y. Ye, "Cvx: Matlab software for disciplined convex programming," 2008.

[127] H. Tuy, "Monotonic optimization: Problems and solution approaches," *SIAM Journal on Optimization*, vol. 11, no. 2, pp. 464–494, 2000.

[128] H. W. Kuhn, "The hungarian method for the assignment problem," *Naval research logistics quarterly*, vol. 2, pp. 83–97, 1955.

[129] M. Wellens, J. Wu, and P. Mahonen, "Evaluation of spectrum occupancy in indoor and outdoor scenario in the context of cognitive radio," in *Proc. 2nd Int. Conf. Cognitive Radio Oriented Wireless Networks and Communication (CROWNCOM)*, pp. 420–427, Aug. 2007.

[130] S. Buzzi, C. I, T. E. Klein, H. V. Poor, C. Yang, and A. Zappone, "A survey of energy-efficient techniques for 5G networks and challenges ahead," *IEEE Journal on Selected Areas in Communications*, vol. 34, pp. 697–709, Apr. 2016.

[131] Z. Luo and S. Zhang, "Dynamic spectrum management: Complexity and duality," *IEEE Journal of Selected Topics in Signal Processing*, vol. 2, pp. 57–73, Feb. 2008.

[132] J.-P. Crouzeix and J. A. Ferland, "Algorithms for generalized fractional programming," *Mathematical Programming*, vol. 52, no. 1-3, pp. 191–207, 1991.

[133] A. Zappone, E. Jorswieck, *et al.*, "Energy efficiency in wireless networks via fractional programming theory," *Foundations and Trends® in Communications and Information Theory*, vol. 11, no. 3-4, pp. 185–396, 2015.

[134] H. Tuy, *Convex Analysis and Global Optimization*, vol. 110. Springer, 2016.

[135] B. Kaufman and B. Aazhang, "Cellular networks with an overlaid device to device network," in *2008 42nd Asilomar Conference on Signals, Systems and Computers (ACSSC)*, pp. 1537–1541, Oct. 2008.

[136] E. Björnson and E. Jorswieck, *Optimal Resource Allocation in Coordinated Multi-Cell Systems*. Foundations and Trends ® in Communications and Information Theory, 2013.

[137] A. Zappone, L. Sanguinetti, G. Bacci, E. Jorswieck, and M. Debbah, "Energy-efficient power control: A look at 5g wireless technologies," *IEEE Transactions on Signal Processing*, vol. 64, pp. 1668–1683, April 2016.

[138] G. Bacci, E. V. Belmega, P. Mertikopoulos, and L. Sanguinetti, "Energy-aware competitive power allocation for heterogeneous networks under qos constraints," *IEEE Transactions on Wireless Communications*, vol. 14, pp. 4728–4742, Sep. 2015.

[139] H. Chour, E. A. Jorswieck, F. Bader, Y. Nasser, and O. Bazzi, "Global optimal resource allocation for efficient fd-d2d enabled cellular network," *IEEE Access*, vol. 7, pp. 59690–59707, 2019.

[140] G. Debreu, "A social equilibrium existence theorem," *Proceedings of the National Academy of Sciences*, vol. 38, no. 10, pp. 886–893, 1952.

[141] R. D. Yates *et al.*, "A framework for uplink power control in cellular radio systems," *IEEE Journal on selected areas in communications*, vol. 13, no. 7, pp. 1341–1347, 1995.

[142] L. Wang, F. Tian, T. Svensson, D. Feng, M. Song, and S. Li, "Exploiting full duplex for device-to-device communications in heterogeneous networks," *IEEE Communications Magazine*, vol. 53, pp. 146–152, May 2015.

[143] S. Xia, B. Chen, K. Zhu, X. Zhai, and S. Gong, "Performance analysis of full-duplex D2D communications in multi-tier heterogeneous wireless networks," in *2017 IEEE International Symposium on Parallel and Distributed Processing with Applications and 2017 IEEE International Conference on Ubiquitous Computing and Communications (ISPA/IUCC)*, pp. 259–266, Dec 2017.

[144] Y. Liu, R. Wang, and Z. Han, "Interference-constrained pricing for d2d networks," *IEEE Transactions on Wireless Communications*, vol. 16, pp. 475–486, Jan 2017.

[145] R. Yin, G. Yu, H. Zhang, Z. Zhang, and G. Y. Li, "Pricing-based interference coordination for d2d communications in cellular networks," *IEEE Transactions on Wireless Communications*, vol. 14, pp. 1519–1532, March 2015.

Titre : La communication terminal-à-terminal avec un mode d'accès Full Duplex en réseau 5G

Mots clés : Full-Duplex, La communication terminal-à-terminal, Allocation de puissance, Allocation du canal

Résumé : Avec la croissance rapide de la demande de trafic de données des clients, l'amélioration de la capacité du système et l'augmentation du débit des utilisateurs sont devenues des préoccupations essentielles pour le futur réseau de communication sans fil de cinquième génération. Dans ce contexte, la communication terminal-à-terminal (Device-to-Device D2D) et le full duplex (FD) sont proposés comme solutions potentielles pour augmenter l'efficacité spectrale et le débit des utilisateurs dans un réseau cellulaire. Le D2D permet à deux périphériques proches de communiquer sans participation de la station de base ou avec une participation limitée. D'autre part, la communication en FD permet une transmission et une réception simultanées dans la même bande de fréquence. En raison de la propriété de distance courte des liaisons D2D, exploiter la technique FD dans la communication D2D est un excellent choix pour améliorer encore l'efficacité spectrale cellulaire et le débit des utilisateurs. Cependant, les émetteurs-récepteurs FD constituent de nouveau défis pour la communication D2D. Par exemple, en FD les émetteurs-récepteurs ne peuvent pas supprimer d'une manière parfaite l'auto-interférence (SI) généré au niveau des récepteurs lors de la transmission des données (par le propre émetteur du dispositif cellulaire). Ainsi, l'auto-interférence résiduelle qui est étroitement liée à la valeur de la puissance de l'émetteur affecte fortement les performances de la transmission FD. De plus, la technique en FD crée des interférences supplémentaires dans le réseau, ce qui peut dégrader ses performances par rapport à la transmission en semi-duplex (Half-duplex FD). Ainsi, une bonne gestion des ressources radio est nécessaire pour exploiter les avantages de la FD et garantir la qualité de service (QoS) des utilisateurs.

Les travaux de cette thèse portent sur l'allocation de puissance et l'attribution de canaux d'un réseau FD-D2D.

En particulier, cette thèse aborde d'abord le problème de l'allocation de puissance et propose une méthode d'allocation de puissance (PA) optimal centralisé simple mais efficace, puis développe le schéma optimal conjoint d'AP et d'AC pour un réseau FD-D2D. Enfin, cette thèse développe une AP efficace et décentralisée utilisant des outils de théorie des jeux qui constitueront une partie essentielle des travaux futurs dans le contexte de la gestion des ressources radio distribuées.

Title: Full-Duplex Device-to-Device Communication for 5G Network

Keywords: Full-Duplex, Device-to-Device, Power allocation, Channel Assignment, Resource allocation

Abstract: With the rapidly growing of the customers' data traffic demand, improving the system capacity and increasing the user throughput have become essential concerns for the future fifth-generation wireless communication network. In this context, D2D communication and full-duplex (FD) are proposed as potential solutions to increase e spatial spectrum utilization and the user rate in a cellular network. D2D allows two nearby devices to communicate without base station participation or with limited participation. On the other hand, FD communication allows simultaneous transmission and reception in the same frequency band. Due to the short distance property of D2D links, exploiting FD technology in D2D communication is an excellent choice to further improve the cellular spectrum efficiency and the users' throughput. However, practical FD transceivers add new challenges for D2D communication. For instance, the existing FD devices cannot perfectly eliminate the self-interference (SI) imposed on the receiver by the node's own transmitter. Thus, the residual SI which is tightly related to the transmitter power value highly affects the performance of FD transmission. Moreover, FD technique creates additional interference in the network which may degrade its performance when compared with the half-duplex transmission. Thus, a proper radio resource management is needed to exploit the benefits of FD and guarantee the quality of service (QoS) of the users. The works in this dissertation focus on the power allocation and channel assignment of an FD-D2D network. This thesis first addresses the power allocation (PA) problem and proposes a simple yet efficient centralized optimal PA framework and next it derives the optimal joint PA and CA scheme for an FD-D2D network. Finally, this dissertation develops an efficient decentralized PA using game theory tools which will be an essential part of future works in the context of distributed radio resource management for FD-D2D network.